Ghent University
Faculty of Sciences
Department of Plant Biotechnology and Bioinformatics

The *Arabidopsis* root cap contributes to root branching by setting the root clock

this thesis is submitted as fulfilment of the requirements for
the degree of Ph.D. in Sciences 2014 by

Wei Xuan

Promoter:
Prof. dr. Tom Beeckman

VIB - Plant Systems Biology
Root Development Group
Technologiepark 927, B-9000 Ghent, Belgium

Xuan, W (2014) "The *Arabidopsis* root cap contributes to root branching by setting the root clock". PhD Thesis, Ghent University, Ghent, Belgium

Wei Xuan was supported by a CSC PhD fellowship grant of China and by the Special Research Funds of Ghent University (BOF, B/06640/01)

JURY MEMBERS

Promotors

Prof. Dr. Tom Beeckman
Department of Plant Biotechnology and Genetics
Ghent University, Belgium

Promotion commission

Prof. dr. Wout Boerjan (chair)
Department of Plant Biotechnology and Genetics
Ghent University, Belgium

Prof. dr. Lieven De Veylder
Department of Plant Systems Biology,
Ghent University, Belgium

Prof. dr. Ive de Smet
Department of Plant Biotechnology and Genetics
Ghent University, Belgium

Prof. dr. Danny Geelen
Department of Plant Production,
Faculty of Bioscience Engineering,
Ghent University, Belgium

Dr. Laurent Laplaze
Institut de Recherche pour le Développement (IRD),
UMR DIADE (IRD/UM2), France

Dr. Dominique Audenaert
Compound Screening Facility,
VIB, Belgium

Dr. Bert de Rybel
Laboratory of Biochemistry,
Wageningen University, the Netherlands

TABLE OF CONTENTS

Spatiotemporal coordination of organ formation is a crucial research topic in both plant and animal biology. In the model plant *Arabidopsis thaliana*, the "root clock" model states that a periodic induction of gene expression occurring in the oscillation zone of the root apex constitutes a temporal signal. This temporal signal can be translated into a spatial message leading to sequential formation of the prebranch sites, patches of cell competent to form lateral roots. The plant hormone auxin controls many aspects of organ growth and development in plants. Particularly for lateral root development, auxin signalling is quintessential for lateral root (LR) initiation, patterning of LR primordia and its emergence. A root cap-specific indole-3-butyric acid (IBA) to indole-3-acetic acid (IAA) conversion was found to contribute to the root branching process. This auxin source modulates the amplitude of the oscillations and subsequently determines whether a prebranch site is created or not.

The aim of this project was to reveal the mechanism how this root cap-source auxin affect the root clock and the nature of this process. To access it, we applied live-imaging approaches to visualize auxin signalling dynamics during the oscillations and the prebranch sites formation. A novel imaging system with a vertically adapted fluorescence microscope was optimized to visualize the dynamics of the root cap auxin response. To identity novel genes controlling the root clock in *Arabidopsis*, we followed two strategies; firstly, an IBA-trascriptome analysis was applied to explore the signalling components downstream of the root cap-source auxin, which led to the identification of MEMBRANE-ASSOCIATED KINASE REGULATOR4 (MAKR4). Secondly, we use Tirlin as a chemical tool to identify the potential signalling components downstream of TIR1/AFB-dependent signalling pathways for lateral root formation.

FREQUENTLY USED ABBREVIATIONS

ACR4: *ARABIDOPSIS* CRINKLY 4
AFB: AUXIN-RELATED F-Box protein
ARF: AUXIN RESPONSE FACTOR
Aux/IAA: AUXIN/INDOLE-3-ACETIC ACID
AXR: AUXIN RESISTANT
Dex: dexamethasone
DMSO: dimethylsulfoxide
DTA: *Diphtheria* toxin A
FC: founder cell
GFP: GREEN FLUORESCENT PROTEIN
GR: glucocorticoid receptor
IAA: indole-3-acetic acid
IAM: indole-3-acetamide
IBA: indole-3-butyric acid
LR: lateral root
LRC: lateral root cap
LRP: lateral root primordium
LRIS: lateral root inducible system
MAKR4: MEMBRANE-ASSOCIATED KINASE REGULATOR 4
NAA: naphthalene-1-acetic acid
Naxillin: non-auxin like lateral root inducer
NLS: nuclear localisation signal
NPA: 1-naphthylphthalamic acid
OZ: oscillation zone
PB: prebranch site
PC: periclinal cell division
PCD: programmed cell death
PI: propidium iodide
PPP: phloem pole pericycle
Q-RT-PCR: quantitative real-time PCR
amiRNA: artificial micro RNA
SLR-1: SOLITARY ROOT-1
SMB: SOMBRERO
T-DNA: transfer DNA
TIR1: transport inhibitor response 1
Tirlin: TIR1-depedent lateral root inducer
TZ: transition zone
tdTOMATO: tandem dimer Tomato red fluorescent protein
UAS: upstream activating sequence
WT: wild type
XPP: xylem pole pericycle

Learn extensively, inquire carefully, think deeply, differentiate clearly, and practice faithfully.
博学之、审问之、慎思之、明辨之、笃行之。”

Doctrine of the Mean
《礼记·中庸》

Chapter 1

Introduction

Adapted from:

Van Norman, J.M., **Xuan, W.**, Beeckman, T., and Benfey, P.N. (Chatfield et al.). To branch or not to branch: the role of pre-patterning in lateral root formation. Development *140*, 4301-4310.

Xuan W., Murphy E., Beeckman T., Audenaert D., De Smet I. (Chatfield et al.). Synthetic molecules: helping to unravel plant signal transduction. J. Chem. Biol. *6*, 43–50

TABLE OF CONTENTS

An introduction to the root clock

The root clock pre-patterns the root system

The plant root system is responsible for the uptake of water and nutrients from the soil, and thus crucial for the plant survival and growth. In response to various growth conditions, plants can optimize their root system by altering root patterning through the formation of lateral roots. Understanding the mechanism underlying root patterning is a major topic both in fundamental and applied research.

In the plant model *Arabidopsis*, root pre-patterning has been linked to the root clock, which manifest itself by a periodic formation of prebranch sites along the axis of primary root *Arabidopsis* (Van Norman et al., 2013). These prebranch sites are prepared to develop as lateral roots when they receive signals to grow further and emerge from the primary root. Molecular evidence showed that the root clock is characterized by a large scale of gene expression oscillations that are in phase with the expression of the auxin response reporter DR5 in a defined zone of the root, the oscillation zone (Moreno-Risueno et al., 2010). Subsequently, this temporal oscillating pattern of gene expression in the oscillation zone is translated into a repetitive spatial pattern of prebranch sites (Moreno-Risueno et al., 2010).

The root clock can be visualized by the use of *DR5:Lucifease* in *Arabidopsis* (Moreno-Risueno et al., 2010). DR5 is a highly active synthetic auxin response element (AuxRE), and it contains tandem direct repeats of 11 base pairs that included the auxin-responsive TGTCTC element found in the soybean GH3 promoter (Ulmasov et al., 1997). The DR5 AuxRE contains 3-bp mutants with thymidine substitutions next to the TGTCTC elements (CCTCGTGTCTC→CCTttTGTCTC), and displays more sensitivity to auxin than the natural composite AuxRE's, and thus provides a useful reporter gene for studying auxin-responsive transcription in *Arabidopsis* and other species. The activity of DR5 is tightly controlled by local auxin signaling capacities and rates of transcription and translation of ARFs. In *Arabidopsis*, DR5 activity can be quantified in transgenic *DR5rev:GFP*, *DR5rev:3xVENUS-N7* and *DR5:Lucifesrase* lines by the analysis of digital images based upon which fluorescence and luciferase signals can be quantified by measuring the analog-digital units (ADU) per pixel using image analysis software (Brunoud et al., 2012; Moreno-Risueno et al., 2010). However, the DR5 reporter does not reflect endogenous auxin concentration in tissue profiles in plants and so far no maker line has been created to evaluate the endogenous IAA status.

The segmentation clock in animals

In segmented animals, such as vertebrates, annelids, and arthropods, body segments are generated sequentially from the presomitic mesoderm (PSM) during somitogenesis (Chipman et al., 2004; Dray et al., 2010; Pueyo et al., 2008; Stollewerk et al., 2003). The segmentation clock and the root clock share the identical mechanism involving a biological clock that periodically convert a temporal signal into a repetitive spatial pattern during sequential organ formation. At the transcriptional level, this process is both controlled by two sets of oscillating genes, in-phase and anti-phase genes, which behave in an opposite way and are required for root clock in plants and segmentation clock in animals.

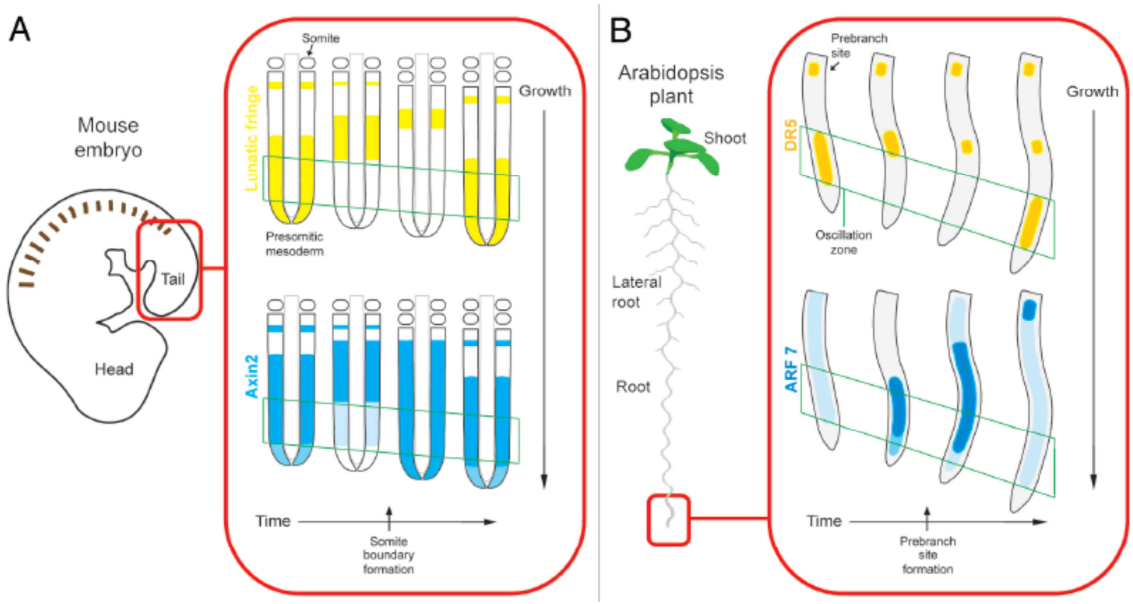

Figure 1. Comparison of the expression patterns of the oscillating genes in the vertebrate segmentation clock in mouse embryo (A) and in the root clock in *Arabidopsis* (B). Both the presomitic mesoderm and the primary root elongate from top to bottom in this schematic, as indicated by the arrow, while gene expression propagates in the opposite direction over time (as depicted from left to right). Gene expression oscillations in two opposite phases occur at the peak of the respective oscillations in the oscillation zones (green frames) as represented by Lunatic fringe (yellow) and Axin2 (blue) in the segmentation clock (A) and by the marker gene DR5 (yellow) and Auxin Response Factor 7 (ARF 7) (Blue) in the root clock (B). (Adapted from Moreno-Risueno and Benfey, 2011)

In animals, the segmentation clock is mainly regulated by three different signaling pathways: Notch, β-catenin/Wnt and Fibroblast Growth Factor (FGF). The Notch and FGF pathway genes oscillate in the same phase, whereas the β-catenin/Wnt pathway genes oscillate in the opposite phase. In plant model *Arabidopsis*, thousands genes were identified as oscillating in-phase or anti-phase. Among them, only few genes were identified to known pathways such as the auxin related pathways, while most of genes have not yet been assigned to any determined signaling pathway. For instance, in *Arabidopsis*, the auxin response maker *DR5* is found to be synchronized with the oscillation of gene expression in the oscillation zone (OZ). The expression of *DR5* starts at the beginning of the OZ close to the root tip, increases over time and moves further from the root tip. When the DR5 signal leaves the OZ, the expression of *DR5* remains static in the prebranch sites. Subsequently, a new cycle of *DR5* oscillation occurs again in the OZ following the primary root elongation. By contrast, expression of *ARF7* in the OZ decreases when the pulse of *DR5* signal rises, and goes up when *DR5* signal is reduced (Fig.1). Interestingly, this opposite expression pattern of *DR5* and *ARF7* in the OZ is similar to that of some oscillating genes identified in the mouse segmentation clock, such as Lunatic fringe (Lfng) and Axin2 (Fig.1) (Dequeant et al., 2006; Moreno-Risueno et al., 2010).

Interestingly, during mouse somitogenesis, Wnt signaling has been implicated in both the segmentation clock and gradient mechanisms (Morimoto et al., 2005; Saga et al., 1997). The establishment of the Wnt/FGF gradient requires a β-catenin protein gradient in the posterior presomitic mesoderm (PSM). This gradient of β-catenin acts downstream of the clock oscillations, and defines the size of the oscillatory field and controls key aspects of PSM maturation and segment formation (Aulehla et al., 2008). Remarkably, the oscillation periodicity is independent of beta-catenin protein levels, whereas the signal intensity and the amplitude of the oscillations is dependent on the presence of high and steady nuclear β-catenin levels (Aulehla et al., 2008). Accordingly, in *Arabidopsis*, the carotenoid biosynthesis pathway was shown to moderate the periodicity of the root clock and also the DR5 activity in the oscillation zone, which determine prebranch sites formation (Van Norman et al., 2014).

The role of indole-3-butyric acid (IBA) in *Arabidopsis*

Auxins are phytohormones involved in controlling plant growth and developmental processes, and indole-3-acetic acid (IAA) has been recognized as the major auxin and is used in most physiological studies. In *Arabidopsis*, IAA is mainly synthesized from tryptophan (Trp) via Trp-dependent, or from an indolic Trp precursor via Trp-independent pathways

(Mashiguchi et al., 2011). However, next to IAA, other abundant auxins in plants have been reported. Indole-3-butyric acid (IBA) has long been used as a synthetic compound that induced root initiation, and several lines of evidence prove the existence of native IBA in plants (Blommaert 1954; Epstein et al, 1993; Ludwig-Muller et al, 1993; Schneider et al., 1985; Sutter and Cohen, 1992). For instance, IBA has been shown to be synthesized in vivo by using IAA and other compounds as precursors in maize (put reference here), and IBA could be extracted from all species belonging to the Salix genus (Ludwig-Müller, 2000; William, 1999). In *Arabidopsis*, IBA comprises approximately 25% to 30% of the total free auxin pool in seedlings (Ludwig-Muller et al., 1993). Unexpectedly, more recently, researchers failed to detect the endogenous IBA in *Arabidopsis* (Novak et al., 2012), which might be due to the very low level of free IBA below detection limit, or still uncharacterized metabolism pathways for IBA in *Arabidopsis*.

Genetic evidence showed that IBA is converted to active indole-3-acetic acid (IAA) in peroxisomes by a process similar to fatty acid β-oxidation (Strader et al., 2010; Zolman et al., 2000). In contrast, IBA transport in vivo is independent of IAA, and facilitated by PLEIOTROPIC DRUG RESISTANCE8 (PDR8)/PENETRATION3/ABCG36 and PDR9/ABCG37 (Liu et al., 2012; Rashotte et al., 2003; Ruzicka et al., 2010; Strader and Bartel, 2009, 2011; Tognetti et al., 2010). As IBA serves as an auxin precursor, it is shares functionality with IAA during plant development. It has been demonstrated that the endogenous IBA-to-IAA conversion is required for proper root growth, such as the root hair elongation and lateral root formation (De Rybel et al., 2012; Strader et al., 2010). Most of the fatty acid β-oxidation enzymes and IBA efflux carriers are located in the root cap cells in the root tip, suggesting the important role of IBA-response on root development.

Several questions remain unanswered, including how, when, and where IBA is synthesized, whether IBA can serve as a signaling molecule on its own, what components regulate IBA distribution in roots, and how IAA derived from IBA in the root cap contributes to the patterning of the root system. For the latter, we hope that the present thesis represents a step forwards towards a better understanding.

References

Aulehla A., Wiegraebe W., Baubet V., Wahl M.B., Deng C., Taketo M., Lewandoski M., Pourquie O. (2008) A beta-catenin gradient links the clock and wavefront systems in mouse embryo segmentation. Nature Cell Biology *10*, 186-193.

Blommaert K. (1954) Growth- and inhibiting-substances in relation to the rest period of the potato tuber. Nature *174*, 970-972.

Brunoud G., Wells D.M., Oliva M., Larrieu A., Mirabet V., Burrow A.H., Beeckman T., Kepinski S., Traas J., Bennett M.J., Vernoux T. (2012) A novel Aux/IAA-based sensor provides a high-resolution spatio-temporal map of auxin response and distribution during plant development. Nature *482*, 103–106.

Chipman, A.D., Arthur, W., and Akam, M. (2004). A double segment periodicity underlies segment generation in centipede development. Current biology : CB *14*, 1250-1255.

De Rybel, B., Audenaert, D., Xuan, W., Overvoorde, P., Strader, L.C., Kepinski, S., Hoye, R., Brisbois, R., Parizot, B., Vanneste, S., *et al.* (2012). A role for the root cap in root branching revealed by the non-auxin probe naxillin. Nature chemical biology *8*, 798-805.

Dequeant, M.L., Glynn, E., Gaudenz, K., Wahl, M., Chen, J., Mushegian, A., and Pourquie, O. (2006). A complex oscillating network of signaling genes underlies the mouse segmentation clock. Science *314*, 1595-1598.

Dray, N., Tessmar-Raible, K., Le Gouar, M., Vibert, L., Christodoulou, F., Schipany, K., Guillou, A., Zantke, J., Snyman, H., Behague, J., *et al.* (2010). Hedgehog signaling regulates segment formation in the annelid Platynereis. Science *329*, 339-342.

Epstein E, Ludwig-Müller J. (1993). Indole-3-butyric acid in plants: occurrence, synthesis, metabolism, and transport. Physiol Plant *88*, 382-389

Liu, X., Barkawi, L., Gardner, G., and Cohen, J.D. (2012). Transport of indole-3-butyric acid and indole-3-acetic acid in *Arabidopsis* hypocotyls using stable isotope labeling. Plant physiology *158*, 1988-2000.

Ludwig-Müller J. (2000) Indole-3-butyric acid in plant growth and development. Plant Growth Regulation. *32*, 2-3.

Ludwig-Muller J, Sass S, Sutter E, Wodner M, Epstein E (1993) Indole-3-butyric acid in *Arabidopsis thaliana*. J Plant Growth Regul *13***,** 179–187

Mashiguchi, K., Tanaka, K., Sakai, T., Sugawara, S., Kawaide, H., Natsume, M., Hanada, A., Yaeno, T., Shirasu, K., Yao, H., *et al.* (2011). The main auxin biosynthesis pathway in *Arabidopsis*. Proceedings of the National Academy of Sciences of the United States of America *108*, 18512-18517.

Moreno-Risueno, M.A., and Benfey, P.N. (2011). Time-based patterning in development: The role of oscillating gene expression. Transcription *2*, 124-129.

Moreno-Risueno, M.A., Van Norman, J.M., Moreno, A., Zhang, J., Ahnert, S.E., and Benfey, P.N. (2010). Oscillating gene expression determines competence for periodic *Arabidopsis* root branching. Science *329*, 1306-1311.

Morimoto, M., Takahashi, Y., Endo, M. & Saga, Y. (2005). The Mesp2 transcription factor establishes segmental borders by suppressing Notch activity. Nature *435*, 354-359

Novak, O., Henykova, E., Sairanen, I., Kowalczyk, M., Pospisil, T., and Ljung, K. (2012). Tissue-specific profiling of the *Arabidopsis* thaliana auxin metabolome. The Plant journal : for cell and molecular biology *72*, 523-536.

Pueyo, J.I., Lanfear, R., and Couso, J.P. (2008). Ancestral Notch-mediated segmentation revealed in the cockroach Periplaneta americana. Proceedings of the National Academy of Sciences of the United States of America *105*, 16614-16619.

Rashotte, A.M., Poupart, J., Waddell, C.S., and Muday, G.K. (2003). Transport of the two natural auxins, indole-3-butyric acid and indole-3-acetic acid, in *Arabidopsis*. Plant physiology *133*, 761-772.

Ruzicka, K., Strader, L.C., Bailly, A., Yang, H., Blakeslee, J., Langowski, L., Nejedla, E., Fujita, H., Itoh, H., Syono, K., *et al.* (2010). *Arabidopsis* PIS1 encodes the ABCG37 transporter of auxinic compounds including the auxin precursor indole-3-butyric acid. Proceedings of the National Academy of Sciences of the United States of America *107*, 10749-10753.

Saga, Y., Hata, N., Koseki, H. & Taketo, M. M. Mesp2: a novel mouse gene expressed in the presegmented mesoderm and essential for segmentation initiation. Genes Dev. 11, 1827–1839

Scheres, B., Benfey, P., and Dolan, L. (2002). Root development. The *Arabidopsis* book / American Society of Plant Biologists *1*, e0101.

Schneider, E.A., Kazakoff, C.W., and Wightman, F. (1985). Gas chromatography-mass spectrometry evidence for several endogenous auxins in pea seedling organs. Planta *165*, 232-241.

Stollewerk, A., Schoppmeier, M., and Damen, W.G. (2003). Involvement of Notch and Delta genes in spider segmentation. Nature *423*, 863-865

Strader, L.C., and Bartel, B. (2009). The *Arabidopsis* PLEIOTROPIC DRUG RESISTANCE8/ABCG36 ATP binding cassette transporter modulates sensitivity to the auxin precursor indole-3-butyric acid. The Plant cell *21*, 1992-2007.

Strader, L.C., and Bartel, B. (2011). Transport and metabolism of the endogenous auxin precursor indole-3-butyric acid. Molecular plant *4*, 477-486.

Strader, L.C., Culler, A.H., Cohen, J.D., and Bartel, B. (2010). Conversion of endogenous indole-3-butyric acid to indole-3-acetic acid drives cell expansion in *Arabidopsis* seedlings. Plant physiology *153*, 1577-1586.

Sutter, E.G., and Cohen, J.D. (1992). Measurement of indolebutyric Acid in plant tissues by isotope dilution gas chromatography-mass spectrometry analysis. Plant physiology *99*, 1719-1722.

Tognetti, V.B., Van Aken, O., Morreel, K., Vandenbroucke, K., van de Cotte, B., De Clercq, I., Chiwocha, S., Fenske, R., Prinsen, E., Boerjan, W., *et al.* (2010). Perturbation of indole-3-butyric acid homeostasis by the UDP-glucosyltransferase UGT74E2 modulates *Arabidopsis* architecture and water stress tolerance. The Plant cell *22*, 2660-2679.

Ulmasov, T., Murfett, J., Hagen, G., and Guilfoyle, T.J. (1997). Aux/IAA proteins repress expression of reporter genes containing natural and highly active synthetic auxin response elements. The Plant cell *9*, 1963-1971.

Van Norman, J.M., Xuan, W., Beeckman, T., and Benfey, P.N. (2013). To branch or not to branch: the role of pre-patterning in lateral root formation. Development *140*, 4301-4310.

Van Norman J. M., Zhang J., Cazzonelli C. I., Pogson B. J., Harrison P. J., Bugg T. D., Chan K.X , Thompson A.J., Benfey P.N. (2014). Periodic root branching in *Arabidopsis* requires synthesis of an uncharacterized carotenoid derivative. Proceedings of the National Academy of Sciences of the United States of America *111*, 1300-1309

William G.H. (1999) Introduction to plant physiology. John Wiley & Sons, Inc., New York City, New York

Zolman, B.K., Yoder, A., and Bartel, B. (2000). Genetic analysis of indole-3-butyric acid responses in *Arabidopsis* thaliana reveals four mutant classes. Genetics *156*, 1323-1337

To branch or not to branch: the role of pre-patterning in lateral root formation

Adapted from:

Van Norman, J.M., **Xuan, W.**, Beeckman, T., and Benfey, P.N. (2013). To branch or not to branch: the role of pre-patterning in lateral root formation. Development *140*, 4301-4310.

Abstract

The establishment of a pre-pattern or competence to form new organs is a key feature of the post-embryonic plasticity of plant development. The elaboration of pre-patterns leads to remarkable heterogeneity in plant form. In root systems, many of the differences in architecture can be directly attributed to the outgrowth of lateral roots. In recent years, efforts have focused on understanding how the pattern of lateral roots is established. Here, we review recent findings that point to a periodic mechanism for establishing this pattern, as well as roles for plant hormones, particularly auxin, in the earliest steps leading up to primordium development. In addition, we compare the development of lateral root primordia with *in vitro* plant regeneration and discuss possible common molecular mechanisms.

Introduction

The post-embryonic formation of lateral organs in plants occurs when cells acquire a new fate, generally based on positional cues, and then undergo a coordinated program of cell division and differentiation to produce an organ primordium. In the root, lateral branches are formed primarily from cells of the pericycle (see Glossary, Box 1), which is an internal tissue surrounding the central vascular cylinder (Fig. 1). On a regular basis, subsets of pericycle cells become competent to form lateral roots (LRs, see Glossary, Box 1) and, depending on the species, this occurs in proximity of phloem (e.g. in maize) or protoxylem strands (e.g. in *Arabidopsis thaliana*) (Casero et al., 1995; Dubrovsky et al., 2000; Hochholdinger and Zimmermann, 2008). The frequency of these events establishes the number of sites competent to form LRs over time and is, therefore, crucial in shaping the final root system architecture, which is a major determinant of agronomic productivity. After competence is established, the development of a lateral root primordium (LRP, see Glossary, Box 1) occurs either strictly through division of cells derived from the pericycle (e.g. in *Arabidopsis*), or through division of pericycle-derived cells and recruitment of cells in the adjacent endodermis (e.g. in maize) (Bell, 1970; Hochholdinger and Zimmermann, 2008).

The development of LRP can be induced or repressed in response to environmental conditions and thus provides a mechanism for the plant to cope with changing edaphic conditions (Malamy, 2005). A great number of environmental variables have been shown to influence LRP development. For example, osmotic (drought) stress inhibits developmental progression of early stage LRP (Deak and Malamy, 2005) and activation of the meristem in emerged LRP is blocked by exogenous abscisic acid, a plant hormone involved in stress responses (De Smet et al., 2003). LRP development is also sensitive to the availability of nutrients including growth limiting nutrients such as nitrogen and phosphorous (recently reviewed in (Jones and Ljung, 2012; Lavenus et al., 2013; Peret et al., 2011). While some environmental stimuli have clear involvement in late stage LRP, nitrogen and phosphorous can also act earlier in LRP development (Lima et al., 2010). It is unclear whether environmental stimuli can only influence the developmental progression of sites already established as competent to form an LRP or if lateral root pre-patterning, which has, to date, been shown to be primarily dependent on time (Moreno-Risueno et al., 2010) can also be impacted by environmental cues. Although the final outcome would be similar, more or fewer LRs, the distinction would reflect a difference in the plant's strategy to achieve developmental plasticity under variable conditions. Therefore, understanding the regulation of LR pre-patterning and subsequent primordia development has captured the interest of many plant biologists.

The molecular and cellular mechanisms of LR formation have been most extensively studied in the model plant *Arabidopsis thaliana*. In this species, relatively regular spacing of LRs was reported, with LR placement coinciding with the outside edge of curves along the primary root, particularly when roots show a bending or wavy growth pattern. To understand the basis for this regular branching pattern, it is crucial to understand the earliest developmental events occurring during LR formation. The *Arabidopsis* primary root tip is classically divided into 3 main developmental zones (Fig. 2A) (Dolan et al., 1993). The rootward-most portion of the root tip, the meristematic zone, contains the stem cell niche and cells that are undergoing active proliferation with relatively little expansion. The meristematic zone is occasionally described as having two parts: the basal and apical meristem. The basal meristem is the shootward-most region of the meristem and is also referred to as the transition zone, as cell division rates slow and cells begin to increase in size (Figure 2A). This is followed by the elongation zone: a region where proliferative cell divisions cease and cells undergo rapid and extensive cell elongation, increasing in length by 300% within three hours (Verbelen et al., 2006). Finally cells enter the differentiation zone where they cease growth and the vast majority attain their final size, begin to differentiate, acquiring their specialized

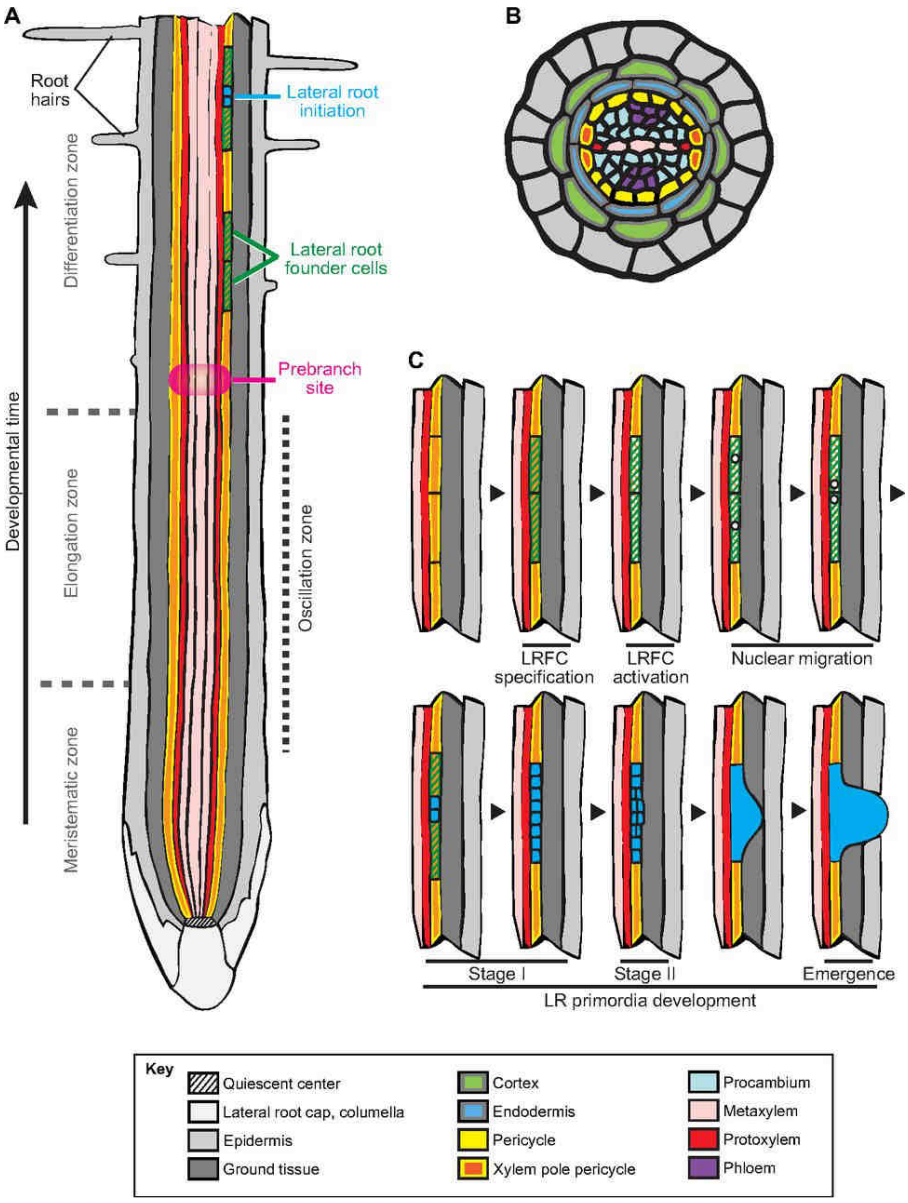

Figure 2. Structure and development of the *Arabidopsis* root. (**A**) Median longitudinal section depicting developmental time (black arrow) in the longitudinal axis. A prebranch site (magenta) forms after an oscillation of gene expression within the oscillation zone (dotted line). Prebranch sites indicate competence to form a lateral root primordium (LRP) in the future. After competence is established, it is predicted that xylem pole pericycle (XPP) cells within a prebranch site can be specified as lateral root founder cells (LRFCs, green hatching). LRP initiate in the differentiation zone through asymmetric cell division of LRFCs, which gives rise to smaller cells (blue). (**B**) Transverse section. Periodic expression of *DR5:GUS* occurs in the protoxylem; however, because lateral root (Choat et al.) initiation occurs in the adjacent XPP cells, signaling between these cell types might be required for LRFC specification. Note that the ground tissue comprises two cell layers: the outermost cortex and the endodermis, which is immediately exterior to the pericycle. (**C**) Cut-away portion of the median longitudinal section focused on a region where an LR will form. XPP cells are predicted to be sequentially specified as LRFCs (green hatching), then activated to undergo cell division (green/white hatching). LRFC activation results in the coordinated migration of nuclei (white circles) towards the common cell wall in a pair of longitudinally abutted cells. These cells then undergo asymmetric division, giving rise to smaller cells (blue), to generate a stage I LRP. The primordium grows through the outer cell layers of the primary root until it emerges from the epidermis. Drawing is not to scale.

cellular features and functions (Figure 2A). Additionally, development of LRP begins in the differentiation zone.

A developing LRP becomes microscopically detectable when a primordium consisting of a single cell layer is generated through asymmetric cell division in the differentiation zone of the root (Fig. 2C) (Malamy and Benfey, 1997). The adjacent pairs of xylem pole pericycle (XPP, see Glossary, Box 1) cells that undergo this cell division, also called LR initiation, are designated as lateral root founder cells (LRFCs, see Glossary, Box 1). Prior to cell division, LRFCs cannot be microscopically distinguished from the other pericycle cells without the use of specific reporter lines. These founder cells first undergo anticlinal cell divisions to generate a single cell-layered primordium containing up to ten small cells (stage I primordium, see Glossary, Box 1). This is followed by periclinal cell divisions in the center-most cells, giving rise to a two cell-layered primordium (stage II primordium, see Glossary, Box 1). Several rounds of division in the central cells lead to an ellipsoid-shaped primordium that eventually grows through the outer cell layers of the parent root and finally emerges from the root surface (Fig. 2C) (Lucas et al., 2013).

Molecular evidence suggests that early events establishing the regular pattern of LRs, prior to LRFC identity and LR initiation, occur at a more root-ward position in the root tip where recurrent expression of reporter constructs driven by the synthetic promoter element DR5 (DIRECT REPEAT5) are observed (De Smet et al., 2007; Moreno-Risueno et al., 2010). DR5 promoter activity, which is used to assay the transcriptional response to auxin, is correlated with subsequent LR initiation, suggesting that an oscillating transcriptional mechanism operates as an upstream driving force for the regular pattern of LRs. Indeed, a large number of genes were identified that oscillate both in phase and in antiphase with the DR5 reporter, although the oscillatory system appears to function independently of local auxin levels (Moreno-Risueno et al., 2010). Furthermore, the 6-hour period of the transcriptional oscillation appears to be shorter than the frequency at which LRs initiate, suggesting that establishment of competence to form a LR and initiation of an LRP are distinct developmental events.

The oscillation in gene expression occurs over a region of the root termed the oscillation zone (OZ, see Glossary, Box 1) (Fig. 2A) (Moreno-Risueno et al., 2010). During the period of the oscillation as many as 12 pericycle cells may exit the OZ (Verbelen et al., 2006), suggesting that several cells may experience the oscillation in gene expression. Yet, generally only pairs of abutted pericycle are specified as LRFCs, suggesting a mechanism exists to refine or restrict the number of pericycle cells that will adopt this fate. At the tissue-specific level, DR5 reporter expression suggested that the oscillatory maximum occurs in the

protoxylem cells adjacent to the pericycle (Fig. 2B). It may, therefore, be that XPP cells receive signals during the oscillation to prepare them for LR initiation, a process that has been termed, priming (see Glossary, Box 1). After the oscillation, a static point of DR5 expression marks pre-branch sites, which are defined as positions competent to produce LRs in the future. Subsequently, auxin signaling-dependent nuclear migration in LRFCs precedes the asymmetric cell divisions that generate stage I primordia.

Hence, the events leading up to and including the specification of LRFCs and LR initiation are crucial for lateral root organogenesis, but many questions surrounding the molecular mechanisms that underlie the earliest stages of lateral root formation remain unanswered. In this review, we focus on these early developmental steps and reflect on the potential mechanisms that contribute to the establishment of the LR distribution pattern, which forms the basis of root system architecture.

Is there a mechanical mechanism involved in establishing the pattern of lateral roots?

Under experimental conditions, *Arabidopsis* roots grow in a serpentine manner, bending from side-to-side as they traverse the culture medium. Root waving has been described as the consequence of differential growth due to re-orientation of growth in the direction of the gravity vector combined with thigmotropic growth (re-orientation based on the touch response, reviewed in (Oliva and Dunand, 2007)). These root growth behaviors are hypothesized to be an evolutionary strategy to facilitate obstacle avoidance under rhizospheric conditions. Accompanying root waving, the development of LRP and the emergence of LRs coincides with the outside edge of these curves (Fortin et al., 1989), suggesting a relationship between the pattern of LRs and root waving.

As root waving results from alternating left- and right-turns by the root tip, the number of outside edges facing towards the left and right is roughly equal. Coincident with the sidedness of the curves, the presence of LRs and LRP is also equal on each side of the root (Fig.3). Furthermore, an agravitropic, auxin transport mutant, *aux1*, which turns in only one direction, shows a shift in LR distribution with more LRs emerging on the outside edge of the coiled root (De Smet et al., 2007). These results suggest that the distribution pattern of LRs is linked with root waving and the gravity response via auxin transport. The co-occurrence of these processes was further investigated by inducing root bending by gravi-stimulation and mechanical methods (Ditengou et al., 2008; Laskowski et al., 2008; Lucas et al., 2008; Richter et al., 2009). Gravi-stimulated bends occur when plants are re-oriented with respect to the gravity vector resulting in a sharp bend as the root tip reorients growth to realign with

gravity. Mechanical bending can be induced through manual manipulation of root or seedling position, growth of the root into a barrier, or through gel sliding assays (Figure 3B-E). Similar to root waving, induction of sharper bends in the root by any method resulted in emergence of LRs at the outside edge of the bends. Intriguingly, LRP develop at the outside edge of a bend even when a root is only transiently bent, however LRP and mechanically-induced bends only coincide when bending occurs a short distance from the root tip (Ditengou et al., 2008; Laskowski et al., 2008; Lucas et al., 2008; Richter et al., 2009).

The molecular link between gravitropism/root waving and LRP development is predicted to be auxin. It was proposed that altered auxin distribution upon root re-orientation is sufficient to establish the pattern of LRs along the root. However, roots that are agravitropic due to defects in auxin signaling or transport or to removal of gravity-sensing tissues still form LRs on the outside of curves, suggesting that gravity response isn't specifically required (Ditengou et al., 2008; Lucas et al., 2008; Richter et al., 2009). Recent observations of roots grown during spaceflight further indicate that the pattern of LRs and gravitropic responses of the primary root are separable; in the micro-*g* environment, roots grow more slowly than those of control plants on Earth (at 1-*g*) but root waving persists and LRs are observed on the outside of curves (Paul et al., 2012). Thus, root waving and the coincidence of LRP with curves occur independent of gravity. These results don't preclude the hypothesis that asymmetric auxin distribution at curves in the root, regardless of its cause, is linked to the development of an LRP.

Indeed, the expression and/or localization of reporters for auxin signaling and transport show rapid changes (observed within 3-7 hours) after the induction of bends, suggesting that mechanical strain on the cells induces changes in auxin distribution and signaling (Ditengou et al., 2008; Laskowski et al., 2008). A computational model was developed whereby the physical deformation of cells upon bending leads to auxin accumulation on the outside of curves, which was suggested to trigger local competence of XPP cells, and then promote the development and emergence of LRP (Laskowski et al., 2008). However, mutants with defects in auxin signaling and/or transport and reduced LR production consistently form LRP or LRs when roots are manually bent (Ditengou et al., 2008; Richter et al., 2009). These results suggest that while the development of LRP may be defective in these mutants, sites competent to form LRP are present. Furthermore, bends induced for very short durations (on the order of 20 seconds) are sufficient to increase the number of LRs observed at the outside of these transient bends. Following these bends, similarly rapid changes in cytosolic Ca^{2+} levels are observed, and treatment with calcium channel blockers inhibited both changes in

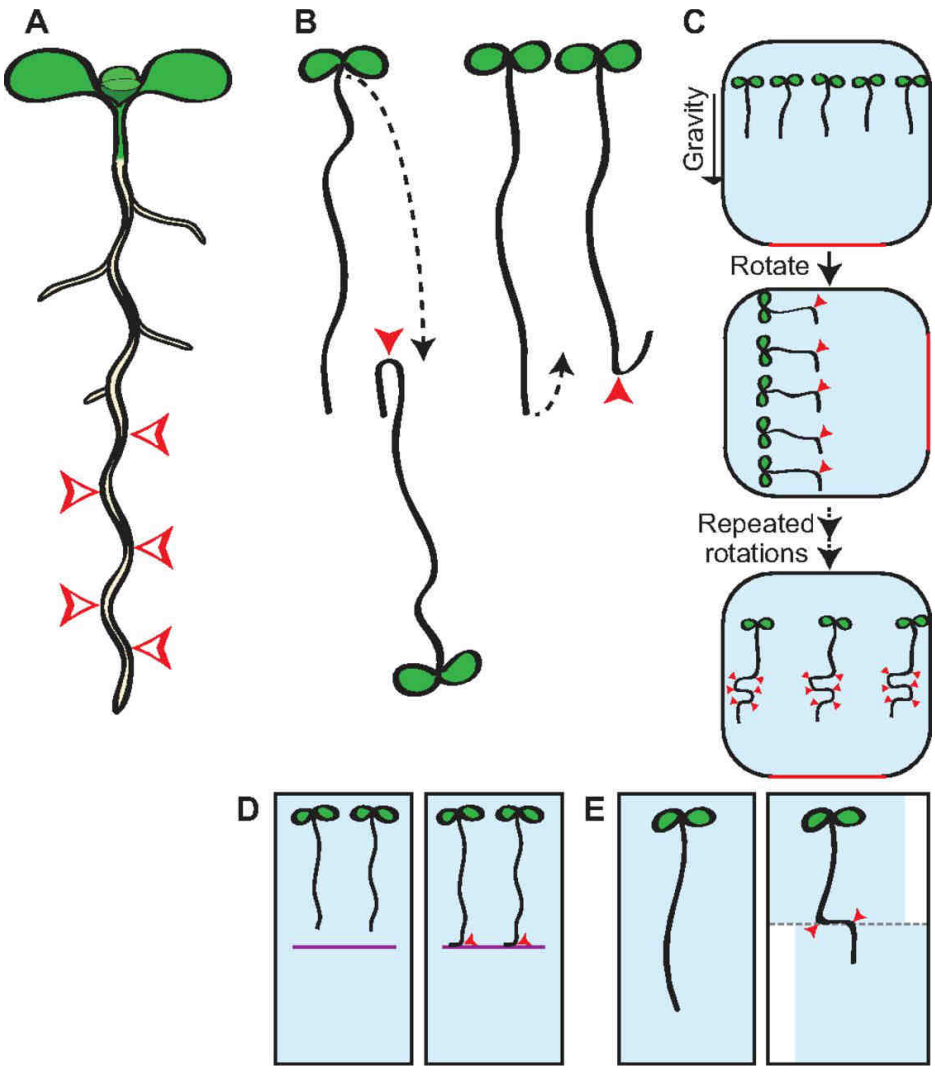

Figure 3. LRs emerge from the outside of curves in the primary root. Schematics of root bends formed under various experimental conditions. (**A**) Root waving occurs as roots grow along the surface of agar plates. LRP develop and eventually emerge from the outside of the curves. The arrowheads indicate positions of incipient LRP. (**B**) Bends can be induced to form in the root through manual manipulation of the seedling either by pulling the shoot downward (left) or by pushing the root tip upward (right). (**C**) Gravistimulation-induced bends. If seedlings are reoriented with respect to the gravity vector, a bend will form as the root tip responds to realign the tip to gravity through differential growth. (**D**) In the absence of gravitropic response in either the root or shoot, a bend can be induced by root growth into a barrier (purple bar). (**E**) Bends can also be induced by cutting the agar on either side of a growing root (gray dotted line) and sliding the agar to one side, thereby creating two bends in the root. In these gel-sliding assays, neither the root tip nor shoot is exposed to manual contact or reorientation. Arrowheads (B-E) indicate the position of LRP emergence in response to induced bends.

cytosolic Ca^{2+} and production of LRP after bending, indicating that Ca^{2+} signaling is required for bend-induced LRP development (Richter et al., 2009). These results suggest that rapid cellular signaling upon bending triggers events that lead to LRP development, prior to changes in cell shape and differential auxin distribution. This implies that events upstream of

signaling can promote LRP development and may indicate that competence to form an LRP is already present at positions of mechanical bending. Alternatively, another interpretation of these results may be that the pattern of LRs is less dependent on developmental pre-patterning and, instead, is a consequence of root growth behaviors.

Nevertheless, evidence for an endogenous pre-patterning mechanism is observed in studies of bend-induced LRP development. Roots subjected to gravistimuli at regular intervals showed a maximum number of LRs when gravistimulation occured at 6-hour intervals. However, LRP formed between the gravity-induced bends when the intervals between gravistimulation were extended to 12- and 24-hours (Lucas et al., 2008). Additionally, removal of the root tip prior to manual bending results in the formation of more LRs between the cut edge and the bent region in both wild type and auxin signaling mutants (Ditengou et al., 2008). These results suggest that the pattern of LRP is established independent of induced bends and indicates that, although a single LR typically emerges at an induced bend, additional nearby sites are competent to develop into LRP. These competent sites may be developmentally stalled by signals from the root tip, by the emerging primordia, or both.

Evidence for an endogenous mechanism in lateral root pre-patterning

An endogenous mechanism for establishing the pattern of LRs was proposed based on a temporal fluctuation in expression of the DR5 reporter. At 15 hour intervals, expression of the DR5 promoter fused to the β-glucuronidase (GUS) reporter gene was observed in the shootward-most portion of the meristematic zone, specifically in the two protoxylem cell files but not in the adjacent XPP cells (Fig. 2B). The longitudinal position of the sites of DR5:GUS expression in the meristem could be correlated with the later development of an LRP (De Smet et al., 2007). Thus, it was suggested that DR5-expressing protoxylem cells signal to adjacent XPP cells to condition them for LRFC identity, a process called priming (see Glossary, Box 1). If the temporal changes in DR5 expression are hypothesized to direct the later formation of an LRP, this recurrent process could explain the regular spacing between LRs under controlled growth conditions. However as DR5 expression occurs in both sets of protoxylem cells, the alternating distribution of LRs on the sides of the root cannot be explained, suggesting that a subsequent mechanism determines LR sidedness (De Smet et al., 2007). For example, the mechanical strain and asymmetric distribution of Ca^{2+} and auxin that is described in cells upon bending occurs in more differentiated regions of the root, therefore it is possible that the sidedness of LR initiation is determined later in response to signals produced as a consequence of changes in cell shape. Expression conferred by the DR5

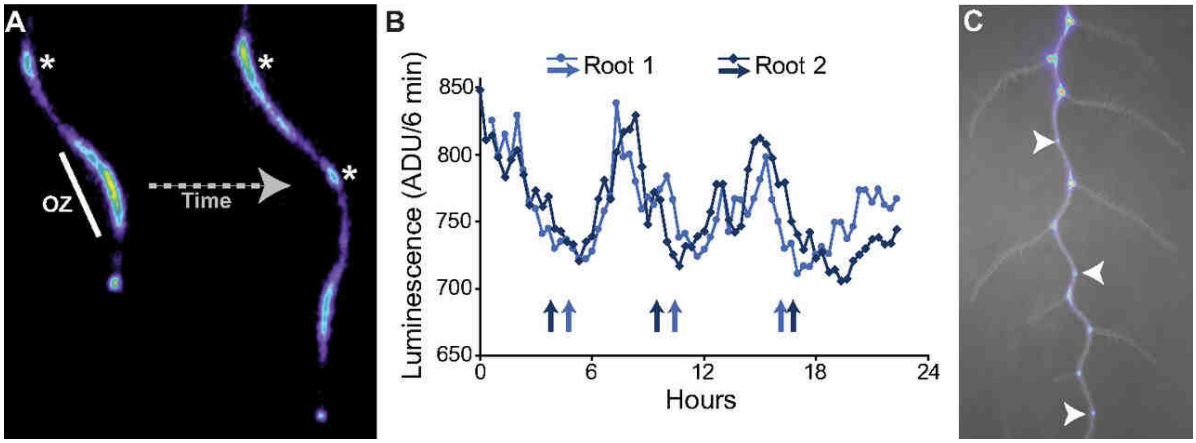

Figure 4. Prebranch sites mark the positions at which LRP will subsequently develop and emerge. (**A**) An oscillation in *DR5:LUC* expression (chemiluminescence signal imaged at 5-6 minute exposure times) in the oscillation zone (OZ) leads to the formation of a prebranch site (asterisk). (**B**) Quantification of the oscillation of *DR5:LUC* expression in two individual roots. The oscillation has a period of ~6 hours and appears to precede the changes in growth direction of the root tip during root waving. Blue/dark blue arrows indicate the time points at which bends were formed in each of the primary roots. ADU, analog-digital units. (**C**) Overlay of a luciferase and brightfield image (taken 5 days after the luciferase image) to show emerged lateral roots. Arrowheads indicate positions at which LRP have yet to emerge. (B,C) Adapted with permission (Moreno-Risueno et al., 2010).

promoter was further examined by fusing it to the Luciferase gene, allowing visualization of its behavior *in vivo* (Moreno-Risueno et al., 2010). Expression of DR5:Luciferase (LUC) in the root tip revealed oscillatory activity with a period of 6 hours. This dynamic expression pattern occurred over a larger region of the root tip than previously described and this region was, therefore, termed the oscillation zone (OZ) (Fig. 4A, B). Following each peak of the DR5 oscillation, a static point of expression was observed, which exhibited a similar longitudinal distribution as LRP and LRs. Indeed, later examination of these points revealed them as the future sites of LRP and LRs, and they were, therefore designated as prebranch sites (see Glossary, Box 1, Fig. 4C) (Moreno-Risueno et al., 2010).

DR5 expression is frequently utilized as a proxy for the distribution of auxin, however an exogenously stimulated peak in auxin levels in the OZ was not able to trigger formation of a prebranch site. Additionally, a reporter gene with similar response dynamics to exogenous auxin as DR5:LUC and expressed in the OZ did not exhibit periodic expression (Moreno-Risueno et al., 2010). These results suggested that oscillatory peaks in auxin itself are not sufficient to account for the dynamic behavior of DR5 and the subsequent formation of prebranch sites. In an effort to determine the underlying cause of the oscillation, microarray analysis of gene expression identified >3400 genes whose expression oscillates either in phase or in antiphase with the DR5 reporter. Several candidate transcriptional regulators were found

to both exhibit oscillatory expression and be functionally important for LR formation (Moreno-Risueno et al., 2010). Although auxin responsive genes do not necessarily show oscillatory expression in the OZ, some oscillating genes have established roles in LR formation and are involved in or downstream of auxin signaling, such as *LATERAL ORGAN BOUNDARIES DOMAIN 16* (*LBD16*) and *AUXIN RESPONSIVE FACTOR 7* (*ARF7*) (Okushima et al., 2007; Okushima et al., 2005). Unexpectedly, *ARF7* was found to oscillate in antiphase to DR5:LUC and in *arf7* mutants the oscillatory expression of DR5:LUC is abnormal and prebranch sites form at irregular intervals, suggesting ARF7 function is important for periodic gene expression in the OZ (Moreno-Risueno et al., 2010). Together these results led to a model describing a lateral root clock, in which a complex periodic transcriptional mechanism specifies sites that are competent to form LRs, thus establishing a LR pre-pattern along the root's axis.

Like the LRs that follow them, prebranch sites are found at curves that are produced during root waving. Although root waving shows a similar periodicity as prebranch site formation, the oscillation of DR5 expression is observed prior to the re-orientation of root growth direction (Moreno-Risueno et al., 2010). This suggests that, despite their occurrence at a similar position along the root, these events are separated by time. The link between bending and prebranch site formation was examined by exposing roots to gravistimuli and manual bending. Roots responded to gravistimulation asynchronously, with individual roots completing the last bend due to root waving prior to re-orienting growth in the direction of the gravity vector, which is consistent with these being distinct growth behaviors. In manual bending assays, prebranch sites were observed at the bend and nearer to the root tip than bends could be made without disrupting the position of the root tip. Manual bending did not result in *de novo* prebranch sites and no LRs emerged from sites not previously marked by a prebranch site; yet, as observed previously, LRP emerged at the outside edge of the bends (Moreno-Risueno et al., 2010). These results are consistent with a hypothesis in which an endogenous patterning mechanism establishes sites competent to form a LR, but LRP development and perhaps sidedness of LRFC specification are subsequent developmental decisions, which integrate multiple cues.

The priming of XPP cells during the oscillation of gene expression in the OZ conceptually links DR5 expression in the protoxylem with later LRP development in the adjacent pericycle. Although priming is thought to be XPP specific, prebranch sites cannot yet be examined at a cellular level for technical reasons (see below). Priming of XPP cells would not be predicted to occur only on one side of the root as DR5 expression is observed at both xylem poles. Additionally, the molecular character of primed XPP cells and the priming

signal remain elusive. An alternative, and not mutually exclusive, hypothesis is that genes oscillating in the pericycle itself may have important roles establishing the LR prepattern. For example, *LBD16* is observed to oscillate and was recently reported to have XPP-specific expression and a key role in LR initiation (Goh et al., 2012; Moreno-Risueno et al., 2010). Because the root tissue examined for oscillating transcriptional profiles was specific to longitudinal regions but encompassed all root tissues, the tissue-specific nature of any oscillating transcripts was not captured (Moreno-Risueno et al., 2010). The necessity for vascular continuity between primary and lateral roots may be a crucial reason for coordination between vascular patterning and LR pre-patterning, and this is supported by additional connections between vascular patterning and the development of LRP (Bonke et al., 2003; Ohashi-Ito and Bergmann, 2007; Parizot et al., 2008). However, the role of cell-to-cell signaling between protoxylem and XPP cells is an intriguing question requiring further investigation.

Lateral root founder cells and prebranch sites

Organogenesis is generally thought to begin with the specification of founder cells (FCs). This specification could involve cells acquiring competence to respond to an activation signal. Activation of FCs typically leads to cell division, which is the first morphological indication that a change in cell fate has occurred. However, prior to activation of cell division, the identification of FCs is difficult as they are histologically indistinguishable from the surrounding cells. Another difficulty is that there are few molecular reporters for FCs, and for those markers that are available, the function of the associated molecules in FC specification, activation or cell division is not entirely clear (Beveridge et al., 2007; Chandler, 2011). These general FC features are also true for lateral root founder cells (LRFCs).

LRFCs are the specific XPP cells that will undergo asymmetric cell division (LR initiation) to produce a stage I LRP. The specification and activation of LRFCs is thought to occur within the differentiation zone of the root, where other cells have ceased division and growth and have become differentiated. However, it is unclear if XPP cells dedifferentiate then re-differentiate into LRFCs, or if they are maintained in an undifferentiated state (Dubrovsky et al., 2000; Laskowski et al., 1995; Malamy and Benfey, 1997). Expression of the DR5:GFP reporter is observed in select XPP cells and precedes LR initiation. Therefore, activation of DR5 expression is considered the first indication that specific XPP cells have acquired LRFC identity (Dubrovsky et al., 2008). Additionally, *aberrant lateral root formation 4 (alf4*) mutants, show DR5:GFP expression in select XPP cells, yet LRP are not

produced as a result of defects in cell division (DiDonato et al., 2004; Dubrovsky et al., 2008). This suggests that *alf4* LRFC are either specified but not activated or are both specified and activated, but cannot undergo cell division to produce a stage 1 LRP. Because DR5:GFP expression precedes LRFC cell division, and pericycle cells appear to be uniformly sensitive to exogenous auxin, it was proposed that local auxin accumulation, rather than increased auxin sensitivity, triggers LRFC specification (Dubrovsky et al., 2008). In addition, one of the first anatomical signs that XPP cells have taken on LRFC fate is the coordinated migration of the nuclei towards the common wall in a pair of cells, however by this point LRFC specification and activation have already occurred, as cell division is imminent (De Rybel et al., 2010; Dubrovsky et al., 2011).

Recent evidence shows that the developmental progression of LRFCs to stage I LRP requires activity of the auxin transporter PIN3 in endodermal cells, which are adjacent to the pericycle cells (Fig 2B). However, LRFCs exhibit DR5:GFP expression prior to PIN3 accumulation in endodermal cells, suggesting that LRFC fate has already been specified (Marhavy et al., 2013). Accumulation of auxin in specific cells requires either directed transport or intracellular biosynthesis, with cellular retention of auxin. Either scenario requires that these select XPP cells attain higher auxin levels, suggesting they may already be distinct from other XPP cells prior to detection of DR5:GFP reporter expression. Thus, in contrast to the proposed role for auxin as a signal in LRFC specification, it may be that auxin acts as an activation signal of LRFC cell division. Based on this hypothesis, it is possible that in *alf4* mutants, LRFCs are specified and receive the activation signal (as visualized by DR5:GFP expression) but, due to mitotic defects, are unable to undergo coordinated cell division. Additionally, *ALF4* expression and protein localization appear to be independent of auxin signaling (DiDonato et al., 2004), suggesting that additional activation signals may exist.

Prebranch sites are the static points of DR5:LUC expression that form at the position of the peak in the periodic oscillation of DR5 after the oscillation is complete (Moreno-Risueno et al., 2010). Expression of DR5, as reported by GFP, is observed in XPP cells at one side of the xylem pole prior to the asymmetric division that gives rise to an LRP, identifying these cells as LRFCs (Dubrovsky et al., 2008). Because the expression of DR5 is used to define both of these terms, they might be considered synonymous. However, it is important to keep in mind the difference between the reporter genes, LUC and GFP. The LUC enzyme cleaves its substrate (luciferin), thereby producing light, and it then becomes inactive. Thus, while monitoring LUC activity is a highly dynamic and sensitive method to assay the *in vivo* activity of a promoter (de Ruijter N.C.A., 2003), it is difficult to obtain cell type-specific

resolution, as light spreads outward in all directions from the source. GFP expression, however, can be localized in a cell type-specific manner using confocal microscopy, although the drawbacks of GFP are long maturation and stability times, higher thresholds for detectability, and a relatively high background fluorescence in plants (de Ruijter N.C.A., 2003). Because the static points of DR5:LUC expression are visible earlier than expected for LRFCs, and because it is not yet possible to determine which cell type the LUC activity originates from or if it is localized to one side of xylem pole, it is not appropriate to describe these points of DR5:LUC expression as LRFCs (Moreno-Risueno et al., 2010). Prebranch sites may indeed be LRFCs that are visible at an earlier time due to the higher sensitivity of LUC. Alternatively, they may indicate a broader, competent site from which specification of a restricted number of XPP cells into LRFCs will subsequently occur specifically at one side of the root.

A developmental window for founder cell identity and the first formative division to produce LRP

LRFC identity has been associated with an increase in the transcriptional response to auxin in select XPP cells briefly before they undergo asymmetric cell division (Benkova et al., 2003; Dubrovsky et al., 2008). The time lag between the DR5:GFP expression in LRFCs and LR initiation is extremely short and, consequently, both events are observed in the same region of the root, namely the early differentiation zone (Fig. 2A) (Dubrovsky et al., 2011). Monitoring auxin response and distribution along the entire *Arabidopsis* primary root revealed a region with low auxin response and levels that was positioned between two distinct auxin maxima: one at the very tip of the root, including the QC and meristematic zone, and a second in the vascular bundle of mature tissue in the shootward-most regions of the root. The region of “auxin minimum” was somewhat paradoxically found to overlap with that in which increased auxin response (as assayed by induction of DR5:GFP expression) in LRFCs and LR initiation occur. Therefore, this region was proposed as the developmental window for LR initiation.

The developmental window is somewhat dynamic, shifting in the direction of the root apex as the root grows thereby guaranteeing a rootward sequence of LR production under controlled growth conditions (Dubrovsky et al., 2006). In this region of lower auxin levels and response, cell- and tissue-specific auxin distribution and TIR1/AFB-dependent auxin signaling modules result in the induction of auxin-responsive genes, such as *GATA23* and *LBD16,* and the subsequent activation of LRFCs to undergo nuclear migration and

asymmetric cell division (De Rybel et al., 2010; Goh et al., 2012). Downstream of the TIR1/AFB auxin receptor proteins, a family of transcriptional repressors AUXIN/INDOLE-3-ACETIC ACID INDUCIBLE (AUX/IAA) proteins are degraded upon auxin perception leading to auxin-induced gene expression (reviewed in (Chapman and Estelle, 2009). In *iaa28*, a gain-of-function mutant, in which the IAA28 protein is stabilized thus suppressing auxin response, nuclear migration is interrupted, leading to inhibition of LRFC activation and a substantial decrease in LR formation (De Rybel et al., 2010). Similarly when *LBD16*, a downstream target of auxin signaling but whose specific function in LR formation remains unknown, is repressed nuclear migration in LRFCs is disrupted, thereby blocking the subsequent initiation of LRs (Goh et al., 2012). Likewise, disrupting polar auxin transport genetically or through chemicals alters auxin distribution in this region and inhibits lateral root initiation (Dubrovsky et al., 2011; Marhavy et al., 2013). The occurrence of these auxin response-maximum driven processes within a region of generally low auxin levels is intriguing and suggests that cells in this region may have enhanced responses to minor fluctuations in endogenous auxin availability. In such an environment, a subset of XPP cells could register local changes in auxin levels providing a signal for developmental progression towards LR initiation, a situation that may not be possible in conditions of high auxin levels.

As opposed to auxin, cytokinins were identified as endogenous suppressors of LR formation. Their inhibitory mode of action was attributed to hindrance of polar auxin transport, which could disturb local auxin distribution patterns and auxin signaling pathways (Benkova et al., 2003; Laplaze et al., 2007; Li et al., 2006). More recently, however, cytokinin response, as monitored by a cytokinin-sensitive sensor (the TCS reporter), in the developmental window was shown to be minimal, although no decrease in active cytokinin levels could be measured within this region of the root (Bielach et al., 2012). Furthermore, exogenous cytokinin failed to induce expression of the TCS reporter, indicating that strong repression of cytokinin signaling is at play in the developmental window and might be an important component for LR initiation. Categorizing the effects of increased cytokinin levels on LR formation either by endogenous expression of cytokinin biosynthesis genes, or by exogenous cytokinin treatment, demonstrated that the early phases of LR formation including the pre-mitotic stages are more sensitive to cytokinin than are the later stages of LRP development. It was suggested that in the developmental window where auxin levels are low, ectopic cytokinin levels are more disruptive to early stage LRP, whereas in more developed primordia, auxin levels are more robust, thus diminishing the impact of cytokinins (Bielach et al., 2012).

Conclusion

During recent years and thanks to the development of novel reporter lines in *Arabidopsis*, insight has been gained into the "invisible phase" of LR formation, namely the events that precede the first asymmetric cell divisions in LRFCs. The uncovering of previously unknown developmental steps has pushed researchers to formulate new concepts so that results obtained by different research groups working on lateral roots can be compared. In this Review, we aim to provide a solid foundation for the coming years during which exciting new insights are expected to surface. We have summarized recent published work on pre-patterning mechanisms in the root, which consist of two important developmental steps: 1) a periodic oscillation of gene expression that triggers competence for LR formation; and 2) the perception of an auxin signal in founder cells to set up LR initiation in the developmental window, a region of the root in which the integration of auxin and cytokinin signaling occurs. However, many questions remain unanswered.

We still lack cellular resolution of the oscillatory gene expression process. The current cellular information from the DR5:GUS reporter implies that signaling from the adjacent vasculature to the XPP cells is important for LRFC specification. However, it is unclear what the identity of such a signal might be and when (in the OZ or later) this signal would be transmitted to the XPP. Because there doesn't appear to be a sidedness to the oscillation in DR5 or endogenous genes, how LR sidedness occurs remains to be determined but signals from the cells exterior to the pericycle upon cellular deformation may be involved. Finally, whether so-called priming signals and the cues that determine sidedness are distinct and sequential remains to be established. Once LRFCs become observable by reporter expression or nuclear migration, asymmetric cell division quickly follows. However, as the positional information transmitted by the oscillation of gene expression occurs earlier, XPP cells may undergo a change in state that we are, as yet, unable to detect. A delay between competence and LRFC specification and activation would further increase the developmental plasticity of the root system by providing another "check-point" for the developmental progression of organogenesis in the root.

Pre-patterning for LR formation is likely to be an example of the trade-off between resource investment and response time during plant development. Unlike animals, plants continually produce new organs in response to environmental cues. One option for a plant would be to wait for the cue and then begin the process of organ formation *de novo*. The obvious downside to this strategy is that the conditions that triggered the response might be short-lived. To reduce response time, plants have instead adopted a strategy of commencing

organ formation, then arresting it at various stages of development. An example is apical branch formation, in which branch points are positioned through phyllotaxis, and primordia are initiated then arrested until the appropriate signal is received. The oscillatory gene expression process that establishes a LR pre-pattern of prebranch sites can be thought of as the equivalent of phyllotaxis, leading to priming of select XPP cells, which then await a signal to form a lateral root primordium.

The presence of pre-patterning mechanisms implies the continuous production of organogenesis-competent cells during root growth. In contrast to this idea, organogenesis during plant regeneration from callus was thought to rely on *de novo* dedifferentiation of mature cells. However, recent comparative analyses of LR and callus formation have revealed clear and striking similarities. One important similarity is the requirement of high hormone levels for induction. In the LRIS (Box 2), the transportable synthetic auxin analogue NAA is applied to seedlings at ~4x the concentration at which the non-transportable analogue 2,4-D is applied to explants in the CIM (Atta et al., 2009; Himanen et al., 2002; Valvekens et al., 1988). However, treatment of root explants with the amount of 2,4-D in CIM or of NAA in the LRIS results in comparable gene expression patterns, indicating that these two treatments induce a similar response (Sugimoto et al., 2010). Unexpectedly, root explants treated with high cytokinin levels or whole seedlings sequentially treated with NAA and cytokinin-enriched media are able to form shoot tissue at early stage LRP, suggesting flexibility in the developmental potential of LRP (Atta et al., 2009; Chatfield et al., 2013). These results suggest that, while the program for callus formation and its initial steps are similarly executed under various hormonal conditions, the formation of root or shoot tissue from callus or early LRP depends on hormonal context.

The comparison between the induction of LR and callus development also revealed that the XPP cells in the root and XPP-like cells in the shoot are unique among cell types in their ability to divide and from new structures/organs in differentiated tissues. Root pericycle cells at poles of either the xylem or phloem are further delineated in that they have distinct cellular morphology, transcriptional profiles, and are the cells of origin for LRP (Brady et al., 2007; Jansen et al., 2012; Laskowski et al., 1995; Malamy and Benfey, 1997). In the *Arabidopsis* shoot, the XPP-like, callus-forming cells are similar to root XPP cells in that they share marker gene expression and are associated with the vasculature, although up to now this shoot tissue has not been specifically defined as XPP (Sugimoto et al., 2010). Given that they are the cells of origin for callus formation from both root and shoot tissues, the meristematic potential and properties of XPP and XPP-like cells has been greatly expanded. Perhaps the structural and molecular similarities, and the notion of a common cell of origin, between LRP

and callus development indicate a common evolutionary origin. Given that hormonal context is a key aspect of determining which type of organ is formed by callus or early LRP, the possibility that LR development is an evolutionary offshoot of regeneration may be a viable hypothesis. In this context, the establishment of a LR pre-pattern may function to confine the meristematic potential of the XPP to specific sites.

What was once considered a largely random event primarily refined by lateral inhibition, lateral root formation is now revealed as a complex developmental process underpinned by a dynamic spatiotemporal pre-patterning mechanism. Advances in methods to interrogate cellular gene expression at finer resolution and the development of dynamic, cell-type specific reporter proteins will be key tools in future studies.

Box 1: Glossary

Oscillation zone (OZ) – The region in which periodic oscillation of the DR5:Luciferase reporter and expression of certain endogenous genes occurs. This region encompasses the shootward-most portion of the meristematic zone, as well as the elongation zone (Figure 2A) (Moreno-Risueno et al., 2010).

Pericycle – A cell layer located between the vascular cylinder and the ground tissue (Figure 2B). Like the vascular tissues, the pericycle has a bilaterally symmetric organization.

Xylem pole pericycle (XPP) – Cells of the pericycle that flank the protoxylem cells (Figure 2B). Xylem pole pericycle cells have distinct cellular morphology, gene expression profiles and the unique capacity within the differentiation zone to re-enter the cell cycle and undergo cell division. Xylem pole pericycle cell division is required for lateral root initiation, as well as for regeneration via callus.

Priming – a process that occurs in select xylem pole pericycle cells, which is proposed to coincide with the oscillation of gene expression. Priming is predicted to condition these cells for subsequent prebranch site and lateral root founder cell specification.

Prebranch site – Static points of DR5:Luciferase expression that occur following the oscillation of DR5:Luciferase in the oscillation zone. Prebranch sites are competent to form lateral roots in the future. Because these sites occur earlier than expected for lateral root founder cells and it hasn't been determined if expression is cell type specific, the relationship between prebranch sites and lateral root founder cells is unclear.

Founder cells – Founder cells are the initial cells specified to become a new organ or tissue. Founder cells are typically histologically similar to related/nearby cells and can only be

identified following other developmental events, such as the activation of cell division(Beveridge et al., 2007; Chandler, 2011).

Lateral root founder cells (LRFC) – A set of two longitudinally abutted cells in each of the 2-3 cell files of the xylem pole pericycle at one side of the root. These cells will undergo asymmetric cell divisions (also called formative divisions) to initiate a lateral root primordium. The first morphological indicator that these cells have a distinct fate is the migration of their nuclei towards the common cell wall. Additionally, expression of DR5:GFP and gLBD16:GFP is induced in these cells prior to asymmetric cell division(Dubrovsky et al., 2008; Goh et al., 2012).

Lateral root primordia (LRP) – A group of cells originating from asymmetric division of lateral root founder cells that progress through a stereotypical set of developmental stages to produce a root *de novo.*

Stage I lateral root primordium – A lateral root primordium comprised of a single cell layer and the first stage of lateral root primordia development. Initially this structure is comprised of two small cells resulting from asymmetric division of the lateral root founder cells, however successive divisions result in a group of 4-10 small longitudinally abutted cells.

Stage II lateral root primordium – Following radial expansion, the cells of the Stage I primordium reorient their division plane, dividing periclinally to the root's longitudinal axis, resulting in a primordium comprised of two cell layers.

Lateral root (Choat et al.) – A root that is branching from a parent root and has activated its apical meristem. In most plants, these organs are formed postembryonically.

Lateral root prepattern – The specification of a spatio-temporal region of the root that is competent to give rise to a lateral root primordium. The lateral root prepattern is predicted to be established by periodic gene expression in the oscillation zone and the formation of prebranch sites. Establishment of the prepattern is stable under various environmental conditions.

Lateral root formation – A term encompassing all of the events leading to the production of an actively growing lateral root.

Lateral root development – A term without a clear and accepted definition. This term can be used to encompass all the developmental stages of a lateral root primordium (from stage I-VII) and is more clearly stated as "lateral root primordium development". The progression of any one lateral root primordium through the developmental stages is impinged upon by environmental cues.

Box 2: The lateral root inducible system

As initiation of an LRP involves few cells and is not coordinated in space or time between seedlings, the use of genome-wide approaches has been challenging. To address this, a method termed the Lateral Root Inducible System (LRIS) was developed, which involves sequential treatment of seedlings with an auxin transport inhibitor and then a synthetic auxin analog, 1-naphthalene acetic acid (NAA) (Himanen et al., 2002). This treatment rapidly induces synchronous cell divisions throughout the XPP. The resulting small cells, which are similar to a stage I LRP, then divide parallel to the root axis similar to a stage II LRP. Finally, extended NAA treatment results in proliferative LRP development along the length of the root at both XPP axes (Himanen et al., 2002).

The LRIS was proposed to override the endogenous prepatterning mechanism and stimulate LRP initiation *en masse*. This allowed application of transcriptional profiling techniques to begin to address the underlying molecular mechanisms. These analyses led to the characterization of novel proteins involved in the early steps of LR formation, including *ARABIDOPSIS* CRINKLY 4 (ACR4) and GATA23 (De Rybel et al., 2010; De Smet et al., 2008) and indicated sequential links between auxin signaling and cell cycle regulation (Himanen et al., 2002; Himanen et al., 2004). In brief, auxin signaling via SOLITARY-ROOT (SLR/IAA14) is required for LR initiation under both standard conditions and in the LRIS (Fukaki et al., 2002; Vanneste et al., 2005). Although, ectopic induction of XPP cell division in *slr/*iaa14 mutants did not promote LR formation (Vanneste et al., 2005), LRs formed proliferatively when induction of XPP cell division was combined with NAA treatment (De Smet et al., 2010). Although endogenous and LRIS-induced LRs have common features, such as tissue of origin and links between auxin signaling and the cell cycle, differences in the pattern/distribution of lateral organs suggest it is less clear how the LRIS informs endogenous LR pre-patterning. While the LRIS may simply shift the endogenous LR patterning program into overdrive, these fundamental patterning differences may indicate that hormonal manipulation elicits a distinct response program in the XPP.

Acknowledgements

In the lab of PNB, this work was funded by grants from DARPA (#D12AP0000), NSF and GBMF. Work in the Lab of TB was in part financed by grants of the Interuniversity Attraction Poles Programme (IAP VI/33 and IUAP P7/29 "MARS") from the Belgian Federal Science Policy Office and WX is supported by a CSC and an Ugent – BOF – cofounding grant.

References

Atta, R., Laurens, L., Boucheron-Dubuisson, E., Guivarc'h, A., Carnero, E., Giraudat-Pautot, V., Rech, P. and Chriqui, D. (2009) Pluripotency of *Arabidopsis* xylem pericycle underlies shoot regeneration from root and hypocotyl explants grown in vitro. *Plant J*, 57, 626-644.
Bell, J. K. a. M., M.E. (1970) A histological study of lateral root initiation and development in *Zea mays*. *Protoplasma*, 70, 179-205.
Benkova, E., Michniewicz, M., Sauer, M., Teichmann, T., Seifertova, D., Jurgens, G. and Friml, J. (2003) Local, efflux-dependent auxin gradients as a common module for plant organ formation. *Cell*, 115, 591-602.
Beveridge, C. A., Mathesius, U., Rose, R. J. and Gresshoff, P. M. (2007) Common regulatory themes in meristem development and whole-plant homeostasis. *Curr Opin Plant Biol*, 10, 44-51.
Bielach, A., Podlesakova, K., Marhavy, P., Duclercq, J., Cuesta, C., Muller, B., Grunewald, W., Tarkowski, P. and Benkova, E. (2012) Spatiotemporal regulation of lateral root organogenesis in *Arabidopsis* by cytokinin. *Plant Cell*, 24, 3967-3981.
Bonke, M., Thitamadee, S., Mahonen, A. P., Hauser, M. T. and Helariutta, Y. (2003) APL regulates vascular tissue identity in *Arabidopsis*. *Nature*, 426, 181-186.
Brady, S. M., Orlando, D. A., Lee, J. Y., Wang, J. Y., Koch, J., Dinneny, J. R., Mace, D., Ohler, U. and Benfey, P. N. (2007) A high-resolution root spatiotemporal map reveals dominant expression patterns. *Science*, 318, 801-806.
Casero, P. J., Casimiro, I. and Lloret, P. G. (1995) Lateral root initiation by asymmetrical transverse divisions of pericycle cells in four plant species: *Raphanus sativus*, *Helianthus annuus*, *Zea mays*, and *Daucus carota*. *Protoplasma*, 188, 49-58.
Celenza, J. L., Jr., Grisafi, P. L. and Fink, G. R. (1995) A pathway for lateral root formation in *Arabidopsis* thaliana. *Genes Dev*, 9, 2131-2142.
Chandler, J. W. (2011) Founder cell specification. *Trends Plant Sci*, 16, 607-613.
Chapman, E. J. and Estelle, M. (2009) Mechanism of auxin-regulated gene expression in plants. *Annu Rev Genet*, 43, 265-285.
Chatfield, S. P., Capron, R., Severino, A., Penttila, P. A., Alfred, S., Nahal, H. and Provart, N. J. (2013) Incipient stem cell niche conversion in tissue culture: using a systems approach to probe early events in WUSCHEL-dependent conversion of lateral root primordia into shoot meristems. *Plant J*, 73, 798-813.
Che, P., Lall, S. and Howell, S. H. (2007) Developmental steps in acquiring competence for shoot development in *Arabidopsis* tissue culture. *Planta*, 226, 1183-1194.
de Ruijter N.C.A., V. J., van Leeuwen W., and van der Krol A.R. (2003) Evaluation and comparison of the GUS, LUC, and GFP reporter system for gene expression studies in plants. *Plant Biol.*, 5, 103-115.
De Rybel, B., Vassileva, V., Parizot, B., Demeulenaere, M., Grunewald, W., Audenaert, D., Van Campenhout, J., Overvoorde, P., Jansen, L., Vanneste, S., *et al.* (2010) A novel aux/IAA28 signaling cascade activates GATA23-dependent specification of lateral root founder cell identity. *Curr Biol*, 20, 1697-1706.
De Smet, I., Lau, S., Voss, U., Vanneste, S., Benjamins, R., Rademacher, E. H., Schlereth, A., De Rybel, B., Vassileva, V., Grunewald, W., *et al.* (2010) Bimodular auxin response controls organogenesis in *Arabidopsis*. *Proc Natl Acad Sci U S A*, 107, 2705-2710.

De Smet, I., Signora, L., Beeckman, T., Inze, D., Foyer, C. H. and Zhang, H. (2003) An abscisic acid-sensitive checkpoint in lateral root development of *Arabidopsis*. *Plant J*, 33, 543-555.
De Smet, I., Tetsumura, T., De Rybel, B., Frey, N. F., Laplaze, L., Casimiro, I., Swarup, R., Naudts, M., Vanneste, S., Audenaert, D., *et al.* (2007) Auxin-dependent regulation of lateral root positioning in the basal meristem of *Arabidopsis*. *Development*, 134, 681-690.
De Smet, I., Vassileva, V., De Rybel, B., Levesque, M. P., Grunewald, W., Van Damme, D., Van Noorden, G., Naudts, M., Van Isterdael, G., De Clercq, R., *et al.* (2008) Receptor-like kinase ACR4 restricts formative cell divisions in the *Arabidopsis* root. *Science*, 322, 594-597.
Deak, K. I. and Malamy, J. (2005) Osmotic regulation of root system architecture. *Plant J*, 43, 17-28.
DiDonato, R. J., Arbuckle, E., Buker, S., Sheets, J., Tobar, J., Totong, R., Grisafi, P., Fink, G. R. and Celenza, J. L. (2004) *Arabidopsis* ALF4 encodes a nuclear-localized protein required for lateral root formation. *Plant J*, 37, 340-353.
Ditengou, F. A., Teale, W. D., Kochersperger, P., Flittner, K. A., Kneuper, I., van der Graaff, E., Nziengui, H., Pinosa, F., Li, X., Nitschke, R., *et al.* (2008) Mechanical induction of lateral root initiation in *Arabidopsis* thaliana. *Proc Natl Acad Sci U S A*, 105, 18818-18823.
Dolan, L., Janmaat, K., Willemsen, V., Linstead, P., Poethig, S., Roberts, K. and Scheres, B. (1993) Cellular organisation of the *Arabidopsis* thaliana root. *Development*, 119, 71-84.
Dubrovsky, J. G., Doerner, P. W., Colon-Carmona, A. and Rost, T. L. (2000) Pericycle cell proliferation and lateral root initiation in *Arabidopsis*. *Plant Physiol*, 124, 1648-1657.
Dubrovsky, J. G., Gambetta, G. A., Hernandez-Barrera, A., Shishkova, S. and Gonzalez, I. (2006) Lateral root initiation in *Arabidopsis*: developmental window, spatial patterning, density and predictability. *Ann Bot*, 97, 903-915.
Dubrovsky, J. G., Napsucialy-Mendivil, S., Duclercq, J., Cheng, Y., Shishkova, S., Ivanchenko, M. G., Friml, J., Murphy, A. S. and Benkova, E. (2011) Auxin minimum defines a developmental window for lateral root initiation. *New Phytol*, 191, 970-983.
Dubrovsky, J. G., Sauer, M., Napsucialy-Mendivil, S., Ivanchenko, M. G., Friml, J., Shishkova, S., Celenza, J. and Benkova, E. (2008) Auxin acts as a local morphogenetic trigger to specify lateral root founder cells. *Proc Natl Acad Sci U S A*, 105, 8790-8794.
Fan, M., Xu, C., Xu, K. and Hu, Y. (2012) LATERAL ORGAN BOUNDARIES DOMAIN transcription factors direct callus formation in *Arabidopsis* regeneration. *Cell Res*, 22, 1169-1180.
Feng, Z., Zhu, J., Du, X. and Cui, X. (2012) Effects of three auxin-inducible LBD members on lateral root formation in *Arabidopsis* thaliana. *Planta*, 236, 1227-1237.
Fortin, M. C., Pierce, F. J. and Poff, K. L. (1989) The pattern of secondary root formation in curving roots of *Arabidopsis* thaliana (L.) Heynh. *Plant Cell Environ*, 12, 337-339.
Fukaki, H., Tameda, S., Masuda, H. and Tasaka, M. (2002) Lateral root formation is blocked by a gain-of-function mutation in the SOLITARY-ROOT/IAA14 gene of *Arabidopsis*. *Plant J*, 29, 153-168.
Goh, T., Joi, S., Mimura, T. and Fukaki, H. (2012) The establishment of asymmetry in *Arabidopsis* lateral root founder cells is regulated by LBD16/ASL18 and related LBD/ASL proteins. *Development*, 139, 883-893.
Himanen, K., Boucheron, E., Vanneste, S., de Almeida Engler, J., Inze, D. and Beeckman, T. (2002) Auxin-mediated cell cycle activation during early lateral root initiation. *Plant Cell*, 14, 2339-2351.

Himanen, K., Vuylsteke, M., Vanneste, S., Vercruysse, S., Boucheron, E., Alard, P., Chriqui, D., Van Montagu, M., Inze, D. and Beeckman, T. (2004) Transcript profiling of early lateral root initiation. *Proc Natl Acad Sci U S A*, 101, 5146-5151.
Hochholdinger, F. and Zimmermann, R. (2008) Conserved and diverse mechanisms in root development. *Curr Opin Plant Biol*, 11, 70-74.
Jansen, L., Roberts, I., De Rycke, R. and Beeckman, T. (2012) Phloem-associated auxin response maxima determine radial positioning of lateral roots in maize. *Philos Trans R Soc Lond B Biol Sci*, 367, 1525-1533.
Jones, B. and Ljung, K. (2012) Subterranean space exploration: the development of root system architecture. *Curr Opin Plant Biol*, 15, 97-102.
Laplaze, L., Benkova, E., Casimiro, I., Maes, L., Vanneste, S., Swarup, R., Weijers, D., Calvo, V., Parizot, B., Herrera-Rodriguez, M. B., *et al.* (2007) Cytokinins act directly on lateral root founder cells to inhibit root initiation. *Plant Cell*, 19, 3889-3900.
Laskowski, M., Grieneisen, V. A., Hofhuis, H., Hove, C. A., Hogeweg, P., Maree, A. F. and Scheres, B. (2008) Root system architecture from coupling cell shape to auxin transport. *PLoS Biol*, 6, e307.
Laskowski, M. J., Williams, M. E., Nusbaum, H. C. and Sussex, I. M. (1995) Formation of lateral root meristems is a two-stage process. *Development*, 121, 3303-3310.
Lavenus, J., Goh, T., Roberts, I., Guyomarc'h, S., Lucas, M., De Smet, I., Fukaki, H., Beeckman, T., Bennett, M. and Laplaze, L. (2013) Lateral root development in *Arabidopsis*: fifty shades of auxin. *Trends Plant Sci*.
Li, X., Mo, X., Shou, H. and Wu, P. (2006) Cytokinin-mediated cell cycling arrest of pericycle founder cells in lateral root initiation of *Arabidopsis*. *Plant Cell Physiol*, 47, 1112-1123.
Lima, J. E., Kojima, S., Takahashi, H. and von Wiren, N. (2010) Ammonium triggers lateral root branching in *Arabidopsis* in an AMMONIUM TRANSPORTER1;3-dependent manner. *Plant Cell*, 22, 3621-3633.
Lucas, M., Godin, C., Jay-Allemand, C. and Laplaze, L. (2008) Auxin fluxes in the root apex co-regulate gravitropism and lateral root initiation. *J Exp Bot*, 59, 55-66.
Lucas, M., Kenobi, K., von Wangenheim, D., Vobeta, U., Swarup, K., De Smet, I., Van Damme, D., Lawrence, T., Peret, B., Moscardi, E., *et al.* (2013) Lateral root morphogenesis is dependent on the mechanical properties of the overlaying tissues. *Proc Natl Acad Sci U S A*, 110, 5229-5234.
Malamy, J. E. (2005) Intrinsic and environmental response pathways that regulate root system architecture. *Plant Cell Environ*, 28, 67-77.
Malamy, J. E. and Benfey, P. N. (1997) Organization and cell differentiation in lateral roots of *Arabidopsis* thaliana. *Development*, 124, 33-44.
Marhavy, P., Vanstraelen, M., De Rybel, B., Zhaojun, D., Bennett, M. J., Beeckman, T. and Benkova, E. (2013) Auxin reflux between the endodermis and pericycle promotes lateral root initiation. *EMBO J*, 32, 149-158.
Moreno-Risueno, M. A., Van Norman, J. M., Moreno, A., Zhang, J., Ahnert, S. E. and Benfey, P. N. (2010) Oscillating gene expression determines competence for periodic *Arabidopsis* root branching. *Science*, 329, 1306-1311.
Ohashi-Ito, K. and Bergmann, D. C. (2007) Regulation of the *Arabidopsis* root vascular initial population by LONESOME HIGHWAY. *Development*, 134, 2959-2968.

Okushima, Y., Fukaki, H., Onoda, M., Theologis, A. and Tasaka, M. (2007) ARF7 and ARF19 regulate lateral root formation via direct activation of LBD/ASL genes in *Arabidopsis*. *Plant Cell*, 19, 118-130.
Okushima, Y., Overvoorde, P. J., Arima, K., Alonso, J. M., Chan, A., Chang, C., Ecker, J. R., Hughes, B., Lui, A., Nguyen, D., *et al.* (2005) Functional genomic analysis of the AUXIN RESPONSE FACTOR gene family members in *Arabidopsis* thaliana: unique and overlapping functions of ARF7 and ARF19. *Plant Cell*, 17, 444-463.
Oliva, M. and Dunand, C. (2007) Waving and skewing: how gravity and the surface of growth media affect root development in *Arabidopsis*. *New Phytol*, 176, 37-43.
Parizot, B., Laplaze, L., Ricaud, L., Boucheron-Dubuisson, E., Bayle, V., Bonke, M., De Smet, I., Poethig, S. R., Helariutta, Y., Haseloff, J., *et al.* (2008) Diarch symmetry of the vascular bundle in *Arabidopsis* root encompasses the pericycle and is reflected in distich lateral root initiation. *Plant Physiol*, 146, 140-148.
Paul, A. L., Amalfitano, C. E. and Ferl, R. J. (2012) Plant growth strategies are remodeled by spaceflight. *BMC Plant Biol*, 12, 232.
Peret, B., Clement, M., Nussaume, L. and Desnos, T. (2011) Root developmental adaptation to phosphate starvation: better safe than sorry. *Trends Plant Sci*, 16, 442-450.
Richter, G. L., Monshausen, G. B., Krol, A. and Gilroy, S. (2009) Mechanical stimuli modulate lateral root organogenesis. *Plant Physiol*, 151, 1855-1866.
Skoog, F. and Miller, C. O. (1957) Chemical regulation of growth and organ formation in plant tissues cultured in vitro. *Symp Soc Exp Biol*, 11, 118-130.
Sugimoto, K., Jiao, Y. and Meyerowitz, E. M. (2010) *Arabidopsis* regeneration from multiple tissues occurs via a root development pathway. *Dev Cell*, 18, 463-471.
Valvekens, D., Montagu, M. V. and Van Lijsebettens, M. (1988) Agrobacterium tumefaciens-mediated transformation of *Arabidopsis* thaliana root explants by using kanamycin selection. *Proc Natl Acad Sci U S A*, 85, 5536-5540.
Vanneste, S., De Rybel, B., Beemster, G. T., Ljung, K., De Smet, I., Van Isterdael, G., Naudts, M., Iida, R., Gruissem, W., Tasaka, M., *et al.* (2005) Cell cycle progression in the pericycle is not sufficient for SOLITARY-ROOT/IAA14-mediated lateral root initiation in *Arabidopsis* thaliana. *Plant Cell*, 17, 3035-3050.
Verbelen, J. P., De Cnodder, T., Le, J., Vissenberg, K. and Baluska, F. (2006) The Root Apex of *Arabidopsis* thaliana Consists of Four Distinct Zones of Growth Activities: Meristematic Zone, Transition Zone, Fast Elongation Zone and Growth Terminating Zone. *Plant Signal Behav*, 1, 296-304.

Synthetic molecules: a helping hand in unravelling plant signal transduction

Adapted from:

Xuan W., Murphy E., Beeckman T., Audenaert D., De Smet I. (2013). Synthetic molecules: helping to unravel plant signal transduction. J. Chem. Biol. *6*, 43–50

ABSTRACT

The application of small molecules has played a crucial role in identifying novel components involved in plant signalling. Compared to classic genetic approaches, small molecule screens offer notable advantages in dissecting plant biological processes, such as technical simplicity, low start-up costs, and most importantly, bypassing the problems of lethality and redundancy. To identify small molecules that target a biological process or protein of interest, robust and well-reasoned high-throughput screening approaches are essential. In this review we present a series of principles and valuable approaches in small molecule screening in the plant model system *Arabidopsis thaliana*. We also provide an overview of small molecules that led to breakthroughs in uncovering phytohormone signalling pathways, endomembrane signalling cascades, novel growth regulators, and plant defence mechanisms. Meanwhile, the strategies to deciphering the mechanisms of these small molecules on *Arabidopsis* are highlighted. Moreover, the opportunities and challenges of small molecule applications in translational biology are discussed.

KEYWORDS

Chemical biology, plant growth and development, small molecules, screening, translational biology

INTRODUCTION

There is a long tradition of small molecule screenings to generate starting points (hit compounds) for drug discovery in animal and microbial systems. This requires a screening collection with a large number of compounds that can be analysed for the desired effect. Pharmaceutical companies have access to collections that often amount to a total of several millions of compounds. In addition, the agro-industry has used similar approaches to identify useful agrochemicals. In recent years, diverse compound collections have become available to academic researchers through commercial suppliers. The availability of these commercial chemical libraries allows exploration of their effect in specific pathways and cellular processes in an academic setting (Iorio et al. 2010).

The effect of these compounds can be tested via two types of screening approaches. In pharmaceutical companies, drug discovery often utilizes a target-based approach, by looking at a protein that plays a role in a specific disease process and subsequently identifying compounds that interfere with the function of that protein (Pandey and Nichols, 2011). But in addition to this, drug discovery can also be approached in a phenotypic way to identify compounds that produce a certain phenotype-of-interest, either in a model organism or in a cell-based system. For this purpose, highly advanced and innovative ways for screening and evaluating compounds have been developed. One such tool that has been extensively used in phenotypic screening is high content imaging. By utilising automated microscopy, scientists can design in-depth qualitative and quantitative paradigms into specific cellular and subcellular processes to discover how these processes respond to certain chemical stimuli (Trask, 2004). This type of screening has led to significant breakthroughs in the field of neurobiology, for example by the discovery of compound FK506 and its respective immunophilin receptors (Liu et al., 2007). Other areas of research that have been significantly advanced include oncology, toxicology, cell cycle research, and protein ligand and receptor identification (Agler et al., 2007; Barabasz et al., 2006; Chuma et al., 2004; Kobayashi et al., 2012).

In agricultural research, synthetic molecules have a longstanding tradition to be applied as fungicides, insecticides and herbicides. Only recently, the application of chemicals to study biological processes (‘chemical biology’ or ‘chemical genetics’) has found its way into the field of plant sciences (Fig. 1). Many of the general methods and principles of chemical biology can also be utilised in the plant field. Here, we will review the screening approaches that were used to identify novel chemical tools and the strategies to identify their mode-of-action.

WHY DO WE NEED TO SCREEN IN PLANTS?

The significance of using synthetic molecules to disrupt highly specific biological processes in plants is evident when looking at the advantages of this technique compared to classical genetics. In plant and animal systems, the highly conserved nature of, for instance, protein kinases or phosphatases, which constitute a large family of signal transduction enzymes, presents a challenging task for the development of chemical inhibitors that target only a subset of these enzymes. RNA interference against non-conserved sequences can be used as a genetic approach to analyse a subset of a large gene family during plant growth and development. However, this approach can become a significant problem when these genes play an essential role in development at the embryonic stage. Mutations in essential genes often lead to embryonic lethality, and thus, prevent the discovery of other roles for that gene later in development. For example, PROTEIN PHOSPHATASE 2A (PP2A) and AURORA (AUR) kinases are comprised of multiple subunits or classes, respectively. Single *aur* kinase mutants show no obvious macroscopic phenotype, whereas double mutants with strong alleles lead to gametophytic lethality and no plants can be recovered (Van Damme et al., 2011). This makes it difficult to determine the potential roles of these proteins at later stages of development. Unlike genetic approaches, in which mutations at the DNA level perturb gene function, synthetic molecules exert their effect directly at the protein level in a manner which is tunable, reversible, and conditional. Therefore, embryonic lethality can be circumvented and the effect of the molecules can be assessed in later developmental stages under variable conditions.

Although inhibitors against animal PP2As, such as cantharidin and okadaic acid, and AUR kinases, such as aurora inhibitor II, are available for the research community, they are ineffective in plants because they abolish overall activity, are not very specific, and/or result in pleiotropic effects (Bajsa et al., 2011; Baskin and Wilson, 1997; Deruere et al., 1999; Mortlock et al., 2005). For instance, the AUR family consists of two classes (Demidov et al., 2005) of which only α AUR kinases (AUR1/2) are involved in formative division plane orientation (Van Damme et al., 2011). Therefore, general inhibitors affecting the activity of all three *Arabidopsis* AUR kinases would not be useful when examining the specific process of plane orientation and cell division. Thus, to modulate the activity of individual proteins within a biological process, novel, (plant-)specific molecules are required.

Small molecules are also very useful as they can address the issue of genetic redundancy, a problem often associated with reverse genetic approaches in plants. If interfering with

multiple pathways simultaneously is required to influence plant growth and development, multiple molecules can be added, which is analogous to multiple gene modifications. Alternatively, synthetic molecules can target several members of the same protein family (i.e. by interacting at conserved sites) and can consequently overcome genetic redundancy. Additionally, due to the highly conserved nature of major plant protein families, such as receptor-like kinases (RLKs), chemical genetics in model systems (like *Arabidopsis thaliana*) allows for techniques to be transferred from one species to another, greatly enhancing the significance of a single chemical screen.

SCREENING PROCEDURES

A prerequisite to find new chemicals that interfere with a certain phenotypic response or biological pathway is the availability of a 'compound screening toolbox'. First, a large collection of compounds needs to be available that, as a whole, is capable of altering the function of a broad range of proteins, including those involved in the biological process of interest. The screening collection can consist of synthetic molecules, natural products, or small signalling peptides (collectively referred to as compounds) (Huggins et al. 2011). There are several compound collections commercially available that can be used for small molecule screening in *Arabidopsis* (Robert et al, 2009). For example, the ChemBridge DIVERSet library contains in total about 100,000 drug-like low molecular mass molecules designed to maximize structural diversity (http://www.chembridge.com/screening_libraries/). Subsets of this collection have been used previously in *Arabidopsis* screenings and have yielded interesting hits and tool compounds (Kim et al., 2011). Similar diverse collections are also available from other suppliers such as Life Chemicals (http://www.lifechemicals.com/), Asinex (http://www.asinex.com/Libraries.html) and TimTec (http://www.timtec.net/Screening-Compound-Libraries.html). During the assembly process of these collections, compounds are selected via *in silico* filtering algorithms based upon physico-chemical properties to enhance bio-availability. In addition, substructure analyses are applied to remove unstable and/or toxic compounds (Vert and Jacob, 2008). Diversity of the compound collection is essential if no prior knowledge of the protein target is known and the screening aims for the identification of compounds that interfere with a phenotypic response rather than a specific protein. On the other hand, if structural information is known about the protein site(s) to target, a more focused library can be designed in which screening compounds are assembled or synthesized based upon one or several structural scaffolds. Most suppliers allow cherry-picking from their collection to assemble custom and/or focused

libraries. In some cases, commercial focused libraries are already available such as collections of kinase inhibitors and ion channel inhibitors.

To assess the potential effect of a compound collection on a particular biological process or protein-of-interest, a robust screening assay has to be developed in cell-free systems, cellular systems, or even small model organisms. In the animal field, these are, for example, *Danio rerio* or *Xenopus laevis* embryos (Kalin et al. 2009; Sun et al. 2012}. In plants, these are mainly *Arabidopsis thaliana* seedlings, but also suspension cells (Noutoshi et al. 2012). In yeast, *Saccharomyces cerevisiae* is used as a tool in the yeast-3-hybrid system, allowing for molecule-protein interactions *in vivo*, which can be used to refute or confirm interactions shown in other model systems (Licitra and Liu, 1996). An important aspect during assay development is miniaturization of the assay to 96- or 384-well plates. This significantly reduces reagent costs during screening campaigns and makes the assay compatible with automation and liquid handling systems, which allows the distribution of compounds, reagents, and model systems in a high-throughput fashion. Because in many screening collections compounds are dissolved in DMSO, determining the sensitivity of the model system to DMSO is essential to avoid toxicity due to too high solvent concentrations. In addition, analysis of positive and negative controls during assay development allows to determine the assay window and to calculate a Z' value, a measure to assess robustness of the screening assay (Zhang et al., 1999). After assay development and acquisition or synthesis of the screening compounds, the compound collection is applied to the assay system with automated liquid handling platforms and the assay output is detected by means of automated plate readers or microscopes. Informatics and databases are required to track, analyse, and retrieve screening data. After hit identification, hits are validated with secondary screening assays and chemical characterization including evaluation of chemical structure and initial structure-activity analysis.

CHEMICAL GENETICS IN PLANT GROWTH

Chemical genetic approaches have been successfully applied to study plant signalling pathways and to modulate plant growth (Armstrong et al. 2004; Dai et al. 2005; (De Rybel et al., 2009b; Hayashi et al., 2008; Kim et al., 2011; Savaldi-Goldstein et al., 2008; Tsuchiya et al., 2010). Initially, chemical screens were mainly applied to gain insight into auxin signal transduction. For example, the small molecule sirtinol was identified because it activated the auxin signal transduction pathway and mimicked auxin-related developmental phenotypes. It led to the identification of SIRTINOL RESISTANT 1 (SIR1), an upstream regulator of auxin

signalling pathways (Zhao et al. 2003). Further studies revealed that the activation of sirtinol required a functional aldehyde oxidase (Dai et al. 2005). In addition, inhibitory small molecules of auxin signalling pathways have also been identified by chemical screens (Armstrong et al. 2004). Only recently, phenotype-based small molecule screens in *Arabidopsis* gave rise to the discovery of various novel signalling pathways in abiotic stress and plant growth development (Robert et al. 2008; Park et al. 2009; De Rybel et al. 2009; Kim et al. 2011). In this section, well-characterized small molecules which were identified from phenotypic screens will be introduced. Furthermore, the screening methods and the mechanism of these chemicals will be briefly discussed.

Pyrabactin

The identification of the synthetic molecule pyrabactin (4-bromo-N-[pyridin-2-yl methyl]naphthalene-1-sulfonamide) as a selective abscisic acid (ABA) agonist has led to major breakthroughs in understanding ABA perception mechanisms (Park et al. 2009). Although many intermediate signalling components had been described before (Finkelstein et al., 2002), knowledge at the level of ABA perception was only marginal. This was mainly due to the high genetic redundancy of the ABA receptor gene family. During a screen of a 10,000-membered chemical library, pyrabactin was identified as a synthetic seed germination inhibitor in an *Arabidopsis thaliana* seed germination assay (Zhao et al. 2007). An ABA-hypersensitive *Arabidopsis* accession was observed to also show hypersensitivity to pyrabactin. Subsequently, pyrabactin-insensitive mutants were identified containing insensitive alleles of *pyrabactin resistance1* (*PYR1*) genes. PYR1 was shown to interact with hypersensitive to aba1 (HAB1) (homolog of ABI1 and ABI2), a protein phosphatase which is a negative regulator of ABA signalling. Thus, the selectivity of pyrabactin for a subset of ABA receptors allowed to bypass this redundancy, and led to the identification of pyr/regulatory component of aba receptor (RCAR) proteins as ABA receptors (Park et al., 2009). The PYR/RCAR proteins act together with PP2Cs and SNF1-related protein kinase2 (SnRK2s) (Fujii et al., 2007; Yoshida et al., 2002) as negative and positive regulators, respectively, of downstream ABA signalling (Ma et al., 2009; Park et al., 2009). This breakthrough, together with further detailed structural and mutational approaches, provided new insights into ABA perception and signalling, and exemplified the need for and use of target-specific agonists in chemical genetics (Melcher et al., 2010; Mosquna et al., 2011).

Bikinin

In addition to specific agonists, such as pyrabactin, general antagonists can also be powerful chemical tools. For example, bikinin, (4-[(5-bromo-2-pyridinyl)amino]-4-oxobutanoic acid), was identified as an activator of brassinosteroid (BR) signalling in a screen for small molecules that induce a constitutive BR response (De Rybel et al., 2009b). A commercial 10,000 compound library (DIVERSet, ChemBridge Corporation) was used for this screen. The structure-activity analysis identified bikinin as a non-steroidal molecule modulating the BR signalling cascade downstream of the brassinosteroid-insensitive1 (BRI1) receptor. A combination of BES1 phosphorylation analysis, kinase assays, surface plasmon resonance binding studies, and microarray analysis showed that bikinin directly targets brassinosteroid-insensitive2 (BIN2) protein, which belongs to the group II glycogen synthase kinase 3 family (GSK3s). To assess the binding mode of bikinin, an ATP-competition assay with BIN2 and modelling of the compound into the crystal structure of the human BIN2 homolog, GSK3β, revealed that bikinin acts as an ATP-competitive kinase inhibitor. In *A. thaliana*, a set of ten GSK3s is present (Jonak and Hirt, 2002). Interestingly, because bikinin targets several subsets of GSK3s, including a subset of three GSK3s shown to be involved in the negative regulation of BR signalling, the compound could act as a conditional and multiple knock-out tool for this subset of GSK3s and therefore induce a BR response (De Rybel et al., 2009b). This type of response would never have been observed by single loss-of-function mutants in genes encoding GSK3s or by a selective GSK3 inhibitor. Thus, the specificity of bikinin for a subset of GSK3s offers the opportunity to study other effects of specifically inhibiting GSK3s in *A. thaliana*.

DFPM

The small molecule [5-(3, 4-dichlorophenyl) furan-2-yl]-piperidine-1-ylmethanethione (DFPM) has been used to determine the coordination and interaction between abiotic stress and plant immunity (Kim et al., 2011). DFPM was first selected from a chemical library of ChemBridge's DIVERSet E library of 9600 compounds (ChemBridge, San Diego) as a negative regulator of the ABA signalling pathway by using a WT-*RAB18* reporter line. Microarray-based whole genome transcriptomic analysis revealed that DFPM down-regulated ABA-induced gene expression, but also stimulates the expression of pathogen-resistance genes, including *pathogenesis-related5* (*PR5*) and *enhanced disease susceptibility1* (*EDS1)*. Interestingly, the inhibitory effects of DFPM on ABA-responsive genes and ABA-induced stomatal closure were impaired in mutants of plant disease resistance pathways, such as *eds1*,

pad4, *sgt1b*, and *rar1*, but not in *npr1*, which is the crucial salicylic acid (SA) response regulator (Cao et al., 1997). This indicated that DFPM-dependent ABA signal transduction required early pathogen resistance response regulators rather than SA signalling. Notably, transcriptional activation of defence-related gene expression or *Pseudomonas syringae* infection can mimic the effect of DFPM on ABA responses, suggesting a negative regulation of ABA signal transduction by activation of plant immunity pathways. Further investigation on the mechanism of DFPM-interfered ABA signal transduction revealed that ABA perception by PYR/RCAR receptors (Park et al., 2009) and subsequent activation of the major ABA signalling kinases, SnRK2s, were not affected by DFPM. However, DFPM blocked ABA-induced Ca^{2+} activated S-type anion channel currents in the wild-type guard cells, but not in *pad4-1*background. This indicated a DES1/PAD4-dependent plant immunity pathway which plays a key role in interrupting early ABA responses by modulation of Ca^{2+} signalling (Kim et al., 2011). Taken together, the synthetic molecule DFPM has provided a comprehensive understanding of cross talk between biotic and ABA signalling networks. DFPM also presents the characteristics of an effective instigator of plant immunity, and could thus be widely applied in abiotic-biotic interaction research.

Naxillin

The non-auxin like probe naxillin was identified as a specific modulator of lateral root development from a marker/phenotype-based small-molecule screen of a commercial 10,000-compound library (DIVERSet, ChemBridge Corporation) in *A. thaliana* (De Rybel et al., 2012). The plant hormone auxin is known as a regulator of many plant developmental processes, including lateral root development (De Rybel et al., 2009a). By contrast, naxillin specifically induces root branching with minimal side effects typical of auxin treatment, such as inhibition of primary root growth. At the transcriptome level, naxillin treatment induced 401 genes, whereas treatment with the synthetic auxin analog naphthalene acetic acid (NAA) induced 2,581 genes, suggesting a much narrower mechanism of action. As such, naxillin represents a valuable tool to decipher the molecular networks involved in lateral root development. To gain insight into the mode-of-action of naxillin, an ethyl methane sulfonate (EMS)-mutagenized population was screened, and a naxillin-resistant mutant allele was selected for further analysis. A positional cloning approach identified a missense mutation in *indole-3-butyric acid response3* (*IBR3*), which acts on conversion of indole-3-butyric acid (IBA) to indole-3-acetic acid (IAA) (Zolman et al., 2007). IBA-to-IAA conversion pathway mutants were further checked upon naxillin treatment and demonstrated that naxillin acts at

the level of the enoyl-CoA hydratase step of the pathway. Expression pattern analysis of IBA-to-IAA conversion genes *indole-3-butyric acid response1 (IBR1)*, *IBR3*, *IBR10*, and *abnormal inflorescence meristem 1 (AIM1)* revealed that expression domains of all these genes overlapped in the root tip of the primary root, specifically in root cap cells. This indicated that root cap-specific auxin production might be involved in root branching. The existence of tissue-specific sources of auxin as a mechanism to fine-tune developmental processes, such as root branching, has never been observed by applying auxins or its analogs, which produce the global effects on plant root developmental processes. This breakthrough provides new insights into the function of auxin homeostasis on root development and nicely illustrates how novel chemical tools can be applied to discover biological mechanisms that are involved in specific plant developmental processes.

Endosidins

The synthetic molecule endosidin1 (ES1) was selected from an automated image-based screen from a chemical library (Microsource Spectrum) contained 2,016 chemicals with known biological activity for inhibitors of pollen germination or effectors of polar growth, and the screen was conducted by using GFP-RIP1, a maker line of apical plasma membrane in *Arabidopsis* and tobacco pollen tubes (Robert et al., 2008). The application of ES1 selectively disrupted the trafficking of pin-formed (PIN) auxin efflux carrier PIN2, auxin insensitive1 (AUX1), and BRI1, and formed intracellular agglomerations termed “endosidin bodies”. Endosidin bodies were further defined as trans-golgi network (TGN)/endosomal proteins SYP61 and the V-ATPase subunit VHA-a1. This suggested that SYP61/VHA-a1 act as components of an early endosome compartment in PIN2 and AUX1 mediated-endomembrane trafficking processes (Robert et al., 2008). To explore more components involved in this pathway, a modified laser scanning confocal microscopy-based high-content intracellular screen was established, which allowed the identification of small-molecules that phenocopy ES1 treatment (Drakakaki et al., 2011). Meanwhile, more chemical libraries, including Chembridge Diverset library, Chembridge, Novacore library and Sigma TimTec Myria library, containing 46,418 compounds in total were screened. After two rounds of screening, 123 small molecules were selected as both inhibitors of pollen germination and effectors of plasma membrane markers. The image database was then transformed by a flexible algorithm into a marker-by-phenotype-by-treatment time matrix and molecules were clustered into groups of endosidins (ESs) depending on the specific profiles of subcellular phenotypes. Although these molecules may induce a similar endomembrane trafficking phenotype,

detailed analysis of different PM makers revealed diverse modes-of-action of these ESs on early events of endosome trafficking. For example, endosidin3 (ES3) was found to target Rho GTPases (ROP) trafficking and exhibited cell polarity defection, whereas endosidin5 (ES5) was linked to PIN cycling and gravitropism. Thus, the direct discovery of endomembrane-defective phenotypes could then easily be linked to developmental phenotypes, which still poses a challenge for exclusively forward genetic screens. This breakthrough is the first time that an automated microscopy-driven phenotypic molecule screen has been used in plants, suggesting that a high-content small molecule screen could serve as an effective tool to illustrate intracellular signalling pathways in *vivo*, and also help to set up a comprehensive systems biology view.

SMALL MOLECULES IN TRANSLATIONAL PLANT SCIENCES

The above examples illustrate the power of chemical genetics to identify chemical 'probes' that can be applied to study biology. From a translational point-of-view, small-molecules could be of great value by forming the starting point in the discovery of new agrochemicals. Evidently, this requires that the compound's target protein(s) and/or the mechanism-of-action be conserved between the species in which the activity of the compound was observed (e.g. *A. thaliana*) and the target crop species.

Based upon analysis of currently available pesticides and herbicides, agrochemicals obey certain structural and physico-chemical rules (Tice, 2001). This is similar to drug-like properties as illustrated by Lipinski's Rule-of-Five, which states that poor bioavailability (poor absorption and permeability) is more likely when more than 5 H-bond donors are present, more than 10 H-bond acceptors are present, the molecular weight (MW) is greater than 500 Da, and the calculated octanol/water coefficient (CLogP) is greater than 5 (Lipinski et al. 2001). The ranges of these parameters for agrochemicals are similar, except for the lower acceptable number of H-bond donors. However, some important differences exist between agrochemicals and pharmaceuticals regarding the types of functional groups (Tice, 2001). For example, to be able to protect a crop, a chemical must persist in the field for several weeks to be of practical value. Therefore, alcohols and amines are much less common in agrochemicals than in pharmaceuticals as these groups are less stable in field environments (due to ease of oxidation). Aromatic rings are also more prevalent among agrochemicals because aromatic rings are more likely to be stable in the environment than alicyclic rings. Finally, acidic groups such as carboxylic acids and acylsulfonamides are prevalent among post-emergence agrochemicals. This is because weakly acidic groups promote phloem

mobility, which is required to transport the chemical to the growing points of the plant. These structural, functional, and physico-chemical constraints should be considered during the assembly of a compound screening collection with the aim to identify new types of agrochemicals. In view of non-GMO applications, synthetic molecules are required that specifically mimic, disturb and/or enhance protein activities, and that can easily and cost-effectively (potentially as a modified variant) be applied to crops (for instance through addition to fertiliser or water). This will generate tools (synthetic molecules) that can be widely applied to non-related species, without requiring genetic modifications. This translational approach is relevant considering the fact that several key signalling pathways are conserved between species.

CONCLUSION

The application of small molecules in plant research has expanded rapidly in the past decade and has made genuine contributions to our comprehensive knowledge of the molecular mechanisms of plant development. However, plant chemical genetics is now at the stage where faster and more efficient ways of screening have to be developed to permit wider accessibility in the plant research field. The establishment of a compound screening platform is of prime importance (Fig. 5), as small molecule use in plant systems has been shown to significantly accelerate and enhance developmental research. This requires development of robust screening assays in plant-based systems and compound collections that a more dedicated for applications in the field of plant sciences. In addition, the application of high-throughput imaging technologies in plant screenings would certainly technically allow us to delve more deeply into complex intracellular networks than previous approaches permitted. In addition, development of small molecules that can modulate protein-protein interactions remains a challenge even in human drug development, and heavily relies on biochemical and biophysical knowledge of the respective target interactions (Arkin and Wells, 2004) and such knowledge unfortunately remains scarce in plant biology. Thus, further investigation will not only be emphasized on searching for protein targets, but also on the mechanistic level where small molecules act as regulators of, for instance, plant receptor-like kinase (RLK) signalling (Marshall et al., 2012). Importantly, one of the greatest challenges remaining is the generation of useful, applicable small molecules in agricultural production. This requires exploration of small molecules that affect specific protein activities, and that can easily and cost-effectively be applied to crops. This in turn could be a potential solution for the non-GMO, and could ultimately lead to a new green revolution.

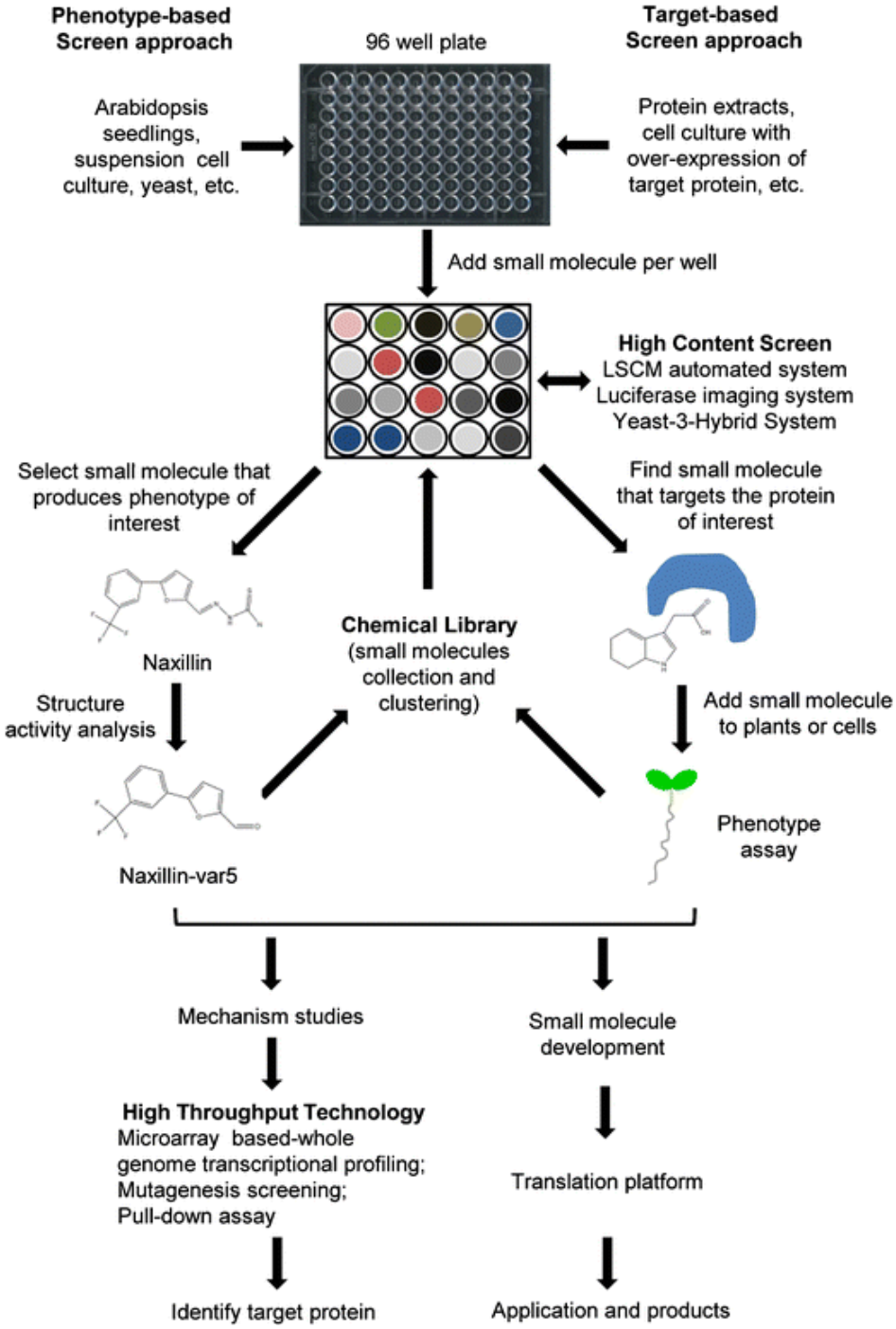

Figure 5. Small molecule screen strategies identify proteins and RLK signalling pathways. The phenotype-based approach (left) is analogous to forward genetics and comprises three different steps. The first step is the assembly of a set of mutation equivalents, i.e. a chemical library with 10,000 or more compounds capable of altering protein function. Subsequently, a high-throughput screen is performed to identify compounds that affect a biological process of interest. A high-content screen can be processed by using advanced technologies. Target-based chemical genetics (right) is comparable to reverse genetics and entails over-expressing a protein of interest, screening for compounds that interact with the protein and finally using this compound to determine the phenotypic consequences of altering the function of this protein in a cellular context. As a final step, the protein targets of these compounds or the potential mechanism are identified. Furthermore, bioactive small molecular would be modified and applied into translation platform. Naxillin was used as example for the structure-activity analysis.

ACKNOWLEDGEMENTS

This work was supported by a Biotechnology and Biological Science Research Council David Phillips Fellowship (BB_BB/H022457/1), a Marie Curie European Reintegration grant (PERG06-GA-2009-256354), the Interuniversity Attraction Poles Programme (IUAP VI/33) initiated by the Belgian State Science Policy Office, VIB, and the Special Research Fund of Ghent University. We thank the School of Biosciences and Malcolm. J. Bennett for studentship funding and acknowledge the University of Nottingham research committee.

REFERENCES

Agler, M., Prack, M., Zhu, Y., Kolb, J., Nowak, K., Ryseck, R., Shen, D., Cvijic, M.E., Somerville, J., Nadler, S., *et al.* (2007). A high-content glucocorticoid receptor translocation assay for compound mechanism-of-action evaluation. J Biomol Screen *12*, 1029-1041.

Arkin, M.R., and Wells, J.A. (2004). Small-molecule inhibitors of protein-protein interactions: progressing towards the dream. Nat Rev Drug Discov *3*, 301-317.

Atta, R., Laurens, L., Boucheron-Dubuisson, E., Guivarc'h, A., Carnero, E., Giraudat-Pautot, V., Rech, P., and Chriqui, D. (2009). Pluripotency of *Arabidopsis* xylem pericycle underlies shoot regeneration from root and hypocotyl explants grown in vitro. The Plant journal : for cell and molecular biology *57*, 626-644.

Bajsa, J., Pan, Z., and Duke, S.O. (2011). Transcriptional responses to cantharidin, a protein phosphatase inhibitor, in *Arabidopsis* thaliana reveal the involvement of multiple signal transduction pathways. Physiol Plant *143*, 188-205.

Barabasz, A., Foley, B., Otto, J.C., Scott, A., and Rice, J. (2006). The use of high-content screening for the discovery and characterization of compounds that modulate mitotic index and cell cycle progression by differing mechanisms of action. Assay Drug Dev Technol *4*, 153-163.

Baskin, T.I., and Wilson, J.E. (1997). Inhibitors of protein kinases and phosphatases alter root morphology and disorganize cortical microtubules. Plant physiology *113*, 493-502.

Bell, J.K.a.M., M.E. (1970). A histological study of lateral root initiation and development in *Zea mays.* Protoplasma *70*, 179-205.

Benkova, E., Michniewicz, M., Sauer, M., Teichmann, T., Seifertova, D., Jurgens, G., and Friml, J. (2003). Local, efflux-dependent auxin gradients as a common module for plant organ formation. Cell *115*, 591-602.

Beveridge, C.A., Mathesius, U., Rose, R.J., and Gresshoff, P.M. (2007). Common regulatory themes in meristem development and whole-plant homeostasis. Current opinion in plant biology *10*, 44-51.

Bielach, A., Podlesakova, K., Marhavy, P., Duclercq, J., Cuesta, C., Muller, B., Grunewald, W., Tarkowski, P., and Benkova, E. (2012). Spatiotemporal regulation of lateral root organogenesis in *Arabidopsis* by cytokinin. The Plant cell *24*, 3967-3981.

Bonke, M., Thitamadee, S., Mahonen, A.P., Hauser, M.T., and Helariutta, Y. (2003). APL regulates vascular tissue identity in *Arabidopsis*. Nature *426*, 181-186.
Brady, S.M., Orlando, D.A., Lee, J.Y., Wang, J.Y., Koch, J., Dinneny, J.R., Mace, D., Ohler, U., and Benfey, P.N. (2007). A high-resolution root spatiotemporal map reveals dominant expression patterns. Science *318*, 801-806.
Cao, H., Glazebrook, J., Clarke, J.D., Volko, S., and Dong, X. (1997). The *Arabidopsis* NPR1 gene that controls systemic acquired resistance encodes a novel protein containing ankyrin repeats. Cell *88*, 57-63.
Casero, P.J., Casimiro, I., and Lloret, P.G. (1995). Lateral root initiation by asymmetrical transverse divisions of pericycle cells in four plant species: *Raphanus sativus*, *Helianthus annuus*, *Zea mays*, and *Daucus carota*. Protoplasma *188*, 49-58.
Chandler, J.W. (2011). Founder cell specification. Trends in plant science *16*, 607-613.
Chapman, E.J., and Estelle, M. (2009). Mechanism of auxin-regulated gene expression in plants. Annual review of genetics *43*, 265-285.
Chatfield, S.P., Capron, R., Severino, A., Penttila, P.A., Alfred, S., Nahal, H., and Provart, N.J. (2013). Incipient stem cell niche conversion in tissue culture: using a systems approach to probe early events in WUSCHEL-dependent conversion of lateral root primordia into shoot meristems. Plant J *73*, 798-813.
Chipman, A.D., Arthur, W., and Akam, M. (2004). A double segment periodicity underlies segment generation in centipede development. Current biology : CB *14*, 1250-1255.
Choat, B., Drayton, W.M., Brodersen, C., Matthews, M.A., Shackel, K.A., Wada, H., and McElrone, A.J. (2010). Measurement of vulnerability to water stress-induced cavitation in grapevine: a comparison of four techniques applied to a long-vesseled species. Plant, cell & environment *33*, 1502-1512.
Chuma, M., Sakamoto, M., Yasuda, J., Fujii, G., Nakanishi, K., Tsuchiya, A., Ohta, T., Asaka, M., and Hirohashi, S. (2004). Overexpression of cortactin is involved in motility and metastasis of hepatocellular carcinoma. J Hepatol *41*, 629-636.
de Ruijter N.C.A., V.J., van Leeuwen W., and van der Krol A.R. (2003). Evaluation and comparison of the GUS, LUC, and GFP reporter system for gene expression studies in plants. Plant Biol *5*, 103-115.
De Rybel, B., Audenaert, D., Beeckman, T., and Kepinski, S. (2009a). The past, present, and future of chemical biology in auxin research. ACS chemical biology *4*, 987-998.
De Rybel, B., Audenaert, D., Vert, G., Rozhon, W., Mayerhofer, J., Peelman, F., Coutuer, S., Denayer, T., Jansen, L., Nguyen, L., *et al.* (2009b). Chemical inhibition of a subset of *Arabidopsis* thaliana GSK3-like kinases activates brassinosteroid signaling. Chem Biol *16*, 594-604.
De Rybel, B., Audenaert, D., Xuan, W., Overvoorde, P., Strader, L.C., Kepinski, S., Hoye, R., Brisbois, R., Parizot, B., Vanneste, S., *et al.* (2012). A role for the root cap in root branching revealed by the non-auxin probe naxillin. Nat Chem Biol *8*, 798-805.
De Rybel, B., Vassileva, V., Parizot, B., Demeulenaere, M., Grunewald, W., Audenaert, D., Van Campenhout, J., Overvoorde, P., Jansen, L., Vanneste, S., *et al.* (2010). A novel aux/IAA28 signaling cascade activates GATA23-dependent specification of lateral root founder cell identity. Current biology : CB *20*, 1697-1706.
De Smet, I., Lau, S., Voss, U., Vanneste, S., Benjamins, R., Rademacher, E.H., Schlereth, A., De Rybel, B., Vassileva, V., Grunewald, W., *et al.* (2010). Bimodular auxin response controls

organogenesis in *Arabidopsis*. Proceedings of the National Academy of Sciences of the United States of America *107*, 2705-2710.
De Smet, I., Signora, L., Beeckman, T., Inze, D., Foyer, C.H., and Zhang, H. (2003). An abscisic acid-sensitive checkpoint in lateral root development of *Arabidopsis*. The Plant journal : for cell and molecular biology *33*, 543-555.
De Smet, I., Tetsumura, T., De Rybel, B., Frey, N.F., Laplaze, L., Casimiro, I., Swarup, R., Naudts, M., Vanneste, S., Audenaert, D., *et al.* (2007). Auxin-dependent regulation of lateral root positioning in the basal meristem of *Arabidopsis*. Development *134*, 681-690.
De Smet, I., Vassileva, V., De Rybel, B., Levesque, M.P., Grunewald, W., Van Damme, D., Van Noorden, G., Naudts, M., Van Isterdael, G., De Clercq, R., *et al.* (2008). Receptor-like kinase ACR4 restricts formative cell divisions in the *Arabidopsis* root. Science *322*, 594-597.
Deak, K.I., and Malamy, J. (2005). Osmotic regulation of root system architecture. The Plant journal : for cell and molecular biology *43*, 17-28.
Demidov, D., Van Damme, D., Geelen, D., Blattner, F.R., and Houben, A. (2005). Identification and dynamics of two classes of aurora-like kinases in *Arabidopsis* and other plants. Plant Cell *17*, 836-848.
Dequeant, M.L., Glynn, E., Gaudenz, K., Wahl, M., Chen, J., Mushegian, A., and Pourquie, O. (2006). A complex oscillating network of signaling genes underlies the mouse segmentation clock. Science *314*, 1595-1598.
Deruere, J., Jackson, K., Garbers, C., Soll, D., and Delong, A. (1999). The RCN1-encoded A subunit of protein phosphatase 2A increases phosphatase activity in vivo. Plant J *20*, 389-399.
DiDonato, R.J., Arbuckle, E., Buker, S., Sheets, J., Tobar, J., Totong, R., Grisafi, P., Fink, G.R., and Celenza, J.L. (2004). *Arabidopsis* ALF4 encodes a nuclear-localized protein required for lateral root formation. The Plant journal : for cell and molecular biology *37*, 340-353.
Ditengou, F.A., Teale, W.D., Kochersperger, P., Flittner, K.A., Kneuper, I., van der Graaff, E., Nziengui, H., Pinosa, F., Li, X., Nitschke, R., *et al.* (2008). Mechanical induction of lateral root initiation in *Arabidopsis* thaliana. Proceedings of the National Academy of Sciences of the United States of America *105*, 18818-18823.
Dolan, L., Janmaat, K., Willemsen, V., Linstead, P., Poethig, S., Roberts, K., and Scheres, B. (1993). Cellular organisation of the *Arabidopsis* thaliana root. Development *119*, 71-84.
Drakakaki, G., Robert, S., Szatmari, A.M., Brown, M.Q., Nagawa, S., Van Damme, D., Leonard, M., Yang, Z., Girke, T., Schmid, S.L., *et al.* (2011). Clusters of bioactive compounds target dynamic endomembrane networks in vivo. Proc Natl Acad Sci U S A *108*, 17850-17855.
Dray, N., Tessmar-Raible, K., Le Gouar, M., Vibert, L., Christodoulou, F., Schipany, K., Guillou, A., Zantke, J., Snyman, H., Behague, J., *et al.* (2010). Hedgehog signaling regulates segment formation in the annelid Platynereis. Science *329*, 339-342.
Dubrovsky, J.G., Doerner, P.W., Colon-Carmona, A., and Rost, T.L. (2000). Pericycle cell proliferation and lateral root initiation in *Arabidopsis*. Plant physiology *124*, 1648-1657.
Dubrovsky, J.G., Gambetta, G.A., Hernandez-Barrera, A., Shishkova, S., and Gonzalez, I. (2006). Lateral root initiation in *Arabidopsis*: developmental window, spatial patterning, density and predictability. Annals of botany *97*, 903-915.
Dubrovsky, J.G., Napsucialy-Mendivil, S., Duclercq, J., Cheng, Y., Shishkova, S., Ivanchenko, M.G., Friml, J., Murphy, A.S., and Benkova, E. (2011). Auxin minimum defines a developmental window for lateral root initiation. The New phytologist *191*, 970-983.

Dubrovsky, J.G., Sauer, M., Napsucialy-Mendivil, S., Ivanchenko, M.G., Friml, J., Shishkova, S., Celenza, J., and Benkova, E. (2008). Auxin acts as a local morphogenetic trigger to specify lateral root founder cells. Proceedings of the National Academy of Sciences of the United States of America *105*, 8790-8794.
Finkelstein, R.R., Gampala, S.S., and Rock, C.D. (2002). Abscisic acid signaling in seeds and seedlings. Plant Cell *14 Suppl*, S15-45.
Fortin, M.C., Pierce, F.J., and Poff, K.L. (1989). The pattern of secondary root formation in curving roots of *Arabidopsis* thaliana (L.) Heynh. Plant, cell & environment *12*, 337-339.
Fujii, H., Verslues, P.E., and Zhu, J.K. (2007). Identification of two protein kinases required for abscisic acid regulation of seed germination, root growth, and gene expression in *Arabidopsis*. Plant Cell *19*, 485-494.
Fukaki, H., Tameda, S., Masuda, H., and Tasaka, M. (2002). Lateral root formation is blocked by a gain-of-function mutation in the SOLITARY-ROOT/IAA14 gene of *Arabidopsis*. The Plant journal : for cell and molecular biology *29*, 153-168.
Goh, T., Joi, S., Mimura, T., and Fukaki, H. (2012). The establishment of asymmetry in *Arabidopsis* lateral root founder cells is regulated by LBD16/ASL18 and related LBD/ASL proteins. Development *139*, 883-893.
Hayashi, K., Tan, X., Zheng, N., Hatate, T., Kimura, Y., Kepinski, S., and Nozaki, H. (2008). Small-molecule agonists and antagonists of F-box protein-substrate interactions in auxin perception and signaling. Proc Natl Acad Sci U S A *105*, 5632-5637.
Himanen, K., Boucheron, E., Vanneste, S., de Almeida Engler, J., Inze, D., and Beeckman, T. (2002). Auxin-mediated cell cycle activation during early lateral root initiation. The Plant cell *14*, 2339-2351.
Himanen, K., Vuylsteke, M., Vanneste, S., Vercruysse, S., Boucheron, E., Alard, P., Chriqui, D., Van Montagu, M., Inze, D., and Beeckman, T. (2004). Transcript profiling of early lateral root initiation. Proceedings of the National Academy of Sciences of the United States of America *101*, 5146-5151.
Hochholdinger, F., and Zimmermann, R. (2008). Conserved and diverse mechanisms in root development. Current opinion in plant biology *11*, 70-74.
Jansen, L., Roberts, I., De Rycke, R., and Beeckman, T. (2012). Phloem-associated auxin response maxima determine radial positioning of lateral roots in maize. Philosophical transactions of the Royal Society of London Series B, Biological sciences *367*, 1525-1533.
Jonak, C., and Hirt, H. (2002). Glycogen synthase kinase 3/SHAGGY-like kinases in plants: an emerging family with novel functions. Trends Plant Sci *7*, 457-461.
Jones, B., and Ljung, K. (2012). Subterranean space exploration: the development of root system architecture. Current opinion in plant biology *15*, 97-102.
Kim, T.H., Hauser, F., Ha, T., Xue, S., Bohmer, M., Nishimura, N., Munemasa, S., Hubbard, K., Peine, N., Lee, B.H., *et al.* (2011). Chemical genetics reveals negative regulation of abscisic acid signaling by a plant immune response pathway. Curr Biol *21*, 990-997.
Kobayashi, H., Harada, H., Nakamura, M., Futamura, Y., Ito, A., Yoshida, M., Iemura, S., Shin-Ya, K., Doi, T., Takahashi, T., *et al.* (2012). Comprehensive predictions of target proteins based on protein-chemical interaction using virtual screening and experimental verifications. BMC Chem Biol *12*, 2.
Laplaze, L., Benkova, E., Casimiro, I., Maes, L., Vanneste, S., Swarup, R., Weijers, D., Calvo, V., Parizot, B., Herrera-Rodriguez, M.B., *et al.* (2007). Cytokinins act directly on lateral root founder cells to inhibit root initiation. The Plant cell *19*, 3889-3900.

Laskowski, M., Grieneisen, V.A., Hofhuis, H., Hove, C.A., Hogeweg, P., Maree, A.F., and Scheres, B. (2008). Root system architecture from coupling cell shape to auxin transport. PLoS biology *6*, e307.
Laskowski, M.J., Williams, M.E., Nusbaum, H.C., and Sussex, I.M. (1995). Formation of lateral root meristems is a two-stage process. Development *121*, 3303-3310.
Lavenus, J., Goh, T., Roberts, I., Guyomarc'h, S., Lucas, M., De Smet, I., Fukaki, H., Beeckman, T., Bennett, M., and Laplaze, L. (2013). Lateral root development in *Arabidopsis*: fifty shades of auxin. Trends in plant science.
Li, X., Mo, X., Shou, H., and Wu, P. (2006). Cytokinin-mediated cell cycling arrest of pericycle founder cells in lateral root initiation of *Arabidopsis*. Plant & cell physiology *47*, 1112-1123.
Licitra, E.J., and Liu, J.O. (1996). A three-hybrid system for detecting small ligand-protein receptor interactions. Proc Natl Acad Sci U S A *93*, 12817-12821.
Lima, J.E., Kojima, S., Takahashi, H., and von Wiren, N. (2010). Ammonium triggers lateral root branching in *Arabidopsis* in an AMMONIUM TRANSPORTER1;3-dependent manner. The Plant cell *22*, 3621-3633.
Liu, D., McIlvain, H.B., Fennell, M., Dunlop, J., Wood, A., Zaleska, M.M., Graziani, E.I., and Pong, K. (2007). Screening of immunophilin ligands by quantitative analysis of neurofilament expression and neurite outgrowth in cultured neurons and cells. J Neurosci Methods *163*, 310-320.
Lucas, M., Godin, C., Jay-Allemand, C., and Laplaze, L. (2008). Auxin fluxes in the root apex co-regulate gravitropism and lateral root initiation. Journal of experimental botany *59*, 55-66.
Lucas, M., Kenobi, K., von Wangenheim, D., Vobeta, U., Swarup, K., De Smet, I., Van Damme, D., Lawrence, T., Peret, B., Moscardi, E., *et al.* (2013). Lateral root morphogenesis is dependent on the mechanical properties of the overlaying tissues. Proceedings of the National Academy of Sciences of the United States of America *110*, 5229-5234.
Ma, Y., Szostkiewicz, I., Korte, A., Moes, D., Yang, Y., Christmann, A., and Grill, E. (2009). Regulators of PP2C phosphatase activity function as abscisic acid sensors. Science *324*, 1064-1068.
Malamy, J.E. (2005). Intrinsic and environmental response pathways that regulate root system architecture. Plant, cell & environment *28*, 67-77.
Malamy, J.E., and Benfey, P.N. (1997). Organization and cell differentiation in lateral roots of *Arabidopsis* thaliana. Development *124*, 33-44.
Marhavy, P., Vanstraelen, M., De Rybel, B., Zhaojun, D., Bennett, M.J., Beeckman, T., and Benkova, E. (2013). Auxin reflux between the endodermis and pericycle promotes lateral root initiation. The EMBO journal *32*, 149-158.
Marshall, A., Aalen, R.B., Audenaert, D., Beeckman, T., Broadley, M.R., Butenko, M.A., Cano-Delgado, A.I., de Vries, S., Dresselhaus, T., Felix, G., *et al.* (2012). Tackling Drought Stress: RECEPTOR-LIKE KINASES Present New Approaches. Plant Cell *24*, 2262.
Melcher, K., Xu, Y., Ng, L.M., Zhou, X.E., Soon, F.F., Chinnusamy, V., Suino-Powell, K.M., Kovach, A., Tham, F.S., Cutler, S.R., *et al.* (2010). Identification and mechanism of ABA receptor antagonism. Nat Struct Mol Biol *17*, 1102-1108.
Moreno-Risueno, M.A., and Benfey, P.N. (2011). Time-based patterning in development: The role of oscillating gene expression. Transcription *2*, 124-129.

Moreno-Risueno, M.A., Van Norman, J.M., Moreno, A., Zhang, J., Ahnert, S.E., and Benfey, P.N. (2010). Oscillating gene expression determines competence for periodic *Arabidopsis* root branching. Science *329*, 1306-1311.
Mortlock, A.A., Keen, N.J., Jung, F.H., Heron, N.M., Foote, K.M., Wilkinson, R.W., and Green, S. (2005). Progress in the development of selective inhibitors of aurora kinases. Curr Top Med Chem *5*, 807-821.
Mosquna, A., Peterson, F.C., Park, S.Y., Lozano-Juste, J., Volkman, B.F., and Cutler, S.R. (2011). Potent and selective activation of abscisic acid receptors in vivo by mutational stabilization of their agonist-bound conformation. Proc Natl Acad Sci U S A *108*, 20838-20843.
Ohashi-Ito, K., and Bergmann, D.C. (2007). Regulation of the *Arabidopsis* root vascular initial population by LONESOME HIGHWAY. Development *134*, 2959-2968.
Okushima, Y., Fukaki, H., Onoda, M., Theologis, A., and Tasaka, M. (2007). ARF7 and ARF19 regulate lateral root formation via direct activation of LBD/ASL genes in *Arabidopsis*. The Plant cell *19*, 118-130.
Okushima, Y., Overvoorde, P.J., Arima, K., Alonso, J.M., Chan, A., Chang, C., Ecker, J.R., Hughes, B., Lui, A., Nguyen, D., *et al.* (2005). Functional genomic analysis of the AUXIN RESPONSE FACTOR gene family members in *Arabidopsis* thaliana: unique and overlapping functions of ARF7 and ARF19. The Plant cell *17*, 444-463.
Oliva, M., and Dunand, C. (2007). Waving and skewing: how gravity and the surface of growth media affect root development in *Arabidopsis*. The New phytologist *176*, 37-43.
Pandey, U.B., and Nichols, C.D. (2011). Human disease models in Drosophila melanogaster and the role of the fly in therapeutic drug discovery. Pharmacol Rev *63*, 411-436.
Parizot, B., Laplaze, L., Ricaud, L., Boucheron-Dubuisson, E., Bayle, V., Bonke, M., De Smet, I., Poethig, S.R., Helariutta, Y., Haseloff, J., *et al.* (2008). Diarch symmetry of the vascular bundle in *Arabidopsis* root encompasses the pericycle and is reflected in distich lateral root initiation. Plant physiology *146*, 140-148.
Park, S.Y., Fung, P., Nishimura, N., Jensen, D.R., Fujii, H., Zhao, Y., Lumba, S., Santiago, J., Rodrigues, A., Chow, T.F., *et al.* (2009). Abscisic acid inhibits type 2C protein phosphatases via the PYR/PYL family of START proteins. Science *324*, 1068-1071.
Paul, A.L., Amalfitano, C.E., and Ferl, R.J. (2012). Plant growth strategies are remodeled by spaceflight. BMC plant biology *12*, 232.
Peret, B., Clement, M., Nussaume, L., and Desnos, T. (2011). Root developmental adaptation to phosphate starvation: better safe than sorry. Trends in plant science *16*, 442-450.
Pueyo, J.I., Lanfear, R., and Couso, J.P. (2008). Ancestral Notch-mediated segmentation revealed in the cockroach Periplaneta americana. Proceedings of the National Academy of Sciences of the United States of America *105*, 16614-16619.
Richter, G.L., Monshausen, G.B., Krol, A., and Gilroy, S. (2009). Mechanical stimuli modulate lateral root organogenesis. Plant physiology *151*, 1855-1866.
Robert, S., Chary, S.N., Drakakaki, G., Li, S., Yang, Z., Raikhel, N.V., and Hicks, G.R. (2008). Endosidin1 defines a compartment involved in endocytosis of the brassinosteroid receptor BRI1 and the auxin transporters PIN2 and AUX1. Proc Natl Acad Sci U S A *105*, 8464-8469.
Savaldi-Goldstein, S., Baiga, T.J., Pojer, F., Dabi, T., Butterfield, C., Parry, G., Santner, A., Dharmasiri, N., Tao, Y., Estelle, M., *et al.* (2008). New auxin analogs with growth-promoting

effects in intact plants reveal a chemical strategy to improve hormone delivery. Proc Natl Acad Sci U S A *105*, 15190-15195.
Stollewerk, A., Schoppmeier, M., and Damen, W.G. (2003). Involvement of Notch and Delta genes in spider segmentation. Nature *423*, 863-865.
Sugimoto, K., Jiao, Y., and Meyerowitz, E.M. (2010). *Arabidopsis* regeneration from multiple tissues occurs via a root development pathway. Developmental cell *18*, 463-471.
Tice, C.M. (2001). Selecting the right compounds for screening: does Lipinski's Rule of 5 for pharmaceuticals apply to agrochemicals? Pest Manag Sci *57*, 3-16.
Trask, O.J. (2004). Nuclear Factor Kappa B (NF-kappaB) Translocation Assay Development and Validation for High Content Screening. In Assay Guidance Manual, G.S. Sittampalam, N. Gal-Edd, M. Arkin, D. Auld, C. Austin, B. Bejcek, M. Glicksman, J. Inglese, V. Lemmon, Z. Li, *et al.*, eds. (Bethesda (MD)).
Tsuchiya, Y., Vidaurre, D., Toh, S., Hanada, A., Nambara, E., Kamiya, Y., Yamaguchi, S., and McCourt, P. (2010). A small-molecule screen identifies new functions for the plant hormone strigolactone. Nat Chem Biol *6*, 741-749.
Valvekens, D., Montagu, M.V., and Van Lijsebettens, M. (1988). Agrobacterium tumefaciens-mediated transformation of *Arabidopsis* thaliana root explants by using kanamycin selection. Proceedings of the National Academy of Sciences of the United States of America *85*, 5536-5540.
Van Damme, D., De Rybel, B., Gudesblat, G., Demidov, D., Grunewald, W., De Smet, I., Houben, A., Beeckman, T., and Russinova, E. (2011). *Arabidopsis* alpha Aurora kinases function in formative cell division plane orientation. Plant Cell *23*, 4013-4024.
Van Norman, J.M., Xuan, W., Beeckman, T., and Benfey, P.N. (2013). To branch or not to branch: the role of pre-patterning in lateral root formation. Development *140*, 4301-4310.
Vanneste, S., De Rybel, B., Beemster, G.T., Ljung, K., De Smet, I., Van Isterdael, G., Naudts, M., Iida, R., Gruissem, W., Tasaka, M., *et al.* (2005). Cell cycle progression in the pericycle is not sufficient for SOLITARY-ROOT/IAA14-mediated lateral root initiation in *Arabidopsis* thaliana. The Plant cell *17*, 3035-3050.
Verbelen, J.P., De Cnodder, T., Le, J., Vissenberg, K., and Baluska, F. (2006). The Root Apex of *Arabidopsis* thaliana Consists of Four Distinct Zones of Growth Activities: Meristematic Zone, Transition Zone, Fast Elongation Zone and Growth Terminating Zone. Plant signaling & behavior *1*, 296-304.
Yoshida, R., Hobo, T., Ichimura, K., Mizoguchi, T., Takahashi, F., Aronso, J., Ecker, J.R., and Shinozaki, K. (2002). ABA-activated SnRK2 protein kinase is required for dehydration stress signaling in *Arabidopsis*. Plant & cell physiology *43*, 1473-1483.
Zhang, J.H., Chung, T.D., and Oldenburg, K.R. (1999). A Simple Statistical Parameter for Use in Evaluation and Validation of High Throughput Screening Assays. J Biomol Screen *4*, 67-73.
Zolman, B.K., Nyberg, M., and Bartel, B. (2007). IBR3, a novel peroxisomal acyl-CoA dehydrogenase-like protein required for indole-3-butyric acid response. Plant molecular biology *64*, 59-72.

“Imagination is more important than knowledge. For knowledge is limited to all we now know and understand, while imagination embraces the entire world, and all there ever will be to know and understand.”

Albert Einstein

Chapter 2

Root cap derived auxin patterns the root system

Adapted From:

Wei Xuan, Dominique Audenaert, Boris Parizot, Barbara Möller, Maria F. Njo, Marlies Demeulenaere, Bert De Rybel, Gert Van Isterdael, Ari Pekka Mähönen, Steffen Vanneste, Tom Beeckman. Root cap derived auxin patterns the root system. Manuscript in preparing.

Root cap derived auxin prepatterns the root system

Authors: Wei Xuan[1,2]*, Dominique Audenaert[1,2]*#, Boris Parizot[1,2], Barbara Möller[1,2], Maria F. Njo[1,2], Marlies Demeulenaere[1,2], Bert De Rybel[1,2†], Gert Van Isterdael[1,2], Ari Pekka Mähönen[3,4], Steffen Vanneste[1,2], Tom Beeckman[1,2§]

Affiliations:

[1]Department of Plant Systems Biology, VIB, Gent, Belgium.

[2]Department of Plant Biotechnology and Bioinformatics, Gent University, Gent, Belgium.

[3]Institute of Biotechnology, University of Helsinki, Helsinki 00014, Finland.

[4]Department of Biosciences, University of Helsinki, Helsinki 00014, Finland.

*These authors contributed equally to this work.

[#]Present address: Compound Screening Facility, VIB, Ghent University, Gent, Belgium

[†]Present address: Laboratory of Biochemistry, Wageningen University, Dreijenlaan 3, 6703HA Wageningen, The Netherlands.

[§] Corresponding author. E-mail: tobee@psb.vib-ugent.be

Abstract:

Spatiotemporal coordination of organ formation is a central question in plant and animal development. In *Arabidopsis thaliana*, root branching begins with oscillatory gene activity in the primary root to create prebranch sites, patches of cells competent to form a lateral root. Thus far, the molecular components that regulate the oscillations were still unknown. Here, we show that auxin perception is required for the oscillations. Furthermore, we reveal a local auxin source in the root cap, derived from the auxin precursor indole-3-butyric acid (IBA), that modulates the oscillation amplitude which in turn determines whether a prebranch site is created or not. Moreover, transcriptome profiling identified novel and IBA-regulated components of root patterning, such as the *MEMBRANE-ASSOCIATED KINASE REGULATOR4 (MAKR4)* that translates the prebranch sites into a regular spacing of lateral organs. Thus, the spatiotemporal patterning of roots is fine-tuned by the root cap-specific conversion pathway of IBA to auxin.

Introduction

Prepatterning is the spatiotemporal specification of subsets of cells to become competent for organogenesis. The characteristics of this process are shared by plants and animals and have been linked to a biological clock that converts temporal information into a periodic spatial pattern (*1-3*). Prepatterning, in which equivalent organs need to be positioned repeatedly along an elongating axis, occurs during somitogenesis in the vertebrate embryo and lateral root (LR) formation in plants (1-4). In case of the root clock in Arabidopsis, periodic induction of gene expression in the transition zone creates oscillations in the growing primary root that are proposed to prepare cells to produce a LR (*1*). These oscillations are recorded in the transition zone of the root apex, also referred to as oscillation zone (OZ), a region close to the tip where meristematic cells stop dividing and rapidly elongate. The oscillations can be visualized by the synthetic auxin signaling output reporter *DR5* (*1, 5*). When cells with high *DR5* expression levels leave the OZ, the expression is maintained and becomes fixed in regularly spaced prebranch sites along the primary root capable to form LRs.

Thus far, the endogenous molecular components that regulate the oscillations are unknown. In addition, whether auxin plays a role in LR prepatterning is still an open question, despite several reported observations. Gravitropic stimulation activates dynamic redistribution of auxin to the lower side of the root in lateral root cap and epidermal cells (*6*). This not only induces root bending but repeated gravistimulation also accelerates the periodicity of *DR5* oscillations (*1*), suggesting that differential auxin distribution might play a role in LR prepatterning. Furthermore, the canonical auxin signaling transcription factor AUXIN RESPONSE FACTOR7 (ARF7) is required for regular oscillations (*1*). However, exogenous application of the most abundant endogenous auxin indole-3-acetic acid (IAA) results in severe and pleiotropic effects on plant growth (*7*), masking its effect on prebranch site formation. Recently, we found that the auxin precursor indole-3-butyric acid (IBA) more specifically induces LR formation by using a chemical biology approach (*8*). IBA-to-IAA conversion depends on several peroxisomal enzymes, such as INDOLE-3-BUTYRIC ACID RESPONSE1 (IBR1), IBR3, and IBR10 (*9, 10*), of which some are specifically produced in the root cap (*8*). The root cap is the first organ that senses the soil during growth; it protects the meristem and directs root growth in response to gravity and other environmental signals. In addition to these functions, we reveal that the root cap represents an auxin resource that controls the regular distribution of lateral organs to optimize the uptake of water and nutrients from the soil.

Results

Auxin perception is required to translate the oscillation signal.

Previously, the *DR5* oscillation in the OZ had been shown to have a mean period of ~6 hours in 2-day-old seedlings (*1*). We obtained a similar time interval of *DR5* pulses in these very young seedlings, but also observed that the oscillation frequency decreased with seedling age, and reached almost a steady-state situation in older seedlings (Fig. 1A). In all experiments described hereafter, we measured *DR5* oscillations in 3-day-old seedlings.

Although local auxin application had been reported to be insufficient to alter the root clock periodicity, several observations suggest that auxin is involved in the establishment of the LR prepattern (*1*, *6*). To clarify the role of auxin in this process, we examined whether auxin perception is required to control the root clock. In the plant model system *Arabidopsis thaliana*, auxin is perceived by the TRANSPORT INHIBITOR RESPONSE1 (TIR1)/AUXIN-RELATED F-BOX (AFB) members of the F-box protein family that act in concert with Aux/IAA transcriptional repressors to control auxin response. Previously, TIR1 and AFB2 have been found to be the predominantly expressed auxin receptors in the root (*11*), and we found *TIR1* and *AFB2* to be expressed in the OZ (fig. S1). Consistently with the role of auxin in LR formation, in the *tir1afb2* double mutant the number of lateral root primordia (LRPs) and emerged LRs was strongly reduced in 8-day-old seedlings (Fig. 1, B and C and fig. S1). We also detected a severely decreased number of prebranch sites in the *tir1afb2* double mutant (Fig. 1, B and C), consistent with a role in LR prepatterning. This reduction in prebranch site number cannot be attributed to an altered gravitropic response (fig. S1). In addition, the *DR5* oscillation frequency was unaltered (Fig. 1E), indicating that the *DR5* oscillation periodicity is not the only factor that controls prebranch site formation. In contrast, the levels of *DR5:Luciferase* expression had decreased strongly in the OZ of *tir1afb2* double mutants (Fig. 1D, Movie S1). Taken together, these results show that auxin perception is required to prepattern the root branching by modulating the oscillation intensity.

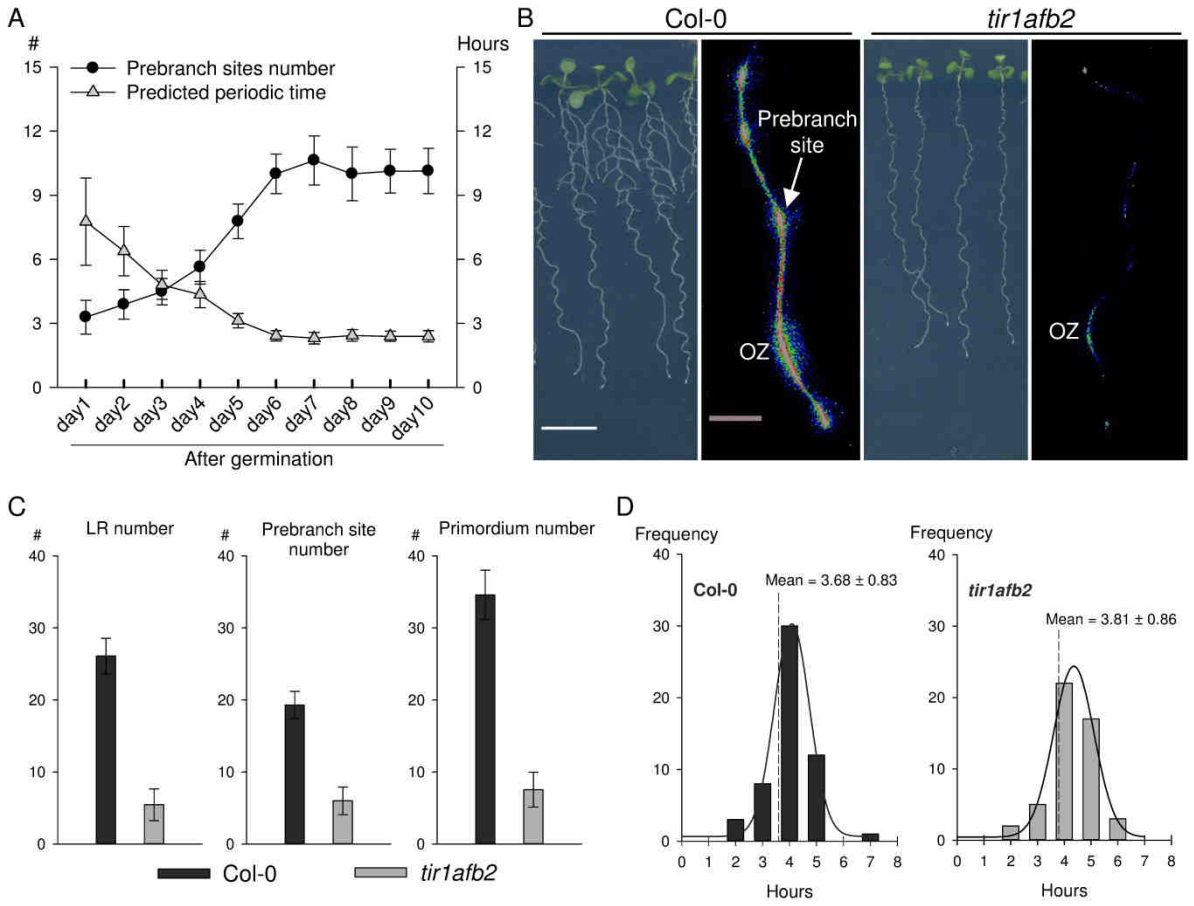

Fig. 1. Auxin receptor-dependent auxin signaling is required for prebranch site formation. (A) Analysis of prebranch site number and predicted periodicity. To count the prebranch site numbers formed daily in Col-0 seedlings of different age, the position of the primary root tip was labeled each day. Twenty-four hours later, static *DR5:Luciferase* expression patches along the newly formed part of the primary root outside the OZ were counted as prebranch sites. Predicted periodic time was calculated by dividing each 24 hour period by the number of prebranch sites established in this period (n > 30 per day). **(B)** Root phenotype and *DR5:Luciferase* expression in roots of Col-0 and *tir1afb2* double mutant seedlings. Bright-field images were taken from 8-day-old seedlings (Scale bar, 1 cm) and *DR5:Luciferase* was expressed in 3-day-old seedlings (Scale bar, 0.1 cm). **(C)** Quantification of the number of LR, prebranch sites, and LRP in 8-day-old Col-0 and *tir1afb2* seedlings. Error-bars are means ± standard deviation (n = 10). **(D)** Distribution of periodic time of *DR5:Luciferase* oscillations in 3-day-old Col-0 and *tir1afb2* seedlings (n > 15).

The IBA-to-IAA conversion controls the oscillation amplitude.

Based on the expression pattern of IBA-to-IAA conversion genes, this conversion pathway might act as a local auxin source that contributes to a spatially restricted auxin response in the OZ (*8*). We investigated whether genetic perturbations of the IBA-to-IAA conversion affect the *DR5* oscillations. The *ibr1ibr3ibr10* triple mutant is defective in enzymes of the IBA-to-IAA conversion pathway and had a reduced number of LRs and early stage LRP (*11*) (Fig. 2A). This was also reflected in failure to induce LRs in ~19.6% of the root curves in gravistimulated seedlings, while the gravitropic response was not altered in the *ibr1ibr3ibr10* triple mutant (fig. S2). Moreover, the number of prebranch sites was reduced in 8-day-old *ibr1ibr3ibr10* triple mutant seedlings (Fig. 2, A and D). ENOYL-CoA HYDRATASE2 (ECH2) is another peroxisomal enzyme required for IBA response (*12*). Consistentl with a stronger defect in IBA-to-IAA conversion (*12*) the number of prebranch sites was lower in the *ech2ibr1ibr3ibr10* quadruple mutant than in the triple mutant (Fig. 2, A and D), revealing a correlation between the IBA-to-IAA conversion and prebranch site formation. Similarly to the *tir1 afb2* mutant, the oscillation frequency in the *ibr1ibr3ibr10* triple mutant was only slightly reduced (~9% compared to the wild type; fig. S2), while the *DR5* expression levels in the OZ of the *ibr1ibr3ibr10* triple mutant seemed to be decreased considerably (Fig. 2D), again implying that the amplitude of the oscillations may be crucial for prebranch site formation.

Altogether, our results suggest that the amplitude of the oscillation modulates the LR prepattern. Therefore, we investigated whether there is any correlation between the amplitude of *DR5* oscillations in the OZ and the subsequent establishment of prebranch sites. To this end, the *DR5* expression levels in the OZ of several subsequent oscillations were measured for 24 hours (Fig. 2B, and Movies S1-S4) and were compared with the number of prebranch sites that were established as a result of these oscillations (Fig. 2C). At least 15 seedlings per genotype (Col-0, *tir1afb2* double mutant, *ibr1ibr3ibr10* triple mutant, *ech2ibr1ibr3ibr10* quadruple mutant and IBA-treated Col-0 seedlings) were analyzed to obtain a large number of measurements (n > 30 per genotype) (Fig. 2, B and C and fig. S2). Exogenous IBA substantially increased the number of LRs in a dose-dependent manner (fig. S2). In seedlings treated with 1 µM IBA, both *DR5* oscillation amplitude (136.3% of wild-type level) and frequency (135.9% of wild-type level) were higher than in mock-treated seedlings, resulting in a strongly increased number of prebranch sites (167.7% of wild-type) (Fig. 2, B and C and fig. S2). In all tested mutant combinations, the decrease in *DR5* oscillation amplitude was followed by a proportional reduction in the prebranch site numbers. In the *ibr1ibr3ibr10* triple

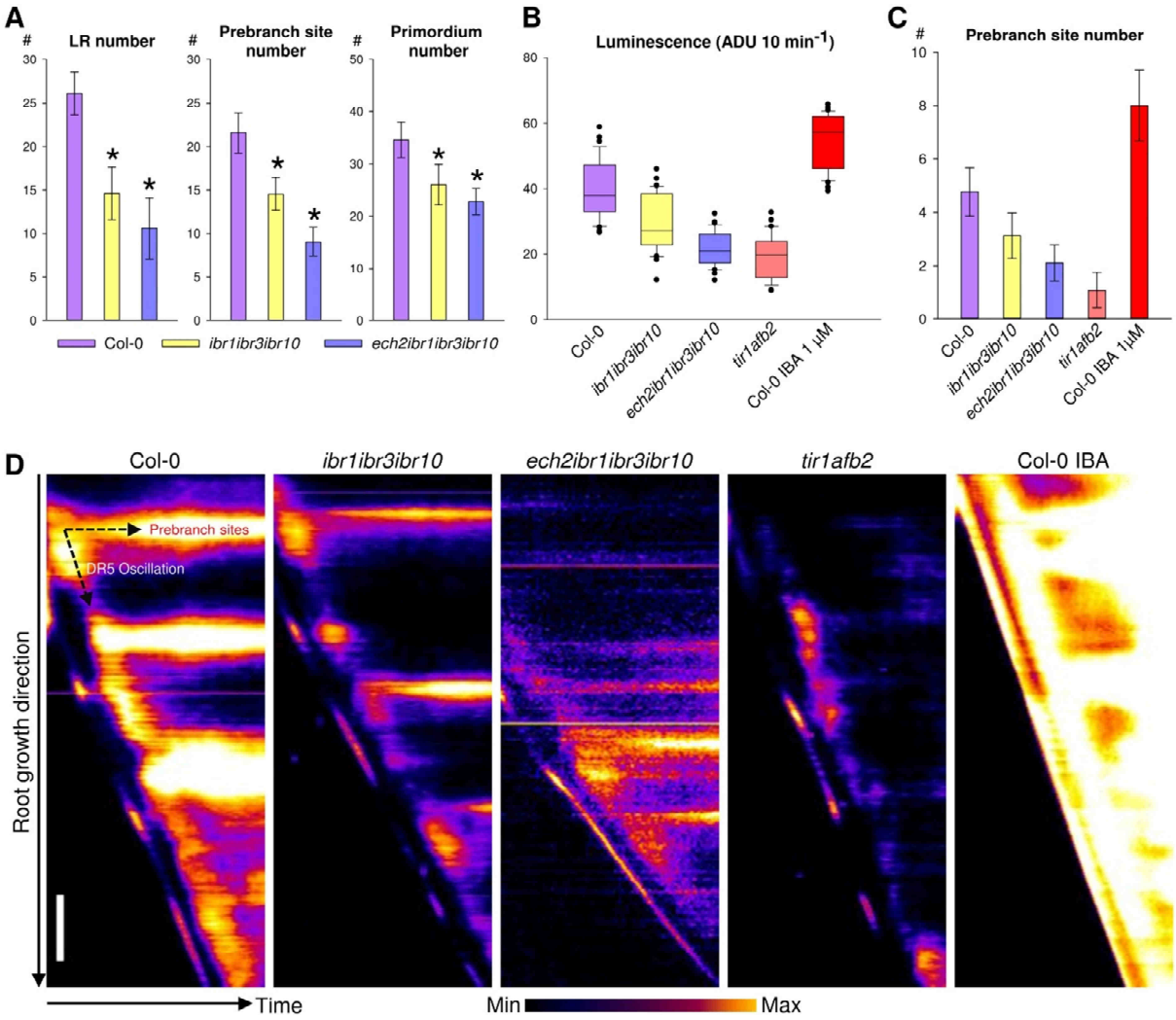

Fig. 2. IBA-to-IAA conversion regulates the oscillation amplitude and the prebranch site numbers. (A) The number of LRs, prebranch sites, and LRPs in 8-day-old Col-0, *ibr1ibr3ibr10* triple mutant, and *ech2ibr1ibr3ibr10* quadruple mutant seedlings (n = 10). **(B)** Box plot of peak intensity values of *DR5:Luciferase* oscillations in 3-day-old Col-0, *ibr1ibr3ibr10* triple mutant, *ech2ibr1ibr3ibr10* quadruple mutant, *tir1afb2* double mutant and IBA-treated Col-0 seedlings. Each box plot was produced from at least 34 measurements from seedlings grown during 24 hours on half-strength MS medium. ADU, analog-digital units. **(C)** Quantification of the number of prebranch sites formed over 24 hours as a result of the oscillations shown in (**B**) for lines with or without IBA treatment. **(D)** Kymograph of *DR5:Luciferase* intensity along the primary root of transgenic 3-day-old lines with or without IBA treatment during 24 hours. Scale bar, 0.1 cm.

mutant, the average amplitude of *DR5* oscillations was 73.8% of the wild-type level (Fig. 2B), whereas 65.5% of the wild-type prebranch site numbers were established as a result of these oscillations (Fig. 2C). In the *ech2ibr1ibr3ibr10* quadruple mutant, the oscillation amplitude was more reduced (54.5% of the wild-type level) and the number of prebranch sites lower (44.2% of the wild-type level) (Fig. 2, B and C). Finally, in the *tir1afb2* double mutant, the

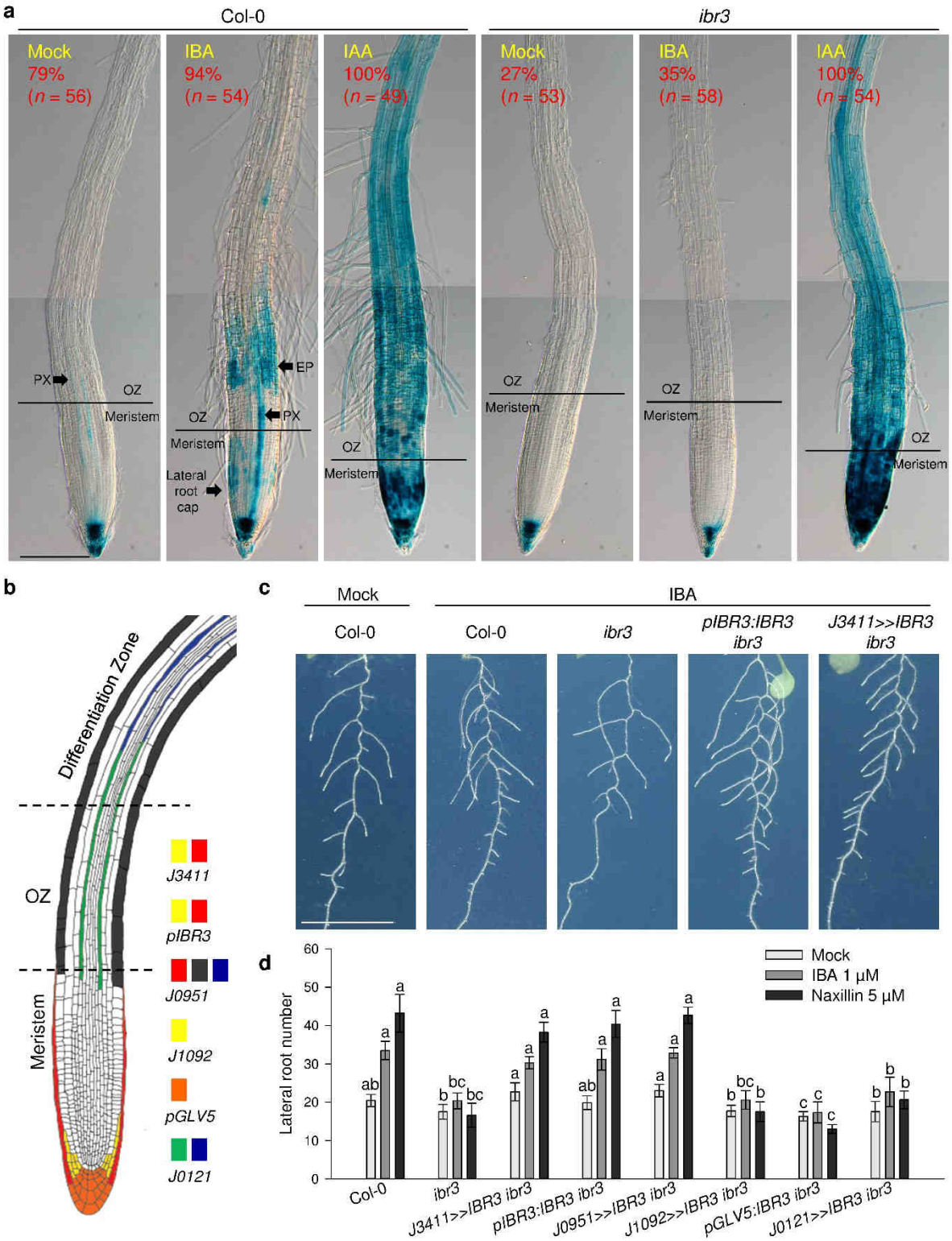

Fig. 3. An auxin source derived from the root cap-specific IBA-to-IAA conversion regulates root patterning. a, *DR5:GUS* expression in the root tips of three-day-old Col-0 and *ibr3* seedlings after 24 hours treatment with or without 3 µM IBA or 0.1 µMIAA. PX, protoxylem pole; Ep, epidermis; OZ, oscillation zone. The percentage indicated the proportion of seedlings showing the same expression pattern in a population of seedlings. **b,** Schematic longitudinal view of root cap cells in the primary root. Enhancer trap lines J3411, J0951, and J1092 were expressed in different LR cap tissue domains; J0121 was expressed in the pericycle associated with the xylem poles; and the IBR3 and GLV5 promoter were lateral root cap and columella specific respectively. **c, d,** Root phenotype and LR

number of enhancer trap lines trans-activating the *IBR3* gene expression in the *ibr3* mutant background. Three-day-old seedlings treated with or without 1 µM IBA or 5 µM Naxillin for 5 days (**c**) and LR number of these seedlings **(d)**. Scale bar, 1 cm. Different letters indicate significant differences among means ($P < 0.05$ by one way ANOVA and Tukey's test as post hoc analysis compared to Col-0 under different treatments respectively, $n > 10$).

lowest oscillation amplitude (46.8% of the wild-type level) correlated with the lowest number of prebranch sites (22.7% of wild-type level) (Fig. 2, B and C). In conclusion, the amplitude of the *DR5* oscillation in the OZ determines whether this temporary signal is transmitted to produce a prebranch site capable to form a LR. We showed that the levels of IBA and IBA-to-IAA conversion regulate the amplitude of the *DR5* oscillation. As such, the level of the IBA-to-IAA conversion represents an important mechanism to regulate the LR prepattern.

An auxin source derived from root cap cells feeds into the root clock.

Based on the expression pattern of IBA-to-IAA conversion genes, we previously suggested that the IBA-to-IAA conversion creates an auxin source in the root cap (*8*). Analysis of the *DR5::GUS* reporter line expression showed that unlike IAA, exogenous IBA specifically induced an auxin response maximum in the root cap and OZ that depends on IBA-to-IAA conversion enzymes (Fig. 3A). Therefore, we investigated the contribution of the root cap and of other tissues for the effect of IBA response on root prepatterning. A GAL4-based transactivation approach was applied to target the expression of *IBR3* in different root cap tissues in the *ibr3* mutant background. The *ibr3 mutant* is not responding to treatments with IBA or with naxillin, a synthetic compound enhancing IBA-to-IAA pathways (*8*) (Fig. 3, C and D). The IBA- or naxillin-insensitivity of the *ibr3* mutant towards LR development could be completely rescued by expressing *IBR3* under the control of the native promoter (lateral root cap), or transactivating *IBR3* in the expression domain of J3411 (lateral root cap) and J0951 (outer lateral root cap cells, epidermis and pericycle in differentiation zone) (*14*), but not of J1092 (lateral root cap initials), J0121 (pericycle cells) or *GOLVEN5* promoter (columella) (Fig. 3, B, C and D). These results imply that the IBA-to-IAA conversion pathway is active specifically in the outer lateral root cap cells to promote LR formation.

Factors downstream of the IBA-to-IAA conversion regulate root patterning.

The high auxin production in outer lateral root cap cells induced an auxin response maximum specifically in the OZ (Fig. 3H). Likewise, exogenous IBA induced an auxin

response maximum in the OZ that depended on IBA-to-IAA conversion enzymes (fig. S3). These results suggest that auxin production in root cap cells regulates auxin signaling in the OZ. To explore downstream components of this signaling process, we performed a transcriptome profiling to identify early transcriptional changes downstream of the IBA-to-IAA conversion in Col-0 and *ibr1ibr3ibr10* triple mutant roots 6 hours after IBA treatment. According to the effect of the root cap-specific IBA-to-IAA conversion on auxin signaling in the OZ, we used a root segment that included root cap, meristem, and OZ (Fig. 4A). We found 66 genes that were induced by IBA in an IBR1 IBR3 IBR10 dependent manner (two-way analysis of variance [ANOVA], fold change [FC] ≥ 3; *P*-value ≤ 0.01; Table S1, see Materials and Methods and eFP browser http://bar.utoronto.ca/~asher/efp_arabidopsis/cgi-bin/efpWeb.cgi?dataSource=Lateral_Root_Initiation) (*16*). Among these genes, gene ontology analysis revealed that genes involved in the response to auxin stimulus were significantly enriched, confirming the validity of our approach (Table S1).

To detect candidate genes downstream of the endogenous IBA-to-IAA conversion pathway, we selected genes that were also significantly upregulated by naxillin, a synthetic IBA-to-IAA pathway-enhancing compound (*8*). We identified two genes involved in auxin homeostasis. Transcript profiling showed that the auxin conjugation enzyme *GH3.3* was highly upregulated after IBA treatment (FC~40), whereas *GH3.6* was upregulated 3.7-fold; quantitative polymerase chain reaction (qPCR) experiments confirmed that the upregulation depended on *IBR1 IBR3 IBR10* (fig. S3) (*17, 18*). By means of transcriptional reporters, *GH3.6* was found to be specifically expressed in the root cap and *GH3.3* in the columella, the meristematic protoxylem pole, and early LRP stages (Fig. 4B and fig. S3). Although the number of LRs in *gh3.3* and *gh3.6* single and double mutants was not altered (fig. S3), estradiol-inducible overexpression of *GH3.3* and *GH3.6* significantly reduced the number of LRs, LRP, and prebranch sites (Fig. 4, C and D and fig. S3). These results suggest that, after IBA application, auxin conjugation enzymes are upregulated to moderate the excess amount of free IAA produced as a result of enhanced IBA-to-IAA conversion. Hence, decreased IAA levels in the root cap reduce the number of prebranch sites, demonstrating the importance of a local auxin source for LR prepatterning.

To select candidate genes that might function downstream of IBA-to-IAA conversion in LR prepatterning, we searched for genes that were expressed in phase or anti-phase with *DR5* oscillations in the OZ (*1*). Among these genes, *MEMBRANE-ASSOCIATED KINASE REGULATOR4 (MAKR4)* was also induced by auxin in the pericycle layer where LR initiation occurs (*19*), and had recently been proposed to be involved in hormone signaling based on homology with another member of this family of seven putative MAKRs (*20*).

qPCR experiments validated that MAKR4 was ~5-fold upregulated upon IBA treatment in an *IBR1 IBR3 IBR10*-dependent manner (fig. S4). We generated a transcriptional reporter with ~1.8 kb of the *MAKR4* promoter, driving Click Beetle luciferase *CBGr99* that has a stronger photon yield than the firefly luciferase (*21*). *MAKR4* was expressed in the protoxylem pole of the meristem and was specifically induced in newly formed prebranch sites following oscillations (Fig. 4, E-G and Movie S5). The MAKR4 protein also accumulated in protoxylem cells in the meristem and in prebranch sites in pericycle cells before nuclear migration, which marks the start of LR initiation (Fig. 4J and K and Movie S6). Subsequently, MAKR4 protein was present in outer root layers of early stage LRP, such as the endodermis and cortex that need to be penetrated by the growing LRP (Fig. 4K). In accordance with the reported localization of the homologous BRI1 KINASE INHIBITOR1 (BKI1) protein (*20*), the MAKR4 protein was localized in the plasma membrane and cytoplasm, and appeared to accumulate relatively densely around the nucleus (Fig. 5J). These results suggest the involvement of MAKR4 in root patterning.

Indeed, the *makr4* mutant and the amiRNAi *MAKR4* lines produced significantly fewer LRs and LRP than the wild type, whereas *MAKR4* overexpression promoted LR formation (Fig. 4, H, I and fig. S4). Expression of the MAKR4 protein under its endogenous promoter complemented the *makr4* mutant, confirming that the loss of MAKR4 was responsible for the *makr4* LR phenotype (fig. S4). However, the estradiol-inducible artificial microRNA interference (amiRNAi) line directed to *MAKR4* had unaltered prebranch site numbers (fig. S4). In conclusion, MAKR4 functions downstream of the IBA-to-IAA conversion and is probably involved in a still unknown signaling process that is required to successfully translate a prebranch site into a LR.

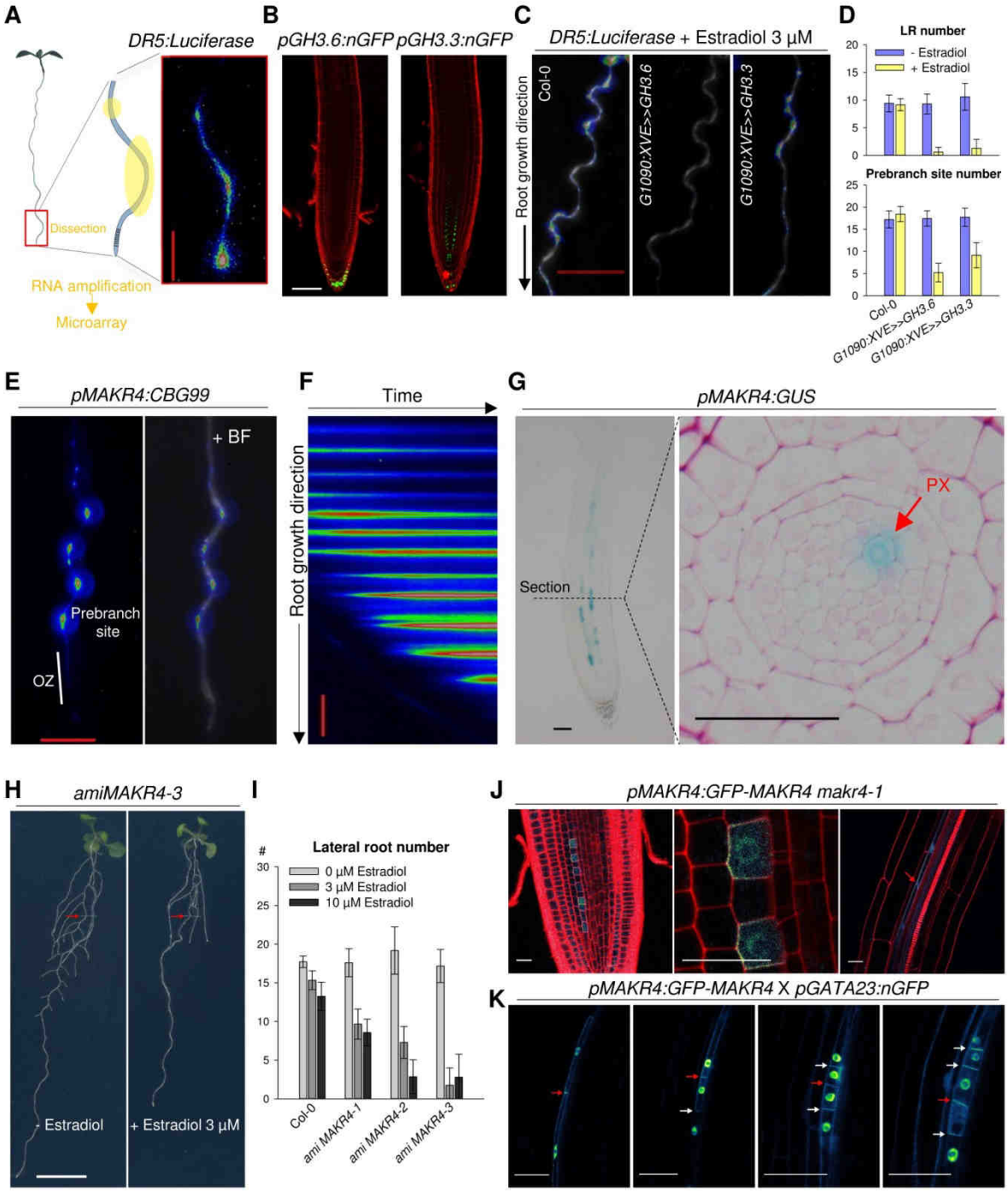

Fig. 4. Auxin homeostasis genes act downstream of the IBA-to-IAA conversion to regulate LR development. (A) Scheme of the root zone (red box) of Col-0 and *ibr1ibr3ibr10* triple mutant seedlings used for transcript profiling after IBA treatment. Scale bar, 0.5 mm. **(B)** Expression pattern of propidium iodide-stained 3-day-old *GH3.6:nGFP* and *GH3.3:nGFP* transcriptional reporter lines in primary root tip. Scale bar, 100 µM. **(C and D)** *DR5:Luciferase* expression and LR and prebranch site numbers of estradiol-inducible *GH3.3* and *GH3.6* overexpression lines. Two-day-old seedlings were treated with or without 3 µM estradiol for 5 more days before LR and prebranch site numbers from the newly grown part of the primary root were quantified. **(E)** *pMAKR4:CBG99* expression in three-day-old seedlings. Luciferase image was overlayed with bright field (BF) image, Scale bar, 0.2 cm. **(F)**

Kymograph based on quantification of *pMAKR4:CBG99* intensity along the primary root during twenty four hours **(G)** Expression pattern of 3-day-old *pMAKR4:GUS* seedlings. The dotted line gives the position of the transversal section shown in the inset. PX, protoxylem. Scale bar, 20 µm. **(H and I)** LR phenotype and LR number of estradiol-inducible *amiMAKR4* lines. Three-day-old seedlings were treated with or without estradiol for 5 more days before images were taken (Scale bar, 1 cm in H) and LR number from the newly grown part of the primary root (red arrow in H) were quantified. **(J)** Localization of pMAKR4:GFP-MAKR4 protein in propidium iodide-stained primary root and prebranch site of 3-day-old seedlings. Scale bar, 20 µM. **(K)** Localization of pMAKR4:GFP-MAKR4 protein during LR initiation in *pGATA23:nGFP* seedlings. Red arrows indicate localization of MAKR4 in the plasma membranes near the anticlinal cell walls of 2 adjacent pericycle founder cells before nuclear migration. White arrows indicate localization of MAKR4 in the plasma membranes adjacent to newly formed anticlinal cell walls of the small daughter cells after asymmetric cell division. Scale bar, 50 µM. Error-bars are means ± standard deviation. $*P < 0.01$ by two-sided Student's *t* test indicated statistically significant differences from Col-0 ($n > 10$).

Discussion.

The role played by the plant hormone auxin in positioning new organs is a central question in plant biology. During LR organogenesis, an auxin-independent mechanism that involves oscillatory gene activity has been proposed to specify subsets of cells competent to form a new organ, a process that is considered as prepatterning of root branching (*1*). Our findings suggest that endogenous auxin levels are both sufficient and necessary to modulate this prepatterning and that auxin perception is essential for this process. We present evidence that root cap-specific IBA-to-IAA conversion creates a local auxin source that modulates both the oscillation amplitude and periodicity. Furthermore, we identified the oscillation amplitude as an important factor determining whether an oscillation is translated into a prebranch site capable of forming a LR. The oscillation amplitude might reflect dynamic fluctuations of the auxin concentration in the OZ. Local auxin accumulation is a shared mechanism to position various organs and tissues in *Arabidopsis* (*22-25*).

Transcriptome profiling has revealed *MAKR4* downstream of the IBA-to-IAA conversion pathway as the first gene reported to be specifically induced in newly formed prebranch sites following oscillations. MAKR4 is a novel membrane-associated kinase regulator, and its membrane localization could hint at cell-cell communication during LR patterning. The cellular localization and the early appearance of MAKR4 during root patterning indicate that MAKR4 is a signaling component that translates the prebranch sites into a regular distribution of lateral organs along the primary root. In vertebrate somitogenesis, the translation of the

prepattern into somites also requires cell-cell communication that depends on Delta-Notch transmembrane signaling (*26*).

In conclusion, our study revealed a crucial role for the root cap in the spatiotemporal patterning of root branching. Already in 1880, Darwin proposed that the very tip of the root is highly suitable to sense external stimuli and to convey them to the upper part of the root to optimize root growth under changing soil conditions (*27*). Our data support this visionary statement by extending the role of the tip to the branching of roots that is required for the increase in surface area of plant root systems.

Acknowledgements

We thank Mark Estelle (University of California, San Diego, CA, USA), Malcolm Bennett (University of Nottingham, UK), Catherine Bellini (Umeå University, Umeå, Sweden/Institut Jean-Pierre Bourgin, INRA-AgroParis Tech, Versailles, France), Lucia C. Strader (Washington University, St. Louis, MO, USA) for the kind gifts of lines and constructs; Matyáš Fendrych for advice on Kymograph; Lorena López-Galvis for help in cloning; and Nicholas Provart and Asher Pasha for help with the eFP browser. This work was funded by grants of the Interuniversity Attraction Poles Programme (IAP VI/33 and IUAP P7/29 'MARS') initiated by the Belgian Science Policy Office, the Research Foundation-Flanders and Ghent University Special Research Fund. W.X. is supported by a grant from the Chinese Scholarship Council (CSC) with cofunding from Ghent University Special Research Fund. B.M. is the recipient of an Omics@vib Marie Curie COFUND fellowship, S.V. is a Postdoctoral Fellow of the Research Foundation-Flanders, and A.P.M is funded by the Academy of Finland.

References

1. M. A. Moreno-Risueno *et al.*, *Science* **329**, 1306-1311 (2010).
2. M. A. Moreno-Risueno, P. N. Benfey, *Transcription* **2**, 124-129 (2011).
3. Y. Harima, R. Kageyama, *Curr. Opin. Genet. Dev.* **23**, 484-490 (2013).
4. J. M. Van Norman, W. Xuan, T. Beeckman, P. N. Benfey, *Development* **140**, 4301-4310 (2013).
5. I. De Smet *et al.*, *Development* **134**, 681-690 (2007).
6. L. R. Band *et al.*, *Proc. Natl. Acad. Sci. USA* **109**, 4668-4673 (2012).

7. M. G. Ivanchenko, S. Napsucialy-Mendivil, J. G. Dubrovsky, *Plant J*. **64**, 740-752 (2010).
8. B. De Rybel *et al., Nat. Chem. Biol*. **8**, 798-805 (2012).
9. B. K. Zolman, M. Nyberg, B. Bartel, *Plant. Mol. Biol*. **64**, 59-72 (2007).
10. B. K. Zolman *et al., Genetics* **180**, 237-251 (2008).
11. G. Parry *et al., Proc. Natl. Acad. Sci. USA* **106**, 22540-22545 (2009).
12. L. C. Strader *et al., Plant Cell* **23**, 984-999 (2011).
13. J. Haseloff, *Methods Cell Biol*. **58**, 139-151 (1999).
14. M. Fendrych *et al., Curr. Biol*. **24**, 931-940 (2014).
15. C. Kares, E. Prinsen, H. Van Onckelen, L. Otten, *Plant Mol. Biol*. **15**, 225-236 (1990).
16. D. Winter *et al., PloS One* **2**, e718 (2007).
17. M. Nakazawa *et al., Plant J.* **25**, 213-221 (2001).
18. P. E. Staswick *et al., Plant Cell* **17**, 616-627 (2005).
19. I. De Smet *et al., Science* **322**, 594-597 (2008).
20. Y. Jaillais *et al., Genes Dev.* **25**, 232-237 (2014).
21. T. Miloud, C. Henrich, G. J. Hämmerling, *J. Biomed. Opt.* **12**, 054018 (2007).
22. Y. Ikeda *et al., Nat. Cell Biol*. **11**, 731-738 (2009).
23. D. Reinhardt *et al., Nature* **426**, 255-260 (2003).
24. M. Ibañes, N. Fàbregas, J. Chory, A. I. Caño-Delgado, *Proc. Natl. Acad. Sci. USA* **106**, 13630-13635 (2009).
25. E. Benková *et al., Cell* **115**, 591-602 (2003).
26. A. C. Oates, L. G. Morelli, S. Ares, *Development* **139**, 625-639 (2012).
27. C. R. Darwin. *The Power of Movement in Plants* (Murray, London, 1880).

SUPPORTING ONLINE MATERIAL

Materials and Methods

Plant growth conditions

Arabidopsis thaliana seeds were surface sterilized with 95% (v/v) ethanol for 5 minutes and 20% (v/v) bleach for 12 minutes. After the seeds had been rinsed 5 times with sterile water, they were imbibed, stratified at 4°C for 3 days, and sown on Petri dishes containing sterile half-strength Murashige and Skoog (1/2MS) medium (0.5 x MS salts, 0.8% sucrose, 0.5 g/L 2-(*N*-morpholino)ethanesulfonic acid MES, pH 5.7, and 1% w/v agar).

Seeds were germinated on vertically positioned Petri dishes in a growth chamber at 21°C under continuous light (100 µmol m^{-2} s^{-1} photosynthetically active radiation), unless otherwise noted. Plants were examined for lateral root phenotypes 8 days after germination (10 days postimbibition [dpi]), unless otherwise noted. For crosses and seed collection, seedlings were transplanted to soil and grown at 22°C with a 16-hour daily illumination (100 µmol m^{-2} s^{-1}).

For hormone and compound treatments, filter-sterilized substances were added to cooled (50°C) molten nutrient medium and mixed in 50-mL Falcon tubes before being poured into Petri dishes. Three-day-old seedlings were transferred to fresh ½MS media with different compounds for an extra 5 days, unless otherwise indicated.

Plant lines used

The *Arabidopsis* accessions Columbia (Col-0) and C24 were used for this study. The auxin-responsive reporter lines *DR5:β-glucuronidase* (*DR5:GUS)* (S*1*) and *DR5:Luciferase* (S*2*) have been described previously. *pGATA23:nGFP* was used as marker line for lateral root initiation in pericycle cells (S*3*). *pTIR1:GUS* and *pAFB2:GUS* lines were kind gifts from Mark Estelle (University of California, San Diego, CA, USA). The GAL4-GFP enhancer trap lines *J0121*, *J0951*, *J3411*, and *J1092* were obtained from the Nottingham Arabidopsis Stock Centre (http://nasc.nott.ac.uk/) and the *UAS:iaaH* line was a gift from Malcolm Bennett (University of Nottingham, UK). The GAL4 enhancer trap lines were crossed with *UAS:iaaH* and the lateral root phenotype of the F1 generation was analyzed.

The origin of the mutant lines used is as follows: the *makr4-1* (Salk_084039) mutant was obtained from the Nottingham Arabidopsis Stock Centre; the auxin receptor mutants were kindly supplied by Mark Estelle (University of California, San Diego, CA, USA); the auxin conjugation mutants *gh3.3-1*, *gh3.3-2*, *gh3.6-1*, *gh3.6-2*, and *gh3.3gh3.6* were kind gifts

from Catherine Bellini (Umeå University, Umeå, Sweden/Institut Jean-Pierre Bourgin, INRA-AgroParis Tech, Versailles, France); and *dlf1-D* was a kind gift from Minami Matsui (RIKEN Plant Science Center, Kanagawa, Japan). The indole-3-buytric acid (IBA) conversion pathway mutants *ibr1-2*, *ibr3-1*, *ibr10-1*, and *ech2-1* have been described previously (S*4*) and *ech2-1ibr1-2ibr3-1ibr10-1* was a kind gift from Lucia C. Strader (Washington University, St. Louis, MO, USA). Double and higher-order mutants harboring various marker lines were generated by crossing. F3 homozygous seedlings were analyzed in all experiments. For the *ibr3* complementation study, F1 seedlings were used to quantify the lateral root phenotype. The primers used to verify that each mutant line was homozygous at the locus of interest are listed in Supplementary Table 2.

Nucleic-acid manipulations and constructs

The Gateway system® (Invitrogen, Carlsbad, CA, USA) was applied to generate most constructs. For transcriptional fusions, ~2-kb promoter fragments upstream of the coding sequence amplified from genomic DNA were cloned into pDONR221 or pDONRP4P1R and subsequently introduced into different expression vectors (S*5*). To generate the *pMAKR4:CBG99* construct, the green luciferase 99-coding sequence of click beetle (*Pyrophorus plagiophthalamus)* was amplified from the pCBG99-Basic Vector (Promega) by polymerase chain reaction (PCR) and introduced into pDONR221; the CBG99-coding sequence was fused to the MAKR4 promoter by Gateway LR reaction. For the *IBR3* transactivation experiment and for the construction of an estradiol-inducible overexpression construct of a translational fusion of the Green Fluorescent Protein (GFP) with MAKR4, the MultiSite Gateway cloning strategy was applied. The promoter fragment and the coding sequence of the target gene were introduced into Entry clones and subsequently cloned into destination vectors. The entry clone carrying the GLV5 promoter was a gift from Ana Fernandez (VIB-Ghent University, Gent, Belgium). To generate estradiol-inducible amiMAKR4 vectors, three unique gene-specific tag sequences designed in Web MicroRNA Designer (http://wmd3.weigelworld.org/) were used to construct the RNAi lines. According to BLAST searches of *Arabidopsis* cDNA, these sequences target MAKR4 only. The plasmids were transformed into Col-0 plants by the standard floral dip method (S*6*), except for the plasmids containing the *UAS:IBR3* and *pMAKR4:GFP-MAKR4* constructs that were transformed into the *ibr3-1* and *makr4-1* mutants, respectively. Primers used are listed in Supplementary Table 2.

Root phenotype analyses

To quantify the lateral root phenotype in wild-type plants and mutants, emerged lateral roots of the whole seedlings were counted under a dissecting microscope 8 days after germination. Subsequently, whole seedlings were scanned for further analysis of the primary root length. For indoleacetamide (IAM) and estradiol treatments, the length of the primary root grown after the treatment was measured and emerged lateral roots in this root region were counted. The gravitropic index was obtained by calculating the ratio of vertical length (VL) and primary root length (RL) (S*7*). To quantify the lateral root phenotype of the *IBR3* transactivation lines, different GAL4-GFP enhancer trap lines were first introgressed into the *ibr3* mutant background, and subsequently crossed with the *ibr3 UAS:IBR3* transgenic line. Primers to verify that each mutant line was homozygous at the locus of interest are listed in **Supplementary Table 2**.

Histochemical analysis and microscopy

GUS assays were done as described previously (S*8*). For microscopic analysis of primordium stages, root samples were cleared (S9). All samples were analyzed by differential interference contrast microscopy (Olympus BX53). For anatomical sections, GUS-stained samples were fixed overnight and embedded as described (S*10*). An Olympus FV10-ASW or Zeiss 710 confocal laser scanning microscope was used for fluorescence imaging of roots. For the propidium iodide (PI)-treated root images, seedlings were stained with 2 µg/mL PI for 3 minutes, washed with water, and used for confocal imaging.

Luciferase imaging and expression analysis

The Luciferase images were taken by a Lumazone machine carrying a charge-coupled device (CCD) camera (Princeton Instruments, Trenton, NJ, USA). The CCD camera that is controlled by a WinView/32 software took movies of the *DR5:Luciferase* expression automatically every 10 minutes (exposure time, 10 minutes) for ~24 hours. Before imaging, plates containing ½MS medium were sprayed with 1 mM D-luciferin solution (Duchefa Biochemie). The picture series were saved as TIFF format for further analysis. To quantify the *DR5:Luciferase* amplitude in the oscillation zone of wild-type plants and mutants, a movie was viewed first; then, the root region from wild-type plants or mutants in which a DR5

oscillation had been observed was selected for luciferase signal measurement for 8 hours. Meanwhile, luciferase signals from regions outside the root were measured as background and subtracted. The luciferase signals were quantified by the measure of the analog-digital units (ADU) per pixel by means of ImagJ (http://imagej.nih.gov/ij/). When movies of mutants were recorded, the wild-type seedlings were always placed next to the mutant seedlings and imaged together. The periodicity of the DR5 oscillations during the primary root growth was calculated by recording the time interval between consecutive DR5 oscillations. More than 70 time points from at least 15 individual seedlings were collected to make a histogram. To visualize the spatiotemporal *DR5:Luciferase* signal changes during primary root elongation, a Kymograph (http://www.embl.de/eamnet/html/body_kymograph.html) was generated with ImageJ. For this purpose, a real-time movie that lasted at least 20 hours was viewed in ImageJ and the *DR5:Luciferase* signal from a newly-grown root region was presented as Kymograph. To monitor the prebranch site numbers of 8-day-old seedling, Col-0 or transgenic *DR5:Luciferase*-harboring seedlings were sprayed with D-luciferin and immediately imaged by Lumazone with a 15-minute exposure time. Static *DR5* expression sites that were visible along the primary root outside the oscillation zone were counted as prebranch sites.

IBA microarray set-up

Seeds were germinated on vertically positioned Petri dishes in a growth chamber at 21°C under continuous light (100 µmol m^{-2} s^{-1} photosynthetically active radiation). Three-day-old Col-0 and *ibr1ibr3ibr10* seedlings (5 days postimbibition) were transferred to fresh ½MS media with or without 10 µM IBA for 6 hours. Filter-sterilized IBA was added to cooled (50°C) molten nutrient medium and mixed in 50-mL Falcon tubes before being poured into Petri dishes. The root tip segments (~4 mm) were dissected from the primary root and harvested for further microarray analysis. For each treatment, at least 120 individual Col-0 or *ibr1ibr3ibr10* mutant root tip segments were sampled and three independent biological replicates were performed.

Microarray analysis

The expression values were normalized with the robust Multi-Array average method (S*11*). Differential analysis was done with linear models and empirical Bayes methods within *affy* and *limma* R packages (www.r-project.org) (S*12*-S*14*). Raw *P*-values were adjusted to q-values with the Benjamini-Hochberg method to control the false discovery rate (S*15*). The Arabidopsis Genome Initiative (AGI) locus identification numbers of the Affymetrix probe sets were assigned with the “affy_ATH1_array_elements-2010-12-20.txt” file from The

Arabidopsis Information Resource (TAIR) (www.arabidopsis.org). Genes that were either ambiguous (multiple gene identifier for one probe set) or microarray controls were discarded. Two-way analysis of variance (ANOVA) *P*-values were computed with the MultiExperiment Viewer (http://www.tm4.org/mev/). Raw and processed microarray data have been deposited in the Gene Expression Omnibus (http://www.ncbi.nlm.nih.gov/geo/query/acc.cgi?token=onutyimizdudzk d&acc=GSE59426) under the accession number: GSE59426. Genes were selected when the following criteria were fulfilled: significant regulation upon 6 hours of IBA treatment in Col seedlings independently of IBR1, IBR3, and IBR10 (fold change [FC] ≥ 3, q-value ≤ 0.01, two-way ANOVA *P*-value ≤ 0.01 for the interaction of the treatment and the *ibr1 ibr3 ibr10* genotype), and genes were rejected when FC ≥ 1.5, q-value ≤ 0.01 in the *ibr1 ibr3 ibr10* genotypes.

Compendium analysis

Datasets corresponding to the published experiments (S*4*, S*16*) were retrieved from the Gene Expression Omnibus (http://www.ncbi.nlm.nih.gov/geo/) accessions GSE42896 and GSE6349 and were analyzed independently with the same procedure as for the IBA dataset. Genes were considered to be significantly regulated in each independent experiment when they fulfilled either the conditions absolute FC ≥ 2, q-value ≤ 0.05 between 0 and 2 hours upon treatment with both compounds (1-naphthaleneacetic acid and naxillin) during the time course (S*4*) or absolute FC ≥ 2, q-value ≤ 0.05 between 0 and 2 hours of the lateral root-inducible system in the sorted pericycle cells (S*16)*. Oscillation cluster data were extracted from Supplementary Table 1 of the corresponding publication (S*2*). A gene was considered a hit when it was expressed in phase or antiphase with the DR5 oscillations with an absolute FC ≥ 2 and an adjusted *P*-value ≤ 0.05. Gene lists were generated and intersected with the Microsoft Excel® software by means of the described methodology (S*17*).

Gene Ontology Enrichment

The Gene Ontology Enrichment of the biological processes was studied with the singular enrichment analysis on the agriGO platform (http://bioinfo.cau.edu.cn/agriGO/) with the ATH1 genome Array (GPL198) as reference background and other parameters set to default (S*18*).

qRT-PCR analysis

Root tips from 3-day-old seedlings were harvested for RNA extraction unless otherwise noted. cDNA was synthesized from 1 µg of RNA with the iScript cDNA Synthesis Kit (Bio-

Rad) according to the manufacturer's instructions and was diluted 20 times for subsequent quantitative (q)PCR. Quantitative reverse-transcription (qRT)-PCR was done on a LightCycler 480 (Roche Diagnostics) in 384-well plates with LightCycler 480 SYBR Green I Master (Roche) according to the manufacturer's instructions. Melting curves were analyzed to check primer specificity. Normalization was done against the average of the housekeeping genes *AT5G60390* and *AT2G32170* with the formula ΔCt = Ct (gene) – Ct (mean [housekeeping genes]) and ΔΔCt = ΔCt (control line) – ΔCt (line of interest). Ct refers to the number of cycles at which SYBR Green fluorescence reaches an arbitrary value during the exponential amplification phase. Primers used in this study are listed in Supplementary Table 2.

Supporting References

S1. T. Ulmasov, J. Murfett, G. Hagen, T. J. Guilfoyle, *Plant Cell* **9**, 1963-1971 (1997).

S2. M. A. Moreno-Risueno, *et al.*,, *Science* **329**, 1306-1311 (2010).

S3. B. De Rybel, *et al.*, *Curr. Biol.* **20**, 1697-1706 (2010).

S4. B. De Rybel, *et al.*, *Nat. Chem. Biol.* **8**, 798-805 (2012).

S5. M. Karimi, A. Depicker, P. Hilson, *Plant Physiol.* **145**, 1144-1154 (2007).

S6. S.J. Clough, A. F. Bent, A.F. *Plant J.* 16, 735-743 (1998).

S7. A. Grabov, *et al.*,, *New Phytol.* **165**, 641-651 (2005).

S8. J. D. Ward, *et al.*, *PLoS Genet.* **9**, e1003992 (2013).

S9. J. E. Malamy, P. N. Benfey, *Development* **124**, 33-44 (1997).

S10. I. De Smet, *et al.*, *J. Microsc.* **213**, 76-80 (2004).

S11. R. A. Irizarry, *et al.*, *Biostatistics* **4**, 249-264 (2003).

S12. L. Gautier, L. Cope, B. M. Bolstad, R. A. Irizarry, *Bioinformatics* **20**, 307-315 (2004).

S13. G. K. Smyth, *Statistical applications in genetics and molecular biology* **3**, Article3 (2004).

S14. G. K. Smyth, J. Michaud, H. S. Scott, *Bioinformatics* **21**, 2067-2075 (2005).

S15. Y. Benjamini, Y. Hochberg, *J. R. Stat. Soc.: Series B (Methodological)* **57**: 289-300 (1995).

S16. I. De Smet, *et al.*, *Science* **322**, 594-597 (2008).

S17. B. Parizot, B. De Rybel, T. Beeckman, *Plant Physiol.* **153**, 34-40 (2010).

S18. Z. Du, X. Zhou, Y. Ling, Z. Zhang, Z. Su, *Nucleic Acids Res.* **38**, W64-W70 (2010).

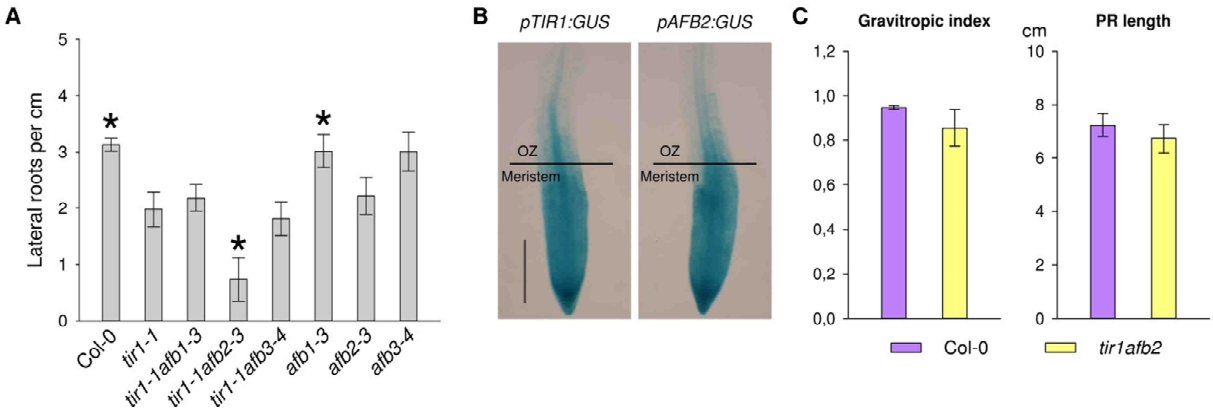

Supplemental Figure S1. Expression patterns of auxin receptor genes and phenotypic characterization of roots in auxin receptor mutants. (A) Lateral root density of single and double auxin receptor mutants quantified from 8-day-old seedlings. *$P < 0.01$ by two-sided Student's *t* test indicated statistically significant differences from *transport inhibitor response 1-1* (*tir1-1*) mutant; n > = 10. **(B)** Expression patterns of 3-day-old transcriptional reporter lines expressing the β-glucuronidase (GUS) gene under the control of the promoter of *TIR1* and *AUXIN-RELATED F-BOX*2 (*AFB2).* Scale bar, 0.2 mm. **(C)** Quantification of gravitropic index and primary root (PR) length in Col-0 and *tir1afb2* 8-day-old seedlings. Error-bars are means ± standard deviation.

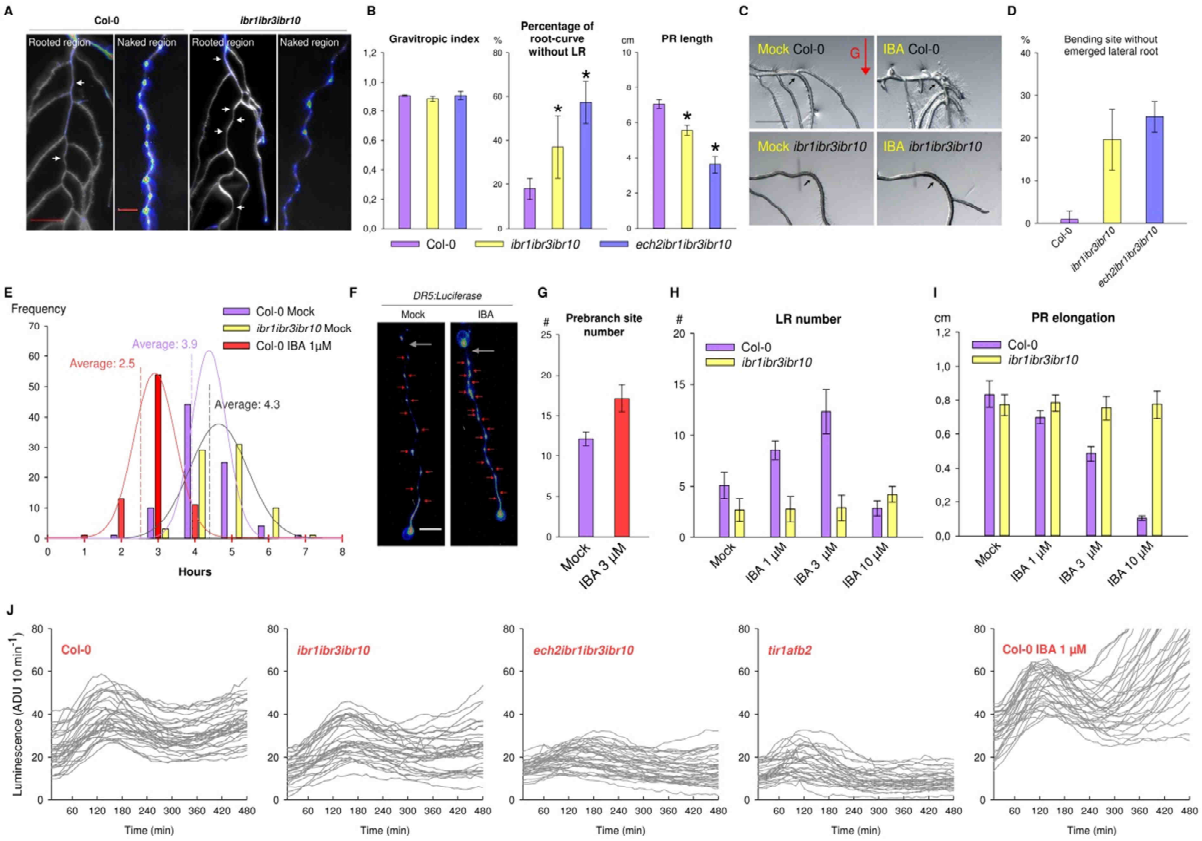

Supplemental Figure S2. Independence on gravity and root elongation of IBA-controlled root branching. (A) *DR5:Luciferase* expression in 8-day-old Col-0 and *ibr1ibr3ibr10* triple mutant seedlings. Images were overlayed with bright-field images. Arrows indicate the convex side of root curves without LR. Scale bars, 0.5 cm (rooted region) and 0.2 cm (naked region). **(B)** Quantification of gravitropic index, percentage of root curves without LR and primary root (PR) length in 8-day-old Col-0, *ibr1ibr3ibr10* triple mutant, and *ech2ibr1ibr3ibr10* quadruple mutant seedlings. Only root curves within the rooted region of the PR were taken into account. **P* < 0.001 by two-sided Student's *t* test; n > 10. **(C and D)** Three-day-old Col-0 and *ibr1ibr3ibr10* triple mutant seedlings transferred to medium with or without 5 µM IBA and immediately gravistimulated by a 90 degree rotation. After 5 additional days, pictures were taken and the percentage of the bending sites without emerged LRs was calculated (n > 30). Scale bar, 2 mm. **(E)** Average periodic time of *DR5:Luciferase* oscillations in 3-day-old *ibr1ibr3ibr10* triple mutant seedlings and Col-0 seedlings treated with or without 1 µM IBA (n >15). **(F and G)** *DR5:Luciferase* expression and number of prebranch sites in 5-day-old Col-0 seedlings treated with 3 µM IBA for 48 hours before the start of the measurement. White arrows indicate transfer of seedlings to ½MS medium containing 3 µM IBA and red arrows mark prebranch sites. Scale bar, 0.6 cm. **(H and I)** LR number and PR elongation measured after 5 days of treatment with different concentrations of IBA in the root region formed after 24 hours of IBA treatment in 3-day-old Col-0 and *ibr1ibr3ibr10* triple mutant seedlings. **(J)** Real-time quantification of the *DR5:Luciferase* signal in the oscillation zone of 3-day-old seedlings of indicated lines with or without IBA treatment (n > 30). Time-lapse imaging of *DR5:Luciferase* signal was taken every 10 minutes for 24 hours. Error-bars are means ± standard deviation.

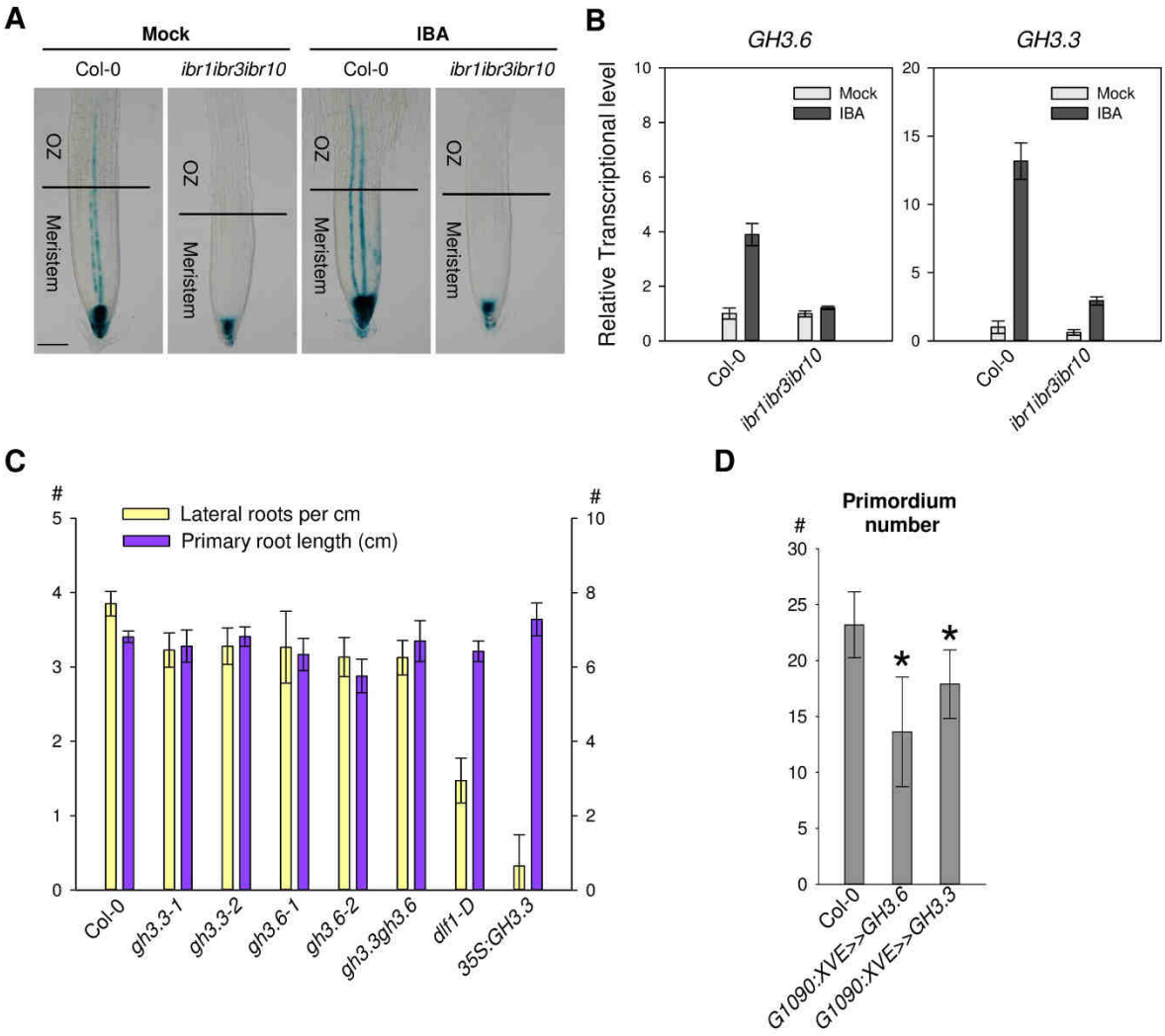
A
Mock
IBA
Col-0
ibr1ibr3ibr10
Col-0
ibr1ibr3ibr10
OZ
Meristem
B
GH3.6
GH3.3
Relative Transcriptional level
Mock
IBA
Col-0
ibr1ibr3ibr10
C
Lateral roots per cm
Primary root length (cm)
Col-0
gh3.3-1
gh3.3-2
gh3.6-1
gh3.6-2
gh3.3gh3.6
dlf1-D
35S:GH3.3
D
Primordium number
Col-0
G1090:XVE>>GH3.6
G1090:XVE>>GH3.3
E
pGH3.6:nGFP
F
pGH3.3:nGFP x 35S:FH6-GFP
Pe
Co
En
Ep

Supplemental Figure S3. Requirement for LR development of IBA-induced genes involved in auxin conjugation. **(A)** *DR5:GUS* expression in root tips of three-day-old Col-0 and *ibr1ibr3ibr10* seedlings after extra two days treatment with or without 3 µM IBA. **(B)** qPCR quantification of transcript levels of *GH3.6* and *GH3.3* in 3-day-old wild-type and transgenic seedlings treated with or without 10 µM IBA for 6 hours. **(C)** Root phenotype of 8-day-old *gh3.3-1*, *gh3.3-2*, *gh3.6-1*, and *gh3.6-2* single mutants, *gh3.3-1gh3.6-1* double mutant, *dlf1-D*, and *35S:GH3.3* overexpression lines. **(D)** LRP number in the newly formed part of the primary root of 2-day-old Col-0 and estradiol inducible *GH3.3* and *GH3.6* overexpression lines treated with 3 µM estradiol for 5 more days. **P* < 0.001 by two-sided Student's *t* test; n > 8. **(E and F)** Expression pattern of five-day-old transcriptional reporter lines for *GH3.3* and *GH3.6* during primordium development. *pGH3.6:NLS-GFP* seedlings were stained with propidium iodide and the *pGH3.3:NLS-GFP* line was crossed with the plasma membrane marker line *35S:FH6-GFP*. Co, Cortex; En, Endodermis; Ep, Epidermis; Pe, Pericycle. Scale bar, 100 µM. Error-bars are means ± standard deviation.

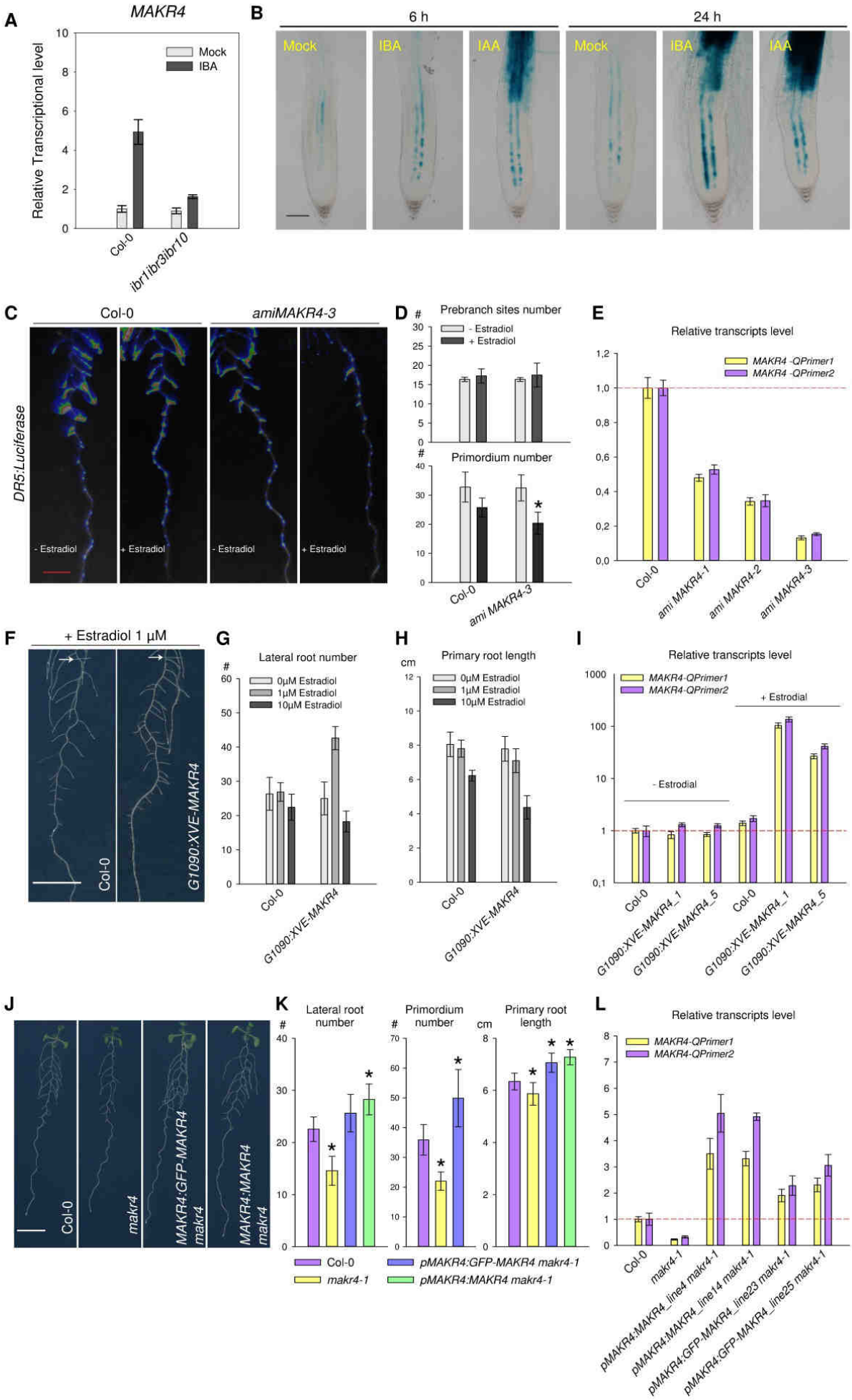
A
MAKR4
Relative Transcriptional level
Mock
IBA
Col-0
ibr1ibr3ibr10
B
6 h
24 h
Mock
IBA
IAA
C
Col-0
amiMAKR4-3
DR5:Luciferase
- Estradiol
+ Estradiol
D
Prebranch sites number
Primordium number
Col-0
ami MAKR4-3
E
Relative transcripts level
MAKR4 -QPrimer1
MAKR4 -QPrimer2
Col-0
ami MAKR4-1
ami MAKR4-2
ami MAKR4-3
F
+ Estradiol 1 µM
Col-0
G1090:XVE-MAKR4
G
Lateral root number
0µM Estradiol
1µM Estradiol
10µM Estradiol
H
Primary root length
I
Relative transcripts level
MAKR4-QPrimer1
MAKR4-QPrimer2
+ Estrodial
- Estrodial
J
Col-0
makr4
MAKR4:GFP-MAKR4 makr4
MAKR4:MAKR4 makr4
K
Lateral root number
Primordium number
Primary root length
Col-0
makr4-1
pMAKR4:GFP-MAKR4 makr4-1
pMAKR4:MAKR4 makr4-1
L
Relative transcripts level
MAKR4-QPrimer1
MAKR4-QPrimer2
pMAKR4:MAKR4_line4 makr4-1
pMAKR4:MAKR4_line14 makr4-1
pMAKR4:GFP-MAKR4_line23 makr4-1
pMAKR4:GFP-MAKR4_line25 makr4-1

Supplemental Figure S4. Root phenotype analysis of transgenic *MAKR4* lines. (A) qPCR quantification of *MAKR4* transcript level in 3-day-old Col-0 and *ibr1ibr3ibr10* seedlings mock-treated or treated for 6 hours with 10 µM IBA. **(B)** Expression pattern of 3-day-old *pMAKR4-GUS* seedlings treated with 5 µM IBA or 0.3 µM indole-3-acetic acid (IAA) for 6 or 12 hours. Scale bar, 0.1 cm. **(C and D)** *DR5:Luciferase* expression, prebranch site number and LRP number in estradiol-inducible *amiMAKR4-3* line. 3-day-old seedlings were treated with or without 3 µM estradiol for 5 more days before prebranch sites and LRP were counted in the newly formed part of the primary root. Scale bar, 0.5 cm. **(E)** qPCR quantification of *MAKR4* transcript level in root tips of three different *amiMAKR4* lines in 3-day-old seedlings treated with 3 µM estradiol for 24 hours. **(F to H)** A 3-day-old estradiol-inducible *MAKR4* overexpression line treated with different concentrations of estradiol for 7 more days before the LR number was counted in the newly formed part of the primary root. White arrows indicate point of transfer of seedlings (n > 10). Scale bar, 1 cm. **(I)** qPCR quantification of *MAKR4* transcript level in root tips of 3-day-old inducible *MAKR4* overexpression lines treated with or without 1 µM estradiol for 24 hours. **(J-L)** LR number, primordium number, and primary root length of 8-day-old *makr4* mutant complemented with or without MAKR4 translational fusion construct. To validate the *MAKR4* mRNA level, primary root tips from 3-day-old transgenic seedlings were harvested and used for real-time PCR quantification (n > 10). Scale bar, 1 cm. Error-bars are means ± standard deviation. **P* < 0.005 by two-sided Student's *t* test indicated statistically significant differences from Col-0 (n ≥10).

Supporting Tables

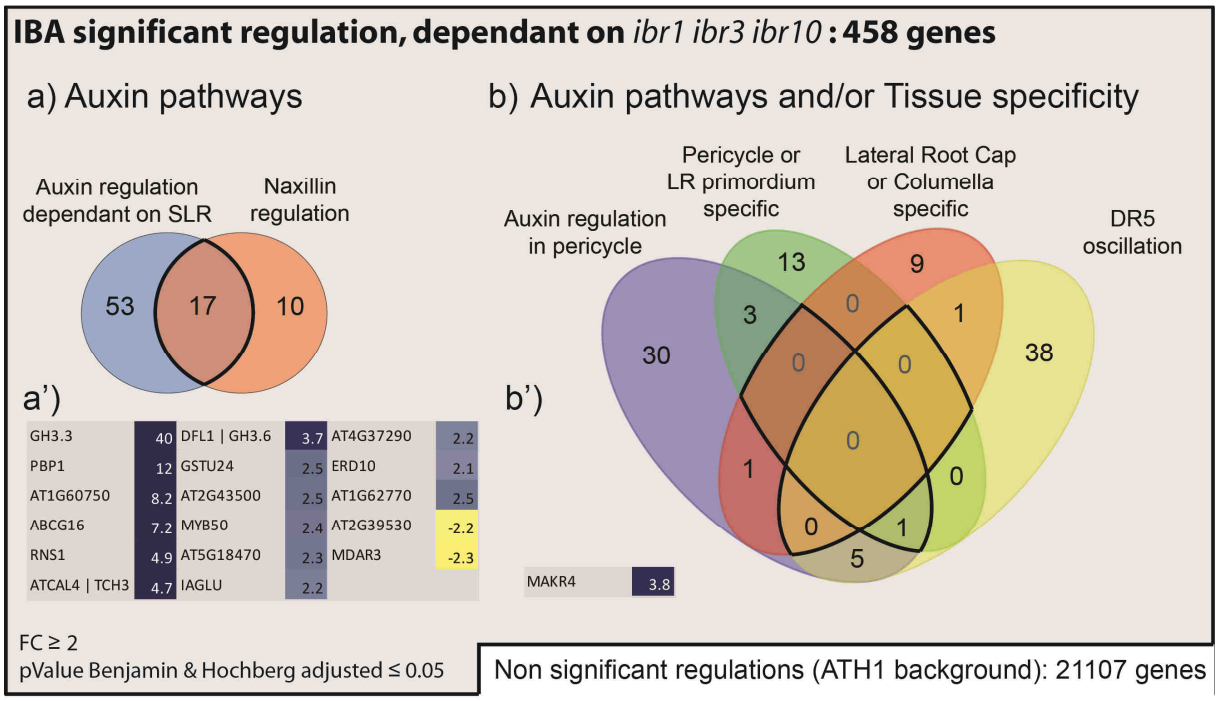

Locus AGI Identifier	Gene Symbol	Gene Name
AT2G39370	MAKR4	MEMBRANE-ASSOCIATED KINASE REGULATOR 4
AT1G30840	PUP4	purine permease 4
AT1G64405		unknown protein
AT5G54510	DFL1	DWARF IN LIGHT 1
AT2G36220		
AT2G42430	LBD16	ASYMMETRIC LEAVES2-LIKE 18
AT2G23170	GH3.3	
AT2G41100	TCH3	ARABIDOPSIS THALIANA CALMODULIN LIKE 4
AT2G33310	IAA13	auxin-induced protein 13
AT3G58190	LBD29	ASYMMETRIC LEAVES 2-LIKE 16
AT5G18470		
AT5G65640	bHLH093	beta HLH protein 93
no_match		embryo sac development arrest 21
AT3G59900	ARGOS	AUXIN-REGULATED GENE INVOLVED IN ORGAN SIZE
AT4G01430		
AT4G15550	IAGLU	indole-3-acetate beta-D-glucosyltransferase
AT5G59780	MYB59	MYB DOMAIN PROTEIN 59
AT1G15740		
AT4G04840	MSRB6	methionine sulfoxide reductase B6
AT2G42440		
AT1G48300		
AT4G39950	CYP79B2	cytochrome P450, family 79, subfamily B, polypeptide 2
AT5G54490	PBP1	pinoid-binding protein 1

Supplemental Table S1. Overlap of genes regulated by IBA in *ibr1ibr3ibr10* dependant manner with auxin pathways and/or tissue specificity. a) Overlap of the 458 IBA regulated genes with SLR dependent NAA induction pathways and naxillin induction pathways. a') list of the 17 genes at the intersection. b) overlap of the 458 IBA regulated genes with NAA induction pathways in the pericycle, specificity of expression in the pericycle or in the primordium tissues, specificity of expression in the columella or in the root cap, expression pattern oscillating in phase or anti-phase with DR5 auxin response marker. b') gene at the intersection of at least 3 of the 4 datasets. The dark lines delimit the regions of the Venn diagram displayed in the tables. Genes are called after their symbol or AGI number and Fold-Change between 0 and 6 hours of IBA treatment is indicated and highlighted with a gradient of blue or yellow color for the genes respectively up- or down-regulated. An extra table shows that twenty-three genes were considered as HITs because they fulfilled the following criteria: significant regulation upon 6 hours of IBA treatment in Col-0 and dependence on IBR1, IBR3, and IBR10. TRUE and FALSE stand for genes that passed or not the selection criteria, respectively (see Materials and Methods).

Supplemental Table S2. Primer sequences for Gateway cloning, T-DNA insertion verification, and qPR-PCR analysis.

Oligo Name	SEQUENCE
IBR3_CDS_attb1F	GGGGACAAGTTTGTACAAAAAAGCAGGCTATATGGGAAGCAGCACGGGCGATC
IBR3_CDS_attb2R	GGGGACCACTTTGTACAAGAAAGCTGGGTGTTAAAGCTTTGAAGCTCTTTGC
GH3.6_Promoter_attb4F	GGGGACAACTTTGTATAGAAAAGTTGGCCGTTATCTTTATGTATAGCGTC
GH3.6_promoter_attb1R	GGGGACTGCTTTTTTGTACAAACTTGCCGTTTAGGTTTTGTGTTTAA
GH3.6_CDS_attb1F	GGGGACAAGTTTGTACAAAAAAGCAGGCTATATGCCTGAGGCACCAAAGAT
GH3.6_CDS_attb2R	GGGGACCACTTTGTACAAGAAAGCTGGGTATTAGTTACTCCCCCATTGCT
GH3.3_Promoter_attb4F	GGGGACAACTTTGTATAGAAAAGTTGGCTCTTACCAAGATACCACCGTA
GH3.3_Promoter_attb1R	GGGGACTGCTTTTTTGTACAAACTTGCGATTAAAATGGTATTTGTAAGTG
GH3.3_CDS_attb1F	GGGGACAAGTTTGTACAAAAAAGCAGGCTGCATGACCGTTGATTCAGCTCT
GH3_3_CDS_attb2R	GGGGACCACTTTGTACAAGAAAGCTGGGTATCAACGACGACGTTCTGGTGA
MAKR4_Promoter_attb4F	GGGGACAACTTTGTATAGAAAAGTTGGCAGTTCACAGTTAGAACATTTGC
MAKR4_Promoter_attb1R	GGGGACTGCTTTTTTGTACAAACTTGCCTTTTTTTTTTTATGTTTCTTC
MAKR4_CDS_attb1F	GGGGACAAGTTTGTACAAAAAAGCAGGCTGCATGGCGGCTTATCTAGAGCGA
MAKR4_CDS_no stop_attb2R	GGGGACCACTTTGTACAAGAAAGCTGGGTAGCCCCTAAACATCTGAGCCCAT
MARK4_CDS_attb2R	GGGGACCACTTTGTACAAGAAAGCTGGGTATTAGCCCCTAAACATCTGAGC
MAKR4_CDS_attb2F	GGGGACAGCTTTCTTGTACAAAGTGGATATGGCGGCTTATCTAGAGCGA
MAKR4_CDS_attb3R	GGGGACAACTTTGTATAATAAAGTTGGTTAGCCCCTAAACATCTGAGC
MAKR4_1_I_miR_s	GATGATATCTTTAGTTAGCGCCTTCTCTCTTTTGTATTCC
MAKR4_1_II_miR_a	GAAGGCGCTAACTAAAGATATCATCAAAGAGAATCAATGA
MAKR4_1_III_miR*s	GAAGACGCTAACTAATGATATCTTCACAGGTCGTGATATG
MAKR4_1_IV_miR*a	GAAGATATCATTAGTTAGCGTCTTCTACATATATATTCCT
MAKR4_2_I_miR_s	GATTTTACTCGCGAATACGTCAATCTCTCTTTTGTATTCC
MAKR4_2_II_miR_a	GATTGACGTATTCGCGAGTAAAATCAAAGAGAATCAATGA
MAKR4_2_III_miR*s	GATTAACGTATTCGCCAGTAAATTCACAGGTCGTGATATG
MAKR4_2_IV_miR*a	GAATTTACTGGCGAATACGTTAATCTACATATATATTCCT
MAKR4_3_I_miR_s	GATTACACTGTCGCATCGCGCTATCTCTCTTTTGTATTCC
MAKR4_3_II_miR_a	GATAGCGCGATGCGACAGTGTAATCAAAGAGAATCAATGA
MAKR4_3_III_miR*s	GATAACGCGATGCGAGAGTGTATTCACAGGTCGTGATATG
MAKR4_3_IV_miR*a	GAATACACTCTCGCATCGCGTTATCTACATATATATTCCT
CBG99_CDS_attb1F	GGGGACAAGTTTGTACAAAAAAGCAGGCTTAATGGTGAAGCGTGAGAAA
CBG99_CDS_attb2R	GGGGACCACTTTGTACAAGAAAGCTGGGTACTAACCGCCGGCCTTCTCCAA
Salk_084039_LP	GGCACCCTTAATCATATTTGG
Salk_084039_RP	GGAGTGCTGTAGAATTCGTCG
GH3.6_qPCR_for	TGGACCATTGGAGATCAAGATG
GH3.6_qPCR_rev	GGCTGAAGTAACTATCAACAACC
GH3.3_qPCR_for	CTCTGCGATCTCCGATGATG
GH3.3_qPCR_rev	CGGTCAGTGAATCCCTTGAG
MAKR4_qPCR1_for	GAAGAGAAGTACGAGTTCGAGTTC
MAKR4_qPCR1_rev	CCCTAAACATCTGAGCCCATTC
MAKR4_qPCR2_for	CGTCTTCCGCTGCGAGAG
MAKR4_qPCR2_rev	GCTTGCCTCCTCATAGAAACTG

Supporting Movies

Video files S1-S6

Movie S1. Movie of *DR5:Luciferase* expression in 3-day-old Col-0 and *tir1afb2* seedlings for 20 hours. The Col-0 root and the *tir1afb2* mutant root were located on the left and right sides, respectively. The root region where DR5 oscillations occurred is indicated by a white arrow. Scale bar, 0.1 cm.

Movie S2. Movie of *DR5:Luciferase* expression in 3-day-old Col-0 seedlings under mock treatment for 20 hours. White arrow indicates the root region where DR5 oscillations occurred. Scale bar, 0.1 cm.

Movie S3. Movie of *DR5:Luciferase* expression in 3-day-old Col-0 seedlings for 20 hours. Seedlings were grown in the presence of 1 µM IBA. White arrow indicates the root region where DR5 oscillations occurred. Scale bar, 0.1 cm.

Movie S4. Movie of *DR5:Luciferase* expression in 3-day-old Col-0 and *ech2ibr1ibr3ibr10* quadruple mutant seedlings for 24 hours. Two roots from the Col-0 seedlings (on the left) and four roots from the *ech2ibr1ibr3ibr10* seedlings were imaged over time. Scale bar, 0.1 cm.

Movie S5. Movie of *pMAKR4:CBG99* expression in 3-day-old Col-0 seedlings for 24 hours. Scale bar, 0.1 cm.

Movie S6. Movie of MAKR4 protein localization during nuclear migration and asymmetric cell division in pericycle cells that are marked by nuclear *GATA23* expression. A 5-day-old *pMAKR4:GFP-MAKR4 x GATA23:nGFP* seedling was used for confocal imaging for 18 hours. Yellow and red arrows indicate GFP signal from the MAKR4 protein and the nuclear GATA23 signal during migration. Scale bar, 200 µm.

“We believe that there is no
structure in plants more wonderful,
as far as its functions are concerned,
than the tip of the radicle.”

Charles Darwin

Chapter 3

Growth dynamics of root cap cells set the root clock

Adapted From:

Wei Xuan, Leah Band, Barbara Möller, Daniel Van Damme, Gieljan De Rop, Davy Opdenacker, Moritz Nowack, Dominique Audenaert, Steffen Vanneste, Tom Beeckman. The growth dynamics of root cap cells set the root clock. Manuscript in preparing.

The growth dynamics of root cap cells set the root clock

Wei Xuan[1,2], Leah Band[3], Barbara Möller[1,2], Daniel Van Damme[1,2], Gieljan De Rop[1,2], Davy Opdenacker[1,2], Moritz Nowack[1,2], Dominique Audenaert[1,2], Steffen Vanneste[1,2], Tom Beeckman[1,2†]

Affiliations:

[1]Department of Plant Systems Biology, VIB, Gent, Belgium.

[2]Department of Plant Biotechnology and Bioinformatics, Gent University, Gent, Belgium.

[3]Centre for Plant Integrative Biology, University of Nottingham, Nottingham LE12 5RD, United Kingdom

[†] Correspondence to: tobee@psb.vib-ugent.be

Summary:

During growth of the plant root system, the root cap is the first organ that interacts with the rhizosphere and senses environmental signals to direct root growth. In *Arabidopsis thaliana*, a root cap-specific auxin source modulates the patterning of lateral organs along the primary root axis. However, thus far the mechanism remained elusive. Here, we reveal that programmed cell death in the root cap is a periodic process that determines the spatiotemporal patterning of root branching. Genetic evidence demonstrated that auxin signaling in the root cap is not required for maintaining the root clock behavior, but depends on the coordination of local auxin biosynthesis and auxin transport. This work shows that the growth dynamics of the root cap are responsible to generate the positional information for periodic root branching to optimize the uptake of water and nutrients from the soil.

Introduction:

During plant growth, the root system contributes to the uptake of water and nutrients by the sequential prodction of lateral roots. In plant model *Arabidopsis thaliana*, the position of lateral organs along the primary root is specified by a prepatterning process. This occurs in the transition zone of the root apex, also referred to as oscillation zone, a region close to the tip where meristematic cells stop dividing and rapidly elongate. During prepatterning, subsets of cells in the OZ experience high levels of gene expression that create oscillations in the growing primary root and that are proposed to prepare cells for the production of a lateral root (De Smet et al., 2007; Moreno-Risueno et al., 2010; Van Norman et al., 2013). The oscillations can be visualized by the synthetic auxin signaling output reporter DR5 (De Smet et al., 2007; Moreno-Risueno et al., 2010). When cells with high DR5 expression levels leave the OZ, the expression is maintained and becomes fixed in regularly spaced prebranch sites along the primary root capable to form LRs.

We recently revealed a crucial role for the root cap in the spatiotemporal patterning of root branching. Root cap-specific conversion of the auxin precursor indole-3-butyric acid (IBA) into the most abundant endogenous auxin indole-3-acetic acid (IAA) creates a local auxin source that modulates the oscillations and thereby controls prebranch site formation (Xuan et al., chapter 2). However, thus far it is unknown how the auxin source in the root cap controls the oscillations. The root cap is the first organ that interacts with the rhizosphere when a root grows through the soil. It is a sensory organ that perceives environmental signals such as gravity, water and nutrients to direct root growth towards nutrient- and water-rich soil patches (Arnaud et al., 2010). The root cap ensheaths and protects the root meristem that continuously produces new root cap cells. In *Arabidopsis*, the root cap consists of centrally located columella cells and peripherally located lateral root cap cells (Dolan et al., 1993). Recently, it was shown that lateral root cap cells undergo programmed cell death (PCD) when they approach the distal boundary of the root cap in the transition zone of the primary root (Fendrych et al., 2014). Moreover, the root cap-specific NAC transcription factor SOMBRERO transcriptionally controls root cap maturation and PCD in the lateral root cap and is involved in LR patterning (Bennett et al., 2010; Moreno-Risueno et al., 2010; Willemsen et al., 2008). Here, we reveal that the growth dynamics of the root cap determine the regular distribution of lateral roots to optimize the uptake of water and nutrients from the soil.

Results

DR5 expression dynamics in root cap and OZ exhibit equal periodicity.

As a first step to investigate how the root cap modulates LR patterning, we determined whether auxin signaling occurs in the root cap. For this purpose, we used a highly sensitive stereo-microscope for fluorescence to visualize a nuclear localized fluorescent DR5 reporter (DR5rev-3xVENUS-N7) (Heisler et al., 2005) at cellular resolution in a vertically growing root. This imaging system uniquely combines the ability to image seedlings while they are growing vertically on solid plant medium with visualization at cellular resolution of a large root portion including the meristem and oscillation zone. We detected a strong DR5 signal in the entire root cap, indicative of a general auxin response (Fig. 1a, b). Long-term imaging of growing seedlings with 10 min. intervals showed that the DR5 signal disappeared every ~4 hours in the most-distal concentric file of root cap cells (Figure 1c, d, Extened Data Fig. 1, and Supplementary Video 1). When we followed the position of the root where DR5 expression had disappeared in the growing seedling, we consistently detected a new LRP at this position in ~89% of events (Supplementary Video 1). Inversely, when we traced back the origin of LRP during root growth, we found that 100% of LRP formed at the position where DR5 expression had disappeared in the root cap. Moreover, we observed that the recurrent disappearance of DR5 expression exhibits the same periodicity as the DR5-Luciferase oscillations in the OZ that were previously shown to mark the position of future LRs (Fig. 1e, f; Moreno-Risueno et al., 2010; Xuan et al., chapter 2). Gravitropic stimulation decreased both the periodicity of disappearance of DR5 expression in the root cap and DR5 oscillations in the OZ to ~2 hours (Fig. 1g). After gravitropic stimulation, the root bended at the position where DR5 disappeared in the root cap and formed a LRP at the bending site (Supplementary Video 2). To study the spatial connection between the root cap and OZ in more detail, we compared the average distance from the QC of the Luciferase signal in the OZ of DR5-Luciferase seedlings and the fluorescent signal in the root cap of DR5rev-3xVENUS-N7 seedlings. We determined that the DR5 signal in the root cap disappeared at the start of the OZ (Fig. 1h, i). All together, these results show that the disappearance of the DR5 signal in the root cap, the oscillations in the OZ and the formation of LRP are temporally and spatially connected.

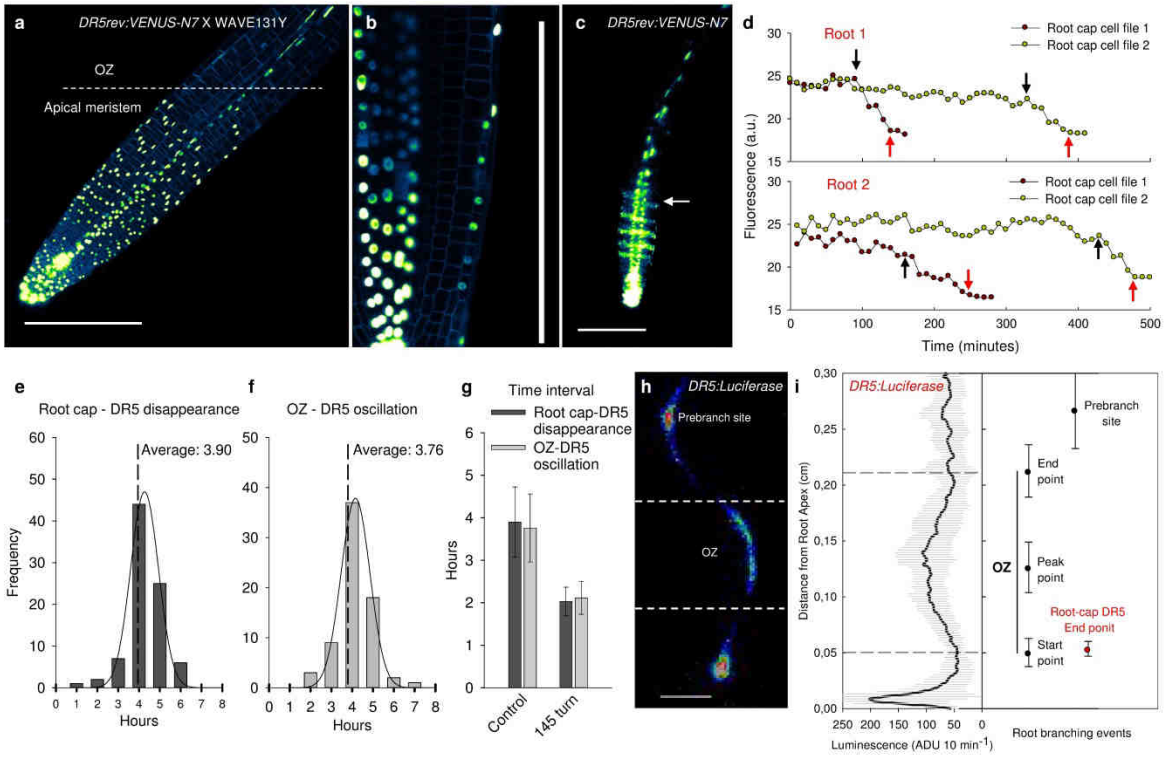

Figure 1: Periodic disappearance of root cap-DR5 expression precedes LRP formation. **a-c**, Confocal fluorescence microscopy images (**a, b**) and stereo microscope image (**c**) of root tip of *DR5rev*:*VENUS-N7* seedlings. Image in **a** was obtained by Z-stack scanning, and arrow in **c** points at a concentric file of root cap cells with *DR5* expression. Scale bar, 100 µm. **d**, Quantification of *DR5* expression in the two most distal adjacent concentric files of root cap cells over time. Black arrows mark the time-point when the *DR5* expression level in the root cap starts decreasing, and red arrows mark the time-point when the *DR5* signal completely disappears in the root cap. **e**, **f**, Histograms showing the distribution of the time interval between the disappearance of *DR5* expression in two adjacent files of root cap cells (e; n = 85 measurements obtained from 25 individual seedlings) and two consecutive *DR5* oscillations in OZ (f; n = 70 from 18 individual seedlings) over time. **g**, Average time interval between the consecutive disappearance of *DR5* expression in two adjacent files of root cap cells and two consecutive *DR5* oscillations in OZ over time under normal conditions and during gravity-induced bending (n > 20). **h,** *DR5:Luciferase* signal in seedling root, Scale bar, 0.5 mm. **i**, Distance from QC of *DR5rev*:*VENUS-N7* signal in the root cap, *DR5:Luciferase* oscillation signal in OZ, and static *DR5-Luciferase* signal in prebranch sites (n > 40). Scale bar, 0.5 mm. In all experiments, 3-day-old seedlings were used for imaging and analysis.

PCD triggers the oscillations in OZ and subsequent LRP formation.

We assesed whether the recurrent disappearance of DR5rev-3xVENUS-N7 expression in the root cap could be controlled by active degradation of fluorescent protein as a result of PCD (Fendrych et al., 2014). Lateral root cap cells show increasing expression of the aspartic protease PASPA3 while they approach the distal end of the root cap and finally die (Fendrych et al., 2014). We created a line expressing the DR5rev-3xVENUS-N7 reporter and the pPASPA3-NLS-tdTomato cell death marker, and detected overlapping expression in the nuclei of the most distal lateral root cap cells (Extended Data Fig. 2a-d). Moreover, real time imaging showed that the DR5 and PASPA3 signal disappeared synchronously in distal lateral root cap cells (Fig. 2a). This indicates that the recurrent disappearance of DR5 signal marks PCD in the lateral root cap and suggests that this PCD is a periodic process. Indeed, we found that expression of the PASPA3 cell death marker disappeared every ~4 hours in the most-distal concentric files of root cap cells (Fig. 2b-d). Gravitropic stimulation decreased the periodicity of disappearance of PASPA3 expression in the root cap to ~2 hours, as was shown for the periodicity of DR5 oscillations in the OZ (Supplementary Video 3 and Extended Data Fig. 2f). When we followed the position where PASPA3 expression disappeared during seedling growth (Supplementary Video 4), we consistently observed the formation of a new LRP at this position (Extended Data Fig. 2e). In addition, the NAC domain transcription factor SMB is specifically expressed in root cap cells and has been shown to transcriptionally control PCD in the lateral root cap (Fig. 2f; Willemsen et al., 2008; Fendrych et al., 2014). Previous transcriptome analysis identified SMB as a putatively oscillating gene in the OZ (Moreno-Risueno et al., 2010), but our analysis of SMB-Luciferase signal showed that SMB expression does not oscillate in root cap cells (Extended Data Fig. 2g). Instead, similar to PASPA3 expression in the root cap, the nuclear pSMB-NLS-GFP signal disappeared every ~4 hours in the most-distal concentric files of root cap cells (Fig. 2e-g and Supplementary Video 5). Thus, the periodicity of PCD in the lateral root cap and the oscillations in the OZ is identical and shifts synchronously in response to gravity. Together, these results reveal that PCD in the lateral root cap is a recurrent process that is spatiotemporally interconnected with LR patterning.

We next disturbed PCD in the lateral root cap to investigate if this will affect LR patterning. Previously, PCD in the lateral root cap had been shown to be disturbed in the smb-3 mutant (Fendrych et al., 2014). Root cap cells in the smb-3 mutant continued to divide and failed to detach from the root, resulting in an increased number of root cap cells that ectopically extended into the oscillation zone (Extended Data Fig. 3e-g; Bennett et al., 2010).

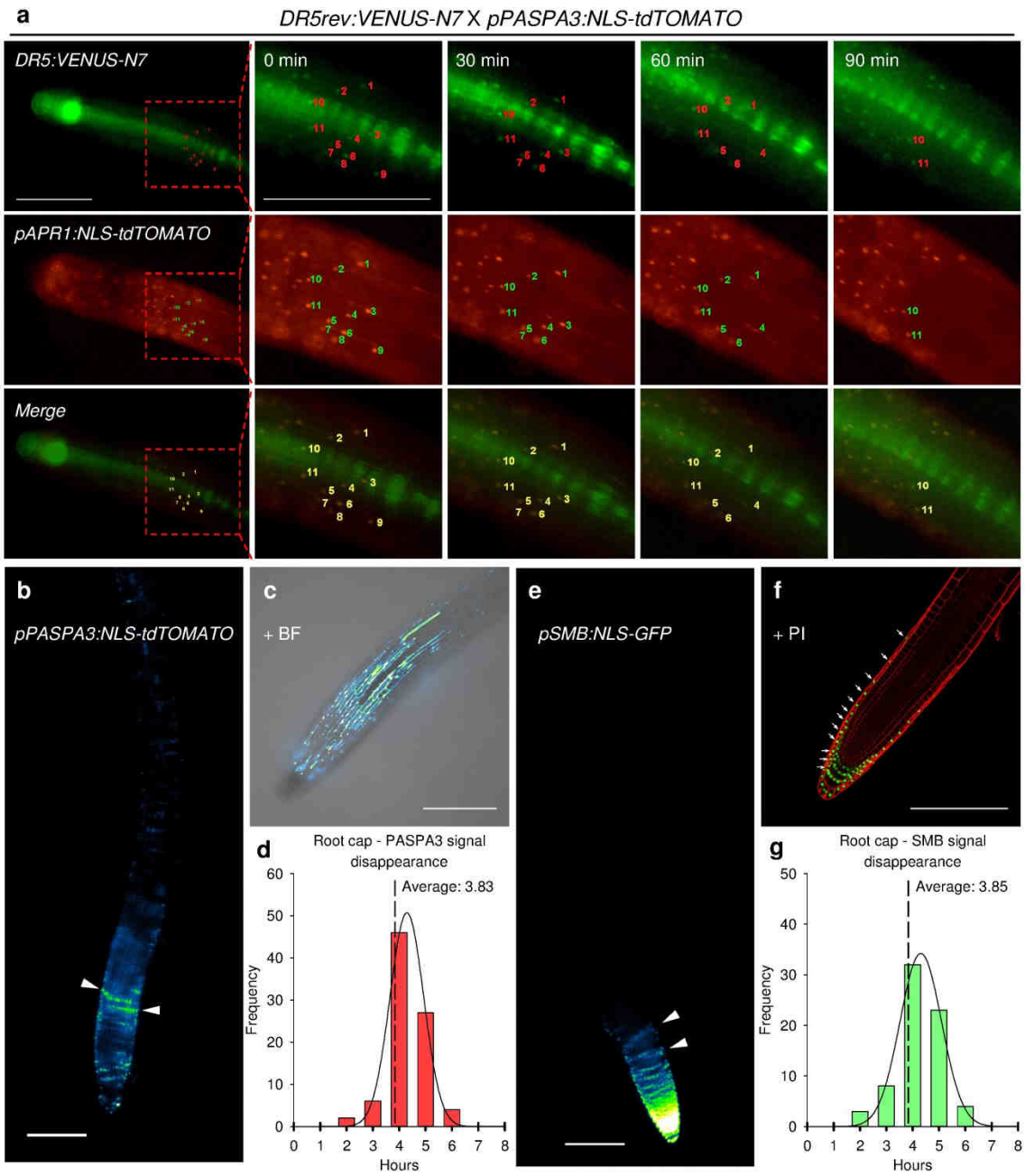

Figure 2: Disappearance of *DR5* expression and cell death in root cap cells exhibit equal periodicity. a, stereo microscope images of *DR5rev:VENUS-N7* and *pPASPA:NLS-tdTOMATO* expressing transgenic seedlings that were imaged over a 90-min period. Images were taken every 15 min. Small numbers mark cells with *DR5* and *PASPA* signal. **b**, **c**, **e**, **f**, stereo microscope (**b**, **e**) and confocal microscopy (**c**, **f**) images of nuclear-tagged *PASPA3* red fluorescent signal and nuclear-tagged *SMB* green fluorescent signal in root cap cells. White arrows in **b** and **e** indicate *PASPA3* and *SMB* nuclear signals in concentric files of root cap cells. Bar = 100 µm. PI, propidium iodide **d**, **g**, Histograms showing the distribution of the time interval between the consecutive disappearance of *PASPA3* and *SMB* signals in two adjacent concentric files of distal root cap cells (n = 85 measurements obtained from 18 individual *pPASPA:NLS-tdTOMATO* seedlings; n = 70 measurements obtained from 18 individual *pSMB:NLS-GFP* seedlings). In all experiments, 3-day-old seedlings were used for imaging and analysis.

The DR5 signal in the root cap was disorganized and significantly reduced in the smb-3 mutant and extended into the oscillation zone (Extended Data Fig. 3e, f, g). Moreover, the oscillations in the OZ were strongly irregular in the *smb-3* mutant, and we observed less LRPs and LRs and a reduced primary root elongation in the *smb-3* mutant (Extended Data Fig. 3a, b, g). In contrast to the smb-3 mutant, dexamethasone (Dex) inducible SMB overexpression triggers a strong release of root cap cells (Fig. 3a, d, g). This is accompanied with a strong reduction in DR5 signal intensity in the root cap and loss of the periodic disappearance of DR5 expression in SMB overexpressing seedlings (Fig. 3c, f, g and Extended Data Fig. 3h). Consequently, the DR5 oscillations in the OZ are completely absent and the number of prebranch sites and LRs is severely diminished upon SMB overexpression (Fig. 2h, i and Supplementary Video 6). When SMB overexpressing seedlings were allowed to grow further on medium without Dex, the newly formed root part produced a normal root cap and LRs. However, the part of the root that had grown on Dex did not produce any LR, confirming the requirement of the root cap for LR patterning (Extended Data Fig. 3i-k). In addition, a strong reduction in the number of lateral root cap cells by inducible transactivation of the toxic diphteria toxin A chain gene in the lateral root cap (J3411) (Birnbaum et al., 2003; Weijers et al., 2003) also significantly suppressed LRP formation (Extended Data Fig. 3l-n). All together, these results suggest that the controlled and recurrent death of root cap cells regulates the oscillations in the OZ and the subsequent formation of LRP.

The root cap modulates the oscillations in OZ via auxin transport.

We next investigated how the recurrent PCD of lateral root cap cells controls the oscillations in the OZ. Previously, we showed that the oscillations are modulated by a local auxin source in the root cap, derived from the auxin precursor IBA (Xuan et al., chapter 2). Therefore, we assessed whether the auxin response that we observed in the root cap (Fig. 1a, b) could be required for this process. Auxin response is inhibited by Aux/IAA transcriptional repressors that are degraded when auxin levels rise (Gray et al., 2001). We expressed a mutant form of the Aux/IAA17 protein, *axr3-1*, which cannot be degraded by auxin and thus constantly represses auxin response (Rouse et al., 1998; Swarup et al., 2005), under the control of the root cap specific SMB promoter in a Dex inducible manner. Induction of axr3-1 resulted in agravitropic root growth and loss of DR5 expression in the root cap, but did not alter LR number (Fig. 4a-c and Extended Data Fig. 4a, b). This indicates that auxin response is not required in the root cap to control LR patterning.

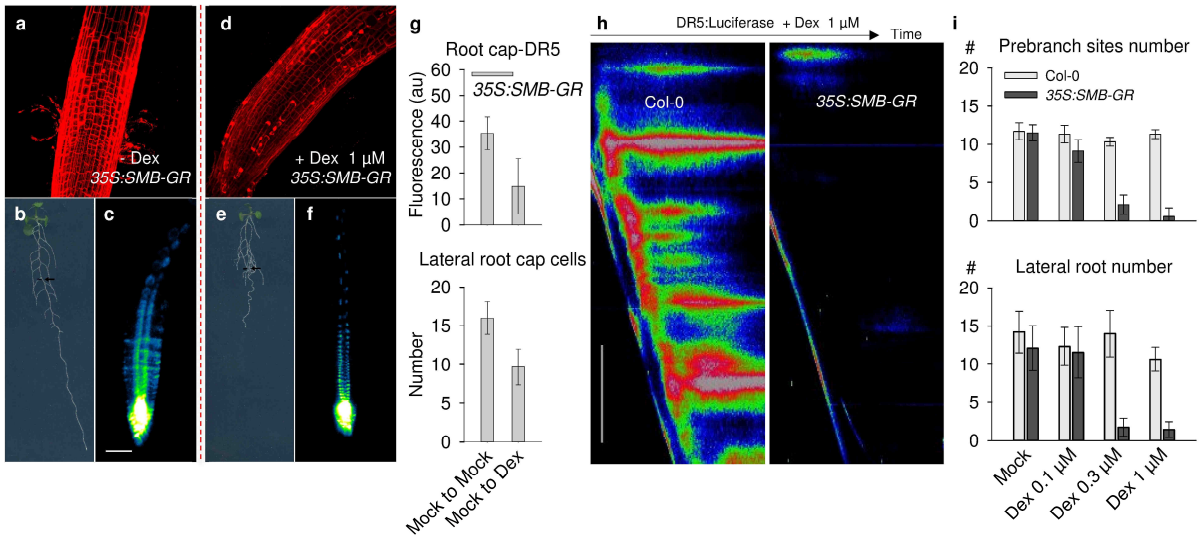

Figure 3: The root cap is required for LR patterning. a, d, c, f, Z-stack confocal microscopy images of transition zone of PI-stained roots (Aida et al., 2004) and stereo microscope images of *DR5rev:VENUS-N7* expressing root tips (**c**, **f**). 5-day-old *35:SMB-GR* transgenic seedlings treated without (**a, c**) or with (**d, f**) 1 µM Dexamethasone (Dex) from day 3 on. Seedlings in **a** and **d** were stained with propidium iodide (PI) before confocal imaging. Pinhole at 1 µm was used for Z-stack scanning; scale bar, 100 µm. **b, e,** Root phenotype of 8-day-old *35:SMB-GR* transgenic seedlings treated without (**c**) or with (**f**) 1 µM Dexamethasone (Dex) from day 3 on. **g**, Quantification of the *DR5* signal intensity in the root cap and number of root cap cells in 5-day-old *DR5rev:VENUS-N7* expressing *35S:SMB-GR* transgenic seedlings that were grown on 1 µM Dex from day 3 on (n > 30). **h**, Kymograph representing *DR5:Luciferase* expression in 3-day-old Col-0 and *35S:SMB-GR* transgenic seedlings after 1 µM Dex application over twenty hours. Scale bar, 1 cm. **i**, Quantification of prebranch sites and LRs number in *35S:SMB-GR* transgenic seedlings that were grown without Dex for 3 days and then grown on indicated Dex concentrations for another 2 days to count the prebranch sites (n =10) or another 5 days to quantify LR number (n = 12). Error-bars are means ± standard deviation.

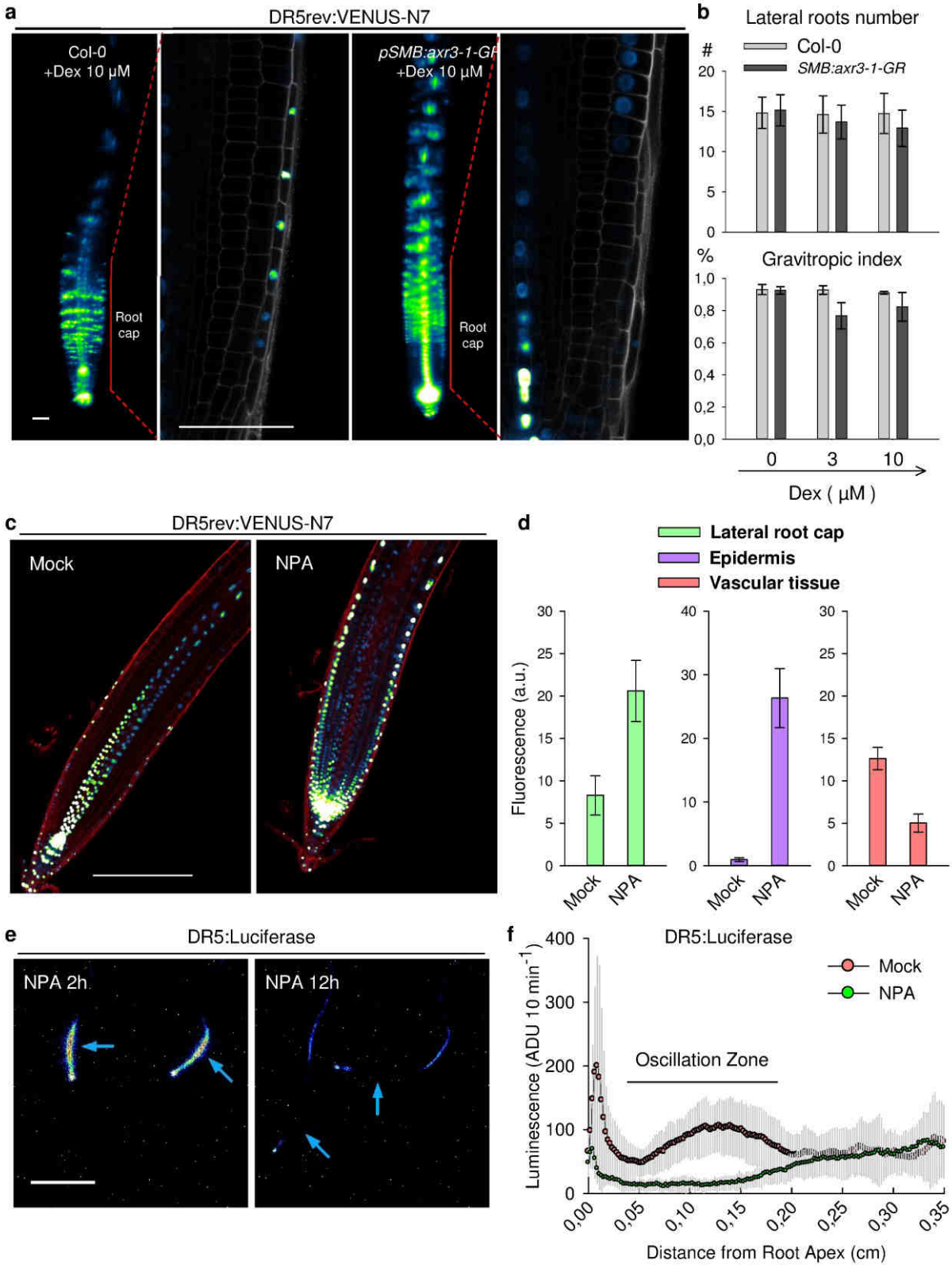
a
DR5rev:VENUS-N7
Col-0
+Dex 10 µM
Root cap
pSMB:axr3-1-GR
+Dex 10 µM
Root cap
b
Lateral roots number
Col-0
SMB:axr3-1-GR
#
Gravitropic index
%
Dex (µM)
c
DR5rev:VENUS-N7
Mock
NPA
d
Lateral root cap
Epidermis
Vascular tissue
Fluorescence (a.u.)
Mock
NPA
e
DR5:Luciferase
NPA 2h
NPA 12h
f
DR5:Luciferase
Mock
NPA
Oscillation Zone
Luminescence (ADU 10 min-1)
Distance from Root Apex (cm)

Figure 4: The auxin reflux loop is required for LR patterning. a, Stereo microscope (left) and confocal microscope (right) images of *DR5rev:VENUS-N7* expression in 3-day-old Col-0 and *pSMB:axr3-GR* seedlings grown on 10 µM Dex. Scale bar, 50 µm. **b**, Quantification of LR number and gravitropic index of Dex-grown primary root part of 8-day-old *pSMB:axr3-GR* seedlings grown on indicated Dex concentrations from day 3 on. **c**, Confocal microscopy images of *DR5rev:VENUS-N7* expression in 3-day-old seedlings after 24 hours treatment by DMSO or 10 µM NPA. Scale bar, 200 µm. **d**, Quantification of *DR5rev:VENUS-N7* signal intensity in indicated tissues in **c** (n > 20). **e**, *DR5:Luciferase* expression in 3-day-old seedlings after 2 hours and 12 hours treatment by 10 µM NPA. Blue arrows indicate the position of OZ. Scale bar, 2 mm. **f**, Quantification of *DR5:Luciferase* signal in the root tips of 3-day-old seedlings treated by DMSO or 10 µM NPA for 12 hours (n > 30).

We next investigated if the IBA-derived auxin source is transported from the root cap to the OZ to modulate the oscillations. We used the polar auxin transport inhibitor N-1-naphthylphthalamic acid (NPA) to determine whether auxin efflux is involved to establish the oscillations in the OZ. Analysis of the PASPA3 cell death marker showed that exogenous application of NPA does not stop the recurrent PCD in lateral root cap cells (Supplementary Video 7 and Extended Data Fig. 4c, d). However, NPA application resulted in a strongly increased DR5rev-3xVENUS-N7 signal in the lateral root cap and epidermis and a decreased DR5 signal in the vascular tissue (Fig. 4f-h and Supplementary Video 8). This suggests that auxin accumulates in the lateral root cap and epidermis and cannot be transported to the vascular tissue in the OZ. When NPA-grown seedlings were allowed to grow further in the absence of NPA, the recurrent degradation of DR5 expression in the lateral root cap is followed by the formation of a LRP at the position where the DR5 expresssion disappeared (Supplementary Video 9). Moreover, NPA addition resulted in loss of DR5-Luciferase oscillations in OZ. (Fig. 4d, e), indicating that auxin efflux carriers are required for LR patterning.

Polar auxin efflux is facilitated by PIN-FORMED (PIN) efflux carriers. Of all tested PIN proteins, only PIN2 is is polarly localized in the apical cell membrane of lateral root cap and epidermis (Extended Data Fig. 4h). In the distal lateral root cap cells, PIN2 is laterally localized on cell membranes of that face the epidermis (Extended Data Fig. 4h), facilitating auxin flux into the epidermis towards the OZ. The protein kinases PINOID (PID), WAG1 and WAG2 redundantly recruit PINs to the apical plasma membrane and are expressed in the epidermis and lateral root cap (Extended Data Fig. 4e) (Dhonukshe et al., 2010). In

pidwag1wag2 triple mutant seedlings, the apical PIN2 polarity in lateral root cap cells is lost (Dhonukshe et al., 2010), and the number of LRPs and LRs was dramatically reduced and cannot be rescued by increased conversion of IBA-into-auxin in root cap cells (Extended Data Fig. 4f and g). This suggests that apical and lateral polar auxin transport in lateral root cap cells towards the OZ is required for LR patterning.

We next investigated whether auxin influx into the lateral root cap is required for LR patterning. The auxin influx carrier AUX1 is specifically expressed in root cap cells and epidermis cells starting from the most distal part of the lateral root cap (Extended Data Fig. 3h). In the aux1 mutant, we observed reduced DR5 expression in the root cap and less prebranch sites and LRs (Extended Data Fig. 4i and Extended Data Fig. 5a-c). A GAL4-based transactivation approach showed that the reduced number of LRs in the *aux1* mutant could be rescued by targeted expression of AUX1 in the domain of J3411 (lateral root cap) but not J0121 (pericycle cells) (Extended Data Fig. 4j). In addition, NPA induced accumulation of DR5 in lateral root cap and epidermis was repressed in *aux1* and *ibr1ibr3ibr10* mutants (Extended Data Fig. 5a-c). This indicates that auxin flux into lateral root cap cells is required for LR patterning, possibly to ensure that the IBA-derived auxin pool can be transported towards the OZ. All together, these results suggest that auxin is transported from the lateral root cap to the OZ to trigger the oscillations.

Discussion:

The molecular mechanism behind the paterning of new organs is a major research topic both in plant and animal biology. In plant roots, lateral roots form periodcically, driven by a molecular oscillator referred to as the root clock, along the primary root axis. The root clock is controlled by the combination of a temporal signal (oscillating of gene expression) to regulate the oscillation periodicity (Moreno-Risueno et al., 2010), and a spatial auxin signal from the root cap to moderate the oscillation strength in the oscillation zone (OZ) (Xuan et al., chapter 2). In this study, we revealed that this root clock is facilitated by a recurrent root cap cell death, which triggers the transition of a considerable amount of auxin from root cap to OZ to set the root clock.

So far, the root cap has been demonstrated as a crucial tissue that mediates the interaction between plant roots and their growth substrate (Filleur et al., 2005; Svistoonoff et al., 2007). Its central role on the patterning of lateral roots along the primary root, that is the central theme of our study, might provide the plants with the possibility to adapt their root architecture to the ever changing soil conditions. During the exploration of the soil, root tips

might sense, via the root cap, the nutrient status when they enter nutrient-poor versus nutrient-rich spots and translate this environmental information to an alteration in the rate of lateral root production. This mechanism might help the plants to take profit from favorable soil conditions and to produce locally a higer number of lateral roots by increasing the lateral root density as is the case for root foraging.

On the other hand, irrespective of environmental conditions, the default settings of the root clock show parallels with the molecular mechanism which controls somitogenesis in vertebrates. Both root cap and tail bud are located at the distal end of the growing structure and are responsible to prepare proliferating cells for the periodic formation of segmentation (segment clock). It is therefore suggested that the apical growing cells of an organism might direct the movement of the organism and pattern the new organs along body axis both in vertebrates and plants.

Darwin once mentioned about the root cap that “We believed there is no structure in plants more wonderful, as far as its functions are concerned, that the tip of the radical” (Darwin and Darwin, 1880). Our results support this vision on the central role of the root cap, the organ at the most tip of root, controling root patterning in Arabidopsis.

Materials and Methods

Plant growth conditions

Arabidopsis thaliana seeds were grown on Petri dishes (12 cm X 12 cm) containing sterile half-strength Murashige and Skoog (1/2MS) medium under continuous light as described before (Xuan et al., chapter 2). For crosses and seed collection, seedlings were transplanted to soil and grown at 22°C with a 16-hour daily illumination (100 µmol m^{-2} s^{-1}).

For compound treatments, filter-sterilized substances were added to cooled (50°C) molten MS medium and mixed in 50-mL Falcon tubes before being poured into Petri dishes. Three-day-old seedlings were transferred to fresh ½MS media with different compounds for extra 5 days, unless otherwise indicated.

Plant lines used

The *Arabidopsis* accessions Columbia (Col-0) and C24 were used for this study. The auxin-responsive reporter lines *DR5rev:VENUS-N7* , *DII-VENUS* and *DR5:Luciferase* have been described previously (Brunoud et al., 2012; Heisler et al., 2005; Moreno-Risueno et al., 2010). *DR5rev:VENUS-N7* has been crossed with Col-0 for three times before being applied in all the experiments. The GAL4-GFP enhancer trap lines *J3411*, *J0951* and J0121 were

obtained from the Nottingham Arabidopsis Stock Centre (http://nasc.nott.ac.uk/) and the *UAS:DTA* line was a gift from Remko Offringa (Leiden University, The Netherlands). The GAL4 enhancer trap lines were crossed with *UAS:DTA* and the lateral root phenotype of the F1 generation was analyzed.

The origin of the mutant lines used is as follows: the *smb-3* (SALK_143526) mutant was obtained from the Nottingham Arabidopsis Stock Centre; the *35S:SMB-GR* transgenic line was kindly supplied by Lieven De Veylder (Ghent University, Belgium); *qua1-3* and *qua2-1* mutants were the gifts from Grégory Mouille (Institut Jean-Pierre Bourgin, INRA, France); the indole-3-buytric acid (IBA) conversion pathway mutant *ibr1-2ibr3-1ibr10-1*, auxin transport mutants *aux1-21* and *pidwag1*(Dhonukshe et al., 2010) *wag2* have been described previously (Strader et al., 2011; Swarup et al., 2004). Double and higher-order mutants harboring various marker lines were generated by crossing. F3 homozygous seedlings were analyzed in all experiments. For the *aux1* complementation study, the enhancer trap lines *J3411* and *J0121* were first induced into *aux1-21* mutant. Homozygous *J3411 aux1-21* and *J0121 aux1-21* seedlings were subsequently crossed with *UAS:AUX1 aux1-22* seedlings. F1 seedlings were used to quantify the lateral root phenotype.

Plant Constructs and Transformations

The Gateway system® (Invitrogen, Carlsbad, CA, USA) was applied to generate most constructs, and the primers used in this study are listed in Supplemental Table 1. For transcriptional fusions, the promoter fragments upstream of the coding sequence amplified from genomic DNA were cloned into pDONR221 or pDONRP4P1R and subsequently introduced into different expression vectors (Karimi et al., 2007). To generate pSMB:axr3-GR construct, the gain-of-function *axr3-1* cDNA fragment were amplified from *UAS:axr3-1* seedling cDNA, and then fused between the SMB promoter and the GR tag in a destination vector. For estradiol-inducible *Diphtheria* toxin a (DTA) translation fusions, the DTA cDNAs was amplified from *UAS:DTA* transgenic seedling cDNA and cloned into pDNOR221. A modified pER8 vector was cloned into the pDONRP4P1R downstream of UAS promoter to enable the compiling of the inducible construct. Transgenic plants were created by Agrobacterium tumefaciens floral dipping with the construct described above into the appropriate genetic background (Clough and Bent, 1998).

Root phenotype analyses

To quantify the lateral root phenotype in wild-type plants and mutants, emerged lateral roots of the whole seedlings were counted under a dissecting microscope 8 days after

germination. Subsequently, whole seedlings were scanned for further analysis of the primary root length. For dexamethasone (Dex) and estradiol treatments, the length of the primary root grown after the treatment was measured and emerged lateral roots in this root region were counted. The gravitropic index was obtained by calculating the ratio of vertical length and primary root length (RL) (Grabov et al., 2005).

Histochemical analysis and confocal microscopy

GUS assays were done as described previously (Vanneste et al., 2005). For microscopic analysis of primordium stages, root samples were cleared (Malamy and Benfey, 1997). All samples were analyzed by differential interference contrast microscopy (Olympus BX53). An Zeiss 710 confocal laser scanning microscope was used for fluorescence imaging of roots. For the propidium iodide (PI)-treated root images, seedlings were stained with 2 µg/mL PI for 3 minutes, washed with water, and used for confocal imaging. To generate 3D projection of z-stacks of root tip sections, stacks of ~ 70 optical z sections (1 µm step-size) were collected from root axes at the meristem zone.

Macroview stereo microscope setting up and imaging

Olympus MXV10 macroview stereo microscope (http://www.olympusamerica.com/seg_section/product.asp?product=1013) was 90 degree turned and adapted to a holder, which enable to image the fluorescence signal from vertical growing *Arabidospsis* root in the square plate. A mobile microscope stage was installed to fix the plate close-up to the lens. For time lapse imaging, the filters were under control of an automated shutter manipulated by the software, and images were taken every two minutes to generate the video files.

Luciferase imaging and expression analysis

The Luciferase images were taken by a Lumazone machine carrying a charge-coupled device (CCD) camera (Princeton Instruments, Trenton, NJ, USA) as described previously (Xuan et al., chapter 2).

Author contributions:

W.X., D.A. and T.B. conceived the project. W.X. and D.V.D. set up the imaging system. W.X., G.D.R. and D.O. performed imaging and analysis. L.B. developed the mathematical

modelling. X.W. and S.V. performed analysis on auxin transport reporters and mutants. M.N. cloned cell death genes. W.X., B.M. and T.B. wrote the manuscript. All authors discussed the results and commented on the manuscript.

Supplementary videos files S1-S9

Video S1. Movie of *DR5rev:VENUS-N7* expression in a 3-day-old seedling for 14 hours. Red arrows indicate the disappearance of *DR5* expression in the root cap; yellow arrows indicate a LRP. Scale bar, 0.2 cm.

Video S2. Movie of *DR5rev:VENUS-N7* expression in a 3-day-old seedling after a gravitropic stimulus (145 degree turn) for 20 hours. Red arrows indicate the disappearance of *DR5* expression in the root cap during root bending; yellow arrows indicate a LRP. Scale bar, 0.5 mm.

Video S3. Movie of *pPASPA3:NLS-tdTOMATO* expression in a 3-day-old seedling after a gravitropic stimulus (145 degree turn) for 11 hours. Red arrows indicate the disappearance of *PASPA3* signal in the root cap during root bending. Scale bar, 0.5 mm.

Video S4. Movie of *pPASPA3:NLS-tdTOMATO* expression in a 3-day-old F1 seedling of a cross between *pPASPA3:NLS-tdTOMATO* and *DR5rev:VENUS-N7* over 18 hours. White arrows indicate the disappearance of *PASPA3* signal in the root cap. Scale bar, 0.1 mm.

Video S5. Movie of *pSMB:NLS-GFP* expression in a 3-day-old seedling over 10 hours. Red arrows indicate the disappearance of *SMB* signal in the root cap. Scale bar, 0.5 mm.

Video S6. Movie of *DR5:Luciferase* expression in 3-day-old seedlings Col-0 and *35S:SMB-GR* Dex-treated seedling over 24 hours. One root from the Col-0 seedlings (on the left) and five roots from the *35S:SMB-GR* seedlings were imaged over time. Scale bar, 0.5 mm.

Video S7. Movie of *pPASPA3:NLS-tdTOMATO* expression in a 3-day-old NPA-treated Col-0 seedling over 22 hours. White arrows indicate the disappearance of *PASPA3* signal in the root cap. NPA was used at 10 µM. Scale bar, 0.2 mm.

Video S8. Movie of *DR5rev:VENUS-N7* expression in a 3-day-old Col-0 seedling treated with NPA for 16 hours. NPA was used at 10 µM. Scale bar, 0.2 mm.

Video S9. Movie of *DR5rev:VENUS-N7* expression in a 3-day-old NPA-grown Col-0 seedling that was transferred to medium without NPA. Red arrow indicates the disappearance of *DR5* signal in the root cap; yellow arrow indicates a LRP. Scale bar, 0.2 mm.

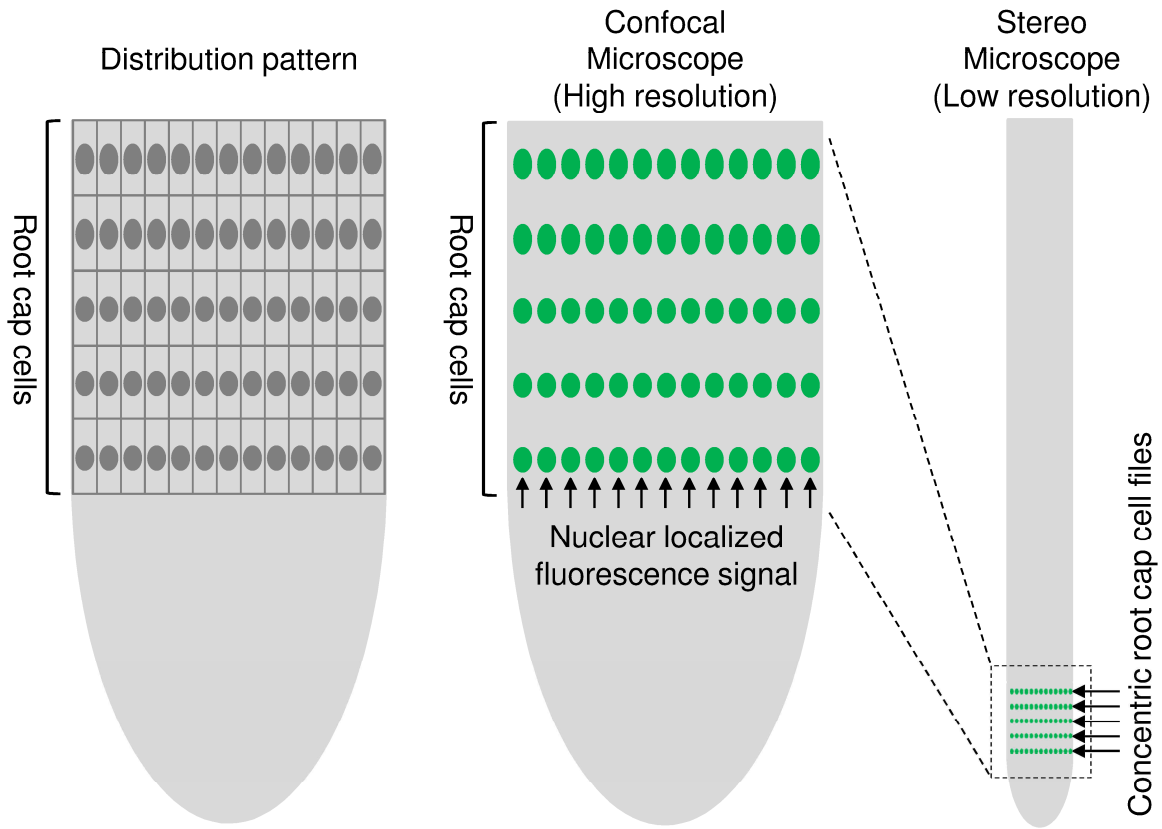

Extended Data Figure 1 | Schematic of the ring-like expression pattern of nuclear localized florescence signal in root cap cells under stereo microscope.

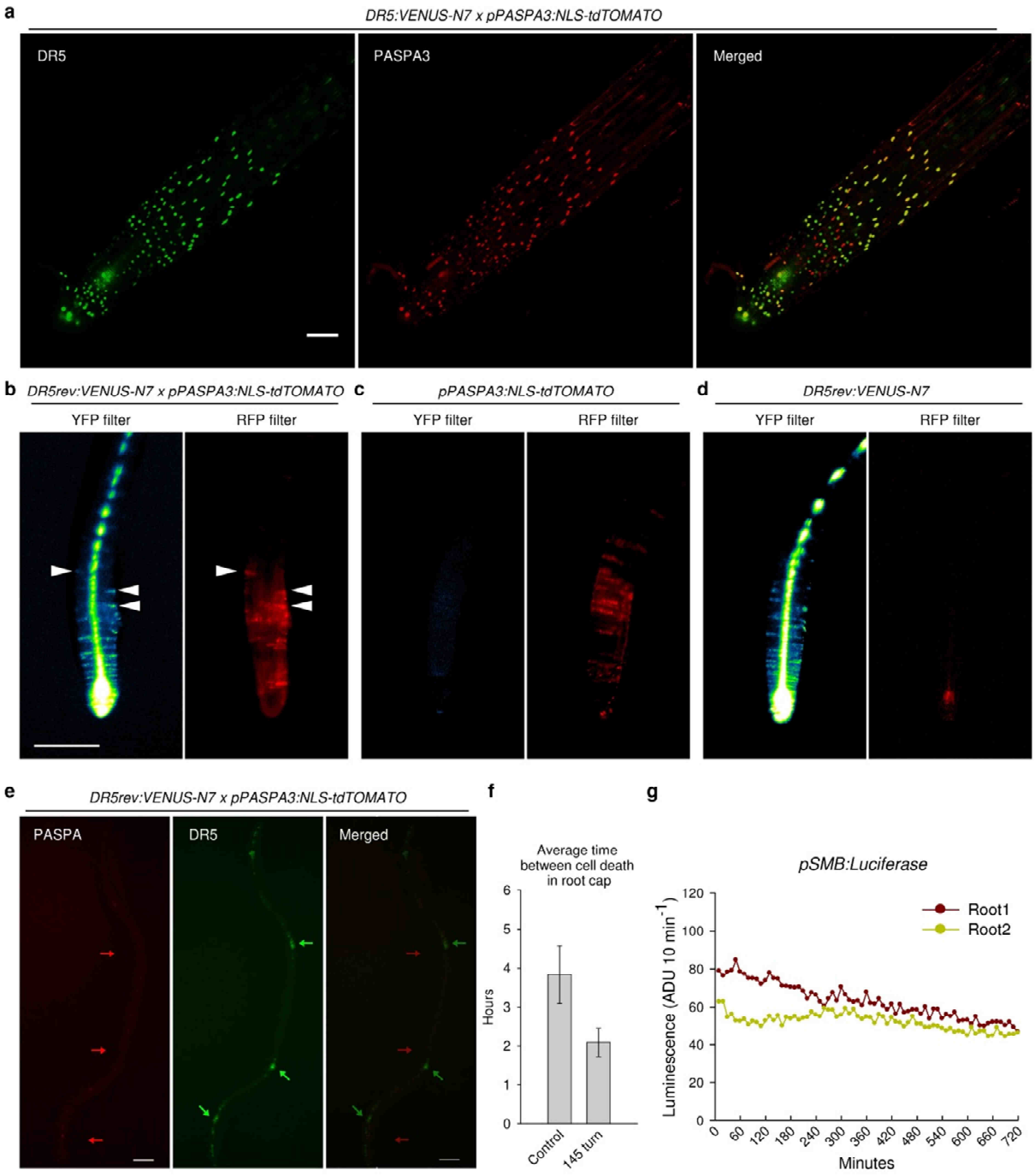
a
DR5:VENUS-N7 x pPASPA3:NLS-tdTOMATO
DR5
PASPA3
Merged
b
DR5rev:VENUS-N7 x pPASPA3:NLS-tdTOMATO
YFP filter
RFP filter
c
pPASPA3:NLS-tdTOMATO
YFP filter
RFP filter
d
DR5rev:VENUS-N7
YFP filter
RFP filter
e
DR5rev:VENUS-N7 x pPASPA3:NLS-tdTOMATO
PASPA
DR5
Merged
f
Average time between cell death in root cap
Hours
Control
145 turn
g
pSMB:Luciferase
Root1
Root2
Luminescence (ADU 10 min-1)
Minutes

Extended Data Figure 2 | Periodic root cap cell death correlates with LRP formation. **a**, Z-stack confocal microscope images of the co-localization of *DR5*-driven nuclear tagged YFP signal and *PASPA3* promoter-driven nuclear tdTOMATO signal in root cap cells. Pinhole, 1.7 µm. Scale bar, 50 µm. **b** - **d**, Macroview stereo microscope images of the localization of *DR5* signal and *PASPA3* signal in the concentric distal cell files of the root cap. Scale bar, 200 µm. **e**, Positional correlation of the *PASPA3* root cap cell death signal and LRPs in the primary root in F1 seedlings of a cross between *pPASPA3:NLS-tdTOMATO* and *DR5rev:VENUS-N7*. Red arrows indicate the disappearance of the PASPA3 signal; green arrows indicated the positions of *DR5* expressing LRP (also see Supplemental video 4). Scale bar, 100 µm. **f**, Quantification of average time interval between disappearance of *pPASPA3:NLS-tdTOMATO* signal in concentric root cap cell files under normal conditions or during gravity-induced bending ($n > 30$). Error-bars are means ± standard deviation. **g**, Quantification of *pSMB-Luciferase* expression in the root cap over twelve hours. 3-day-old seedlings were used for in all experiments.

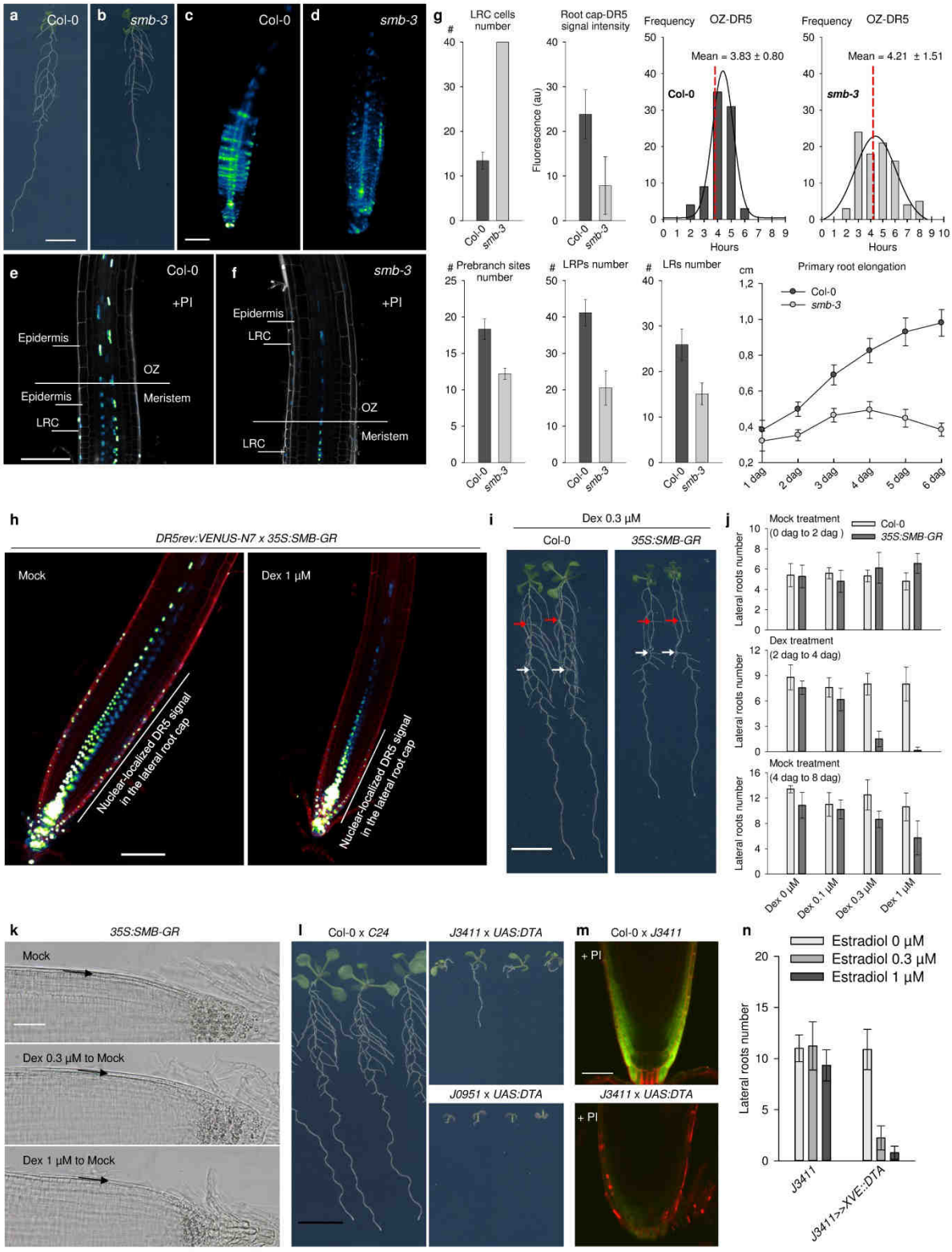
a Col-0
b smb-3
c Col-0
d smb-3
e Col-0 +PI
Epidermis
OZ
Epidermis
Meristem
LRC
f smb-3 +PI
Epidermis
LRC
OZ
Meristem
LRC
g
LRC cells number
Root cap-DR5 signal intensity
Fluorescence (au)
Frequency OZ-DR5
Mean = 3.83 ± 0.80
Col-0
Hours
Frequency OZ-DR5
Mean = 4.21 ± 1.51
smb-3
Hours
Prebranch sites number
LRPs number
LRs number
Primary root elongation
cm
Col-0
smb-3
1 dag
2 dag
3 dag
4 dag
5 dag
6 dag
h
DR5rev:VENUS-N7 x 35S:SMB-GR
Mock
Dex 1 µM
Nuclear-localized DR5 signal in the lateral root cap
i
Dex 0.3 µM
Col-0
35S:SMB-GR
j
Mock treatment (0 dag to 2 dag)
Col-0
35S:SMB-GR
Lateral roots number
Dex treatment (2 dag to 4 dag)
Mock treatment (4 dag to 8 dag)
Dex 0 µM
Dex 0.1 µM
Dex 0.3 µM
Dex 1 µM
k
35S:SMB-GR
Mock
Dex 0.3 µM to Mock
Dex 1 µM to Mock
l
Col-0 x C24
J3411 x UAS:DTA
J0951 x UAS:DTA
m
Col-0 x J3411
+ PI
J3411 x UAS:DTA
+ PI
n
Estradiol 0 µM
Estradiol 0.3 µM
Estradiol 1 µM
Lateral roots number
J3411
J3411>>XVE::DTA

Extended Data Figure 3 | Root clock requires the root cap. a, Root phenotype of 8-day-old Col-0 and *smb-3* seedlings. **c-f**, Macroview microscope images (**c, d**) and confocal microscope images (**e, f**) of *DR5rev:VENUS-N7* expression in root tips of 3-day-old Col-0 and *smb-3* seedlings. PI, propidium iodide. **g**, Quantification of the indicated parameters in Col-0 and *smb-3* seedlings. 3-day-old seedlings were used to measure the number of lateral root cap cells (n > 30), the *DR5* signal intensity in the root cap (n > 30) and the *DR5* oscillation frequency in OZ (n > 70 obtained from individual 15 seedlings); numbers of prebranch sites (PBs), LRPs, and LRs were obtained from 8-day-old seedlings (n > 12). Primary root elongation was measured in 6-day-old seedlings (n > 14). **h**, *DR5rev:VENUS-N7* expression in 5-day-old *35S:SMB-GR* transgenic seedlings that were Mock or Dex treated from day 3 on. **i-k**, Quantification of LR number in 8-day-old Col-0 and *35S:SMB-GR* seedlings treated with Dex from day 2 (red arrows), then transferred to medium without Dex on day 4 (black arrows). LR numbers from the root regions that only formed on indicated medium (with or without Dex), and images of root phenotype (**i**) and root tip (**k**) were taken. Arrows indicated the time of the transfer. n = 10. **l**, **m**, Root phenotype and expression pattern of J3411 of 8-day-old F1 progeny of indicated lines. **n**, Quantification of LR number in 8-day-old indicated transgenic lines treated with various concentrations of estradiol from day 3 on (n > 10). Black scale bars, 1 cm; white scale bars, 100 µm.

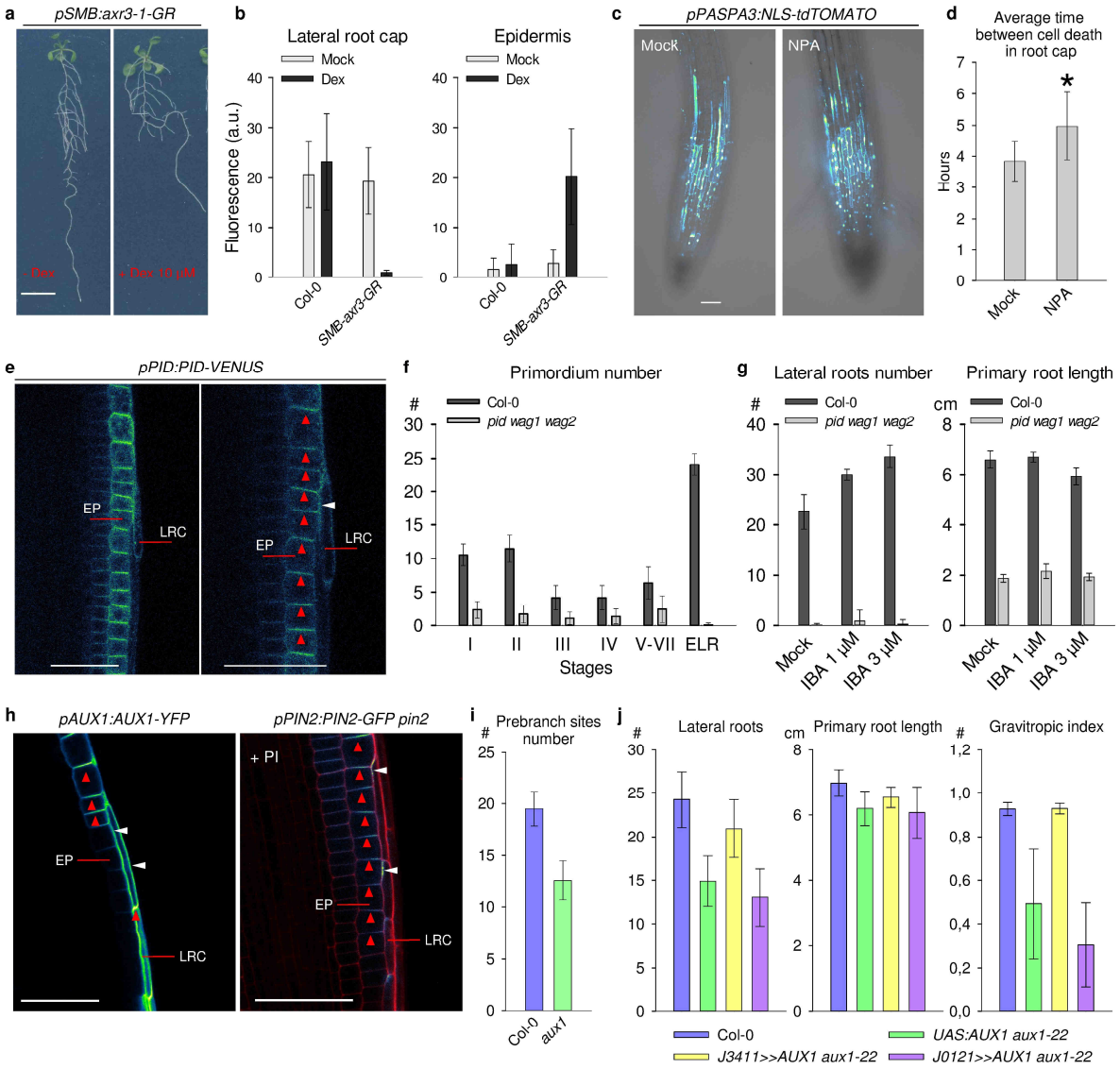

Extended Data Figure 4 | Auxin transport regulates LR patterning. a, Root phenotype of 8-day-old *pSMB:axr3-GR* transgenic seedlings transferred to ½ MS medium with or without Dex from day 3 on. Bar = 1 cm. **b**, Quantification of DR5 signal intensity in lateral root cap and epidermis in 3-day-old indicated lines treated with or without 10 µM Dex since germination. **c**, *pPASPA3:NLS-tdTOMATO* expression in 3-day-old Mock- or NPA-treated seedlings. **d**, Quantification of average time interval between the disappearance of *pPASPA3:NLS-tdTOMATO* signal in concentric root cap cell files under indicated treatments ($n > 30$, $*P < 10^{-5}$). **e**, Quantification of root phenotype in 8-day-old Col-0 and *pidwag1wag2* seedlings transferred to medium containing different concentrations of IBA from day 3 on ($n > 10$). **f**, *pAUX1:AUX1-YFP* and *pPIN2:PIN2-GFP* protein accumulation in root cap cells. **g**, **h**, Quantification of the root phenotype in 8-day-old Col-0 and *aux1* single mutant seedlings and F1 seedlings of *J3411>>AUX1 aux1-22* and *J0121>>AUX1 aux1-22*. Error-bars are means ± standard deviation. Scale bar, 50 µm.

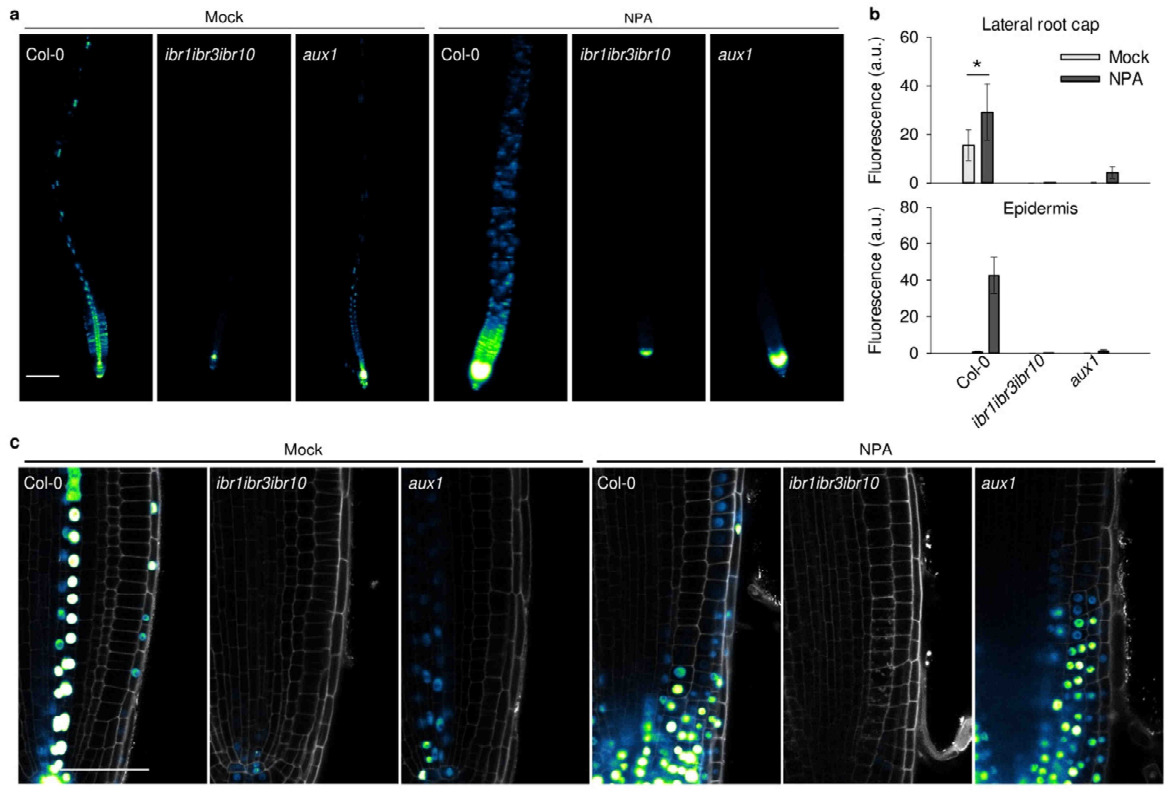

Extended Data Figure 5 | Inhibition of auxin transport changes *DR5* expression pattern. **a**, **c**, Macroview stereo microscope images (**a**) and confocal microscope images (**c**) of *DR5rev:VENUS-N7* expression in 3-day-old Col-0, *ibr1ibr3ibr10* triple mutant, and *aux1* single mutant seedlings grown with or without 10 µM NPA. Scale bar, 50 µm. **b**, Quantification of *DR5rev:VENUS-N7* signal intensity in lateral root cap and epidermis tissues in 3-day-old indicated seedlings under Mock- or 10 µM NPA treatment (n = 24, $*P < 10^{-6}$). Error-bars are means ± standard deviation.

Reference

Aida, M., Beis, D., Heidstra, R., Willemsen, V., Blilou, I., Galinha, C., Nussaume, L., Noh, Y.S., Amasino, R., and Scheres, B. (2004). The PLETHORA genes mediate patterning of the Arabidopsis root stem cell niche. Cell *119*, 109-120.
Arnaud, C., Bonnot, C., Desnos, T., and Nussaume, L. (2010). The root cap at the forefront. Comptes rendus biologies *333*, 335-343.
Bennett, T., van den Toorn, A., Sanchez-Perez, G.F., Campilho, A., Willemsen, V., Snel, B., and Scheres, B. (2010). SOMBRERO, BEARSKIN1, and BEARSKIN2 regulate root cap maturation in Arabidopsis. The Plant cell *22*, 640-654.
Birnbaum, K., Shasha, D.E., Wang, J.Y., Jung, J.W., Lambert, G.M., Galbraith, D.W., and Benfey, P.N. (2003). A gene expression map of the Arabidopsis root. Science *302*, 1956-1960.
Brunoud, G., Wells, D.M., Oliva, M., Larrieu, A., Mirabet, V., Burrow, A.H., Beeckman, T., Kepinski, S., Traas, J., Bennett, M.J., *et al.* (2012). A novel sensor to map auxin response and distribution at high spatio-temporal resolution. Nature *482*, 103-106.
Clough, S.J., and Bent, A.F. (1998). Floral dip: a simplified method for Agrobacterium-mediated transformation of Arabidopsis thaliana. The Plant journal : for cell and molecular biology *16*, 735-743.
De Smet, I., Tetsumura, T., De Rybel, B., Frey, N.F., Laplaze, L., Casimiro, I., Swarup, R., Naudts, M., Vanneste, S., Audenaert, D., *et al.* (2007). Auxin-dependent regulation of lateral root positioning in the basal meristem of Arabidopsis. Development *134*, 681-690.
Dhonukshe, P., Huang, F., Galvan-Ampudia, C.S., Mahonen, A.P., Kleine-Vehn, J., Xu, J., Quint, A., Prasad, K., Friml, J., Scheres, B., *et al.* (2010). Plasma membrane-bound AGC3 kinases phosphorylate PIN auxin carriers at TPRXS(N/S) motifs to direct apical PIN recycling. Development *137*, 3245-3255.
Dolan, L., Janmaat, K., Willemsen, V., Linstead, P., Poethig, S., Roberts, K., and Scheres, B. (1993). Cellular organisation of the Arabidopsis thaliana root. Development *119*, 71-84.
Fendrych, M., Van Hautegem, T., Van Durme, M., Olvera-Carrillo, Y., Huysmans, M., Karimi, M., Lippens, S., Guerin, C.J., Krebs, M., Schumacher, K., *et al.* (2014). Programmed Cell Death Controlled by ANAC033/SOMBRERO Determines Root Cap Organ Size in Arabidopsis. Current biology : CB.
Filleur, S., Walch-Liu, P., Gan, Y., and Forde, B.G. (2005). Nitrate and glutamate sensing by plant roots. Biochemical Society transactions *33*, 283-286.
Grabov, A., Ashley, M.K., Rigas, S., Hatzopoulos, P., Dolan, L., and Vicente-Agullo, F. (2005). Morphometric analysis of root shape. The New phytologist *165*, 641-651.
Gray, W.M., Kepinski, S., Rouse, D., Leyser, O., and Estelle, M. (2001). Auxin regulates SCF(TIR1)-dependent degradation of AUX/IAA proteins. Nature *414*, 271-276.
Heisler, M.G., Ohno, C., Das, P., Sieber, P., Reddy, G.V., Long, J.A., and Meyerowitz, E.M. (2005). Patterns of auxin transport and gene expression during primordium development revealed by live imaging of the Arabidopsis inflorescence meristem. Current biology : CB *15*, 1899-1911.
Karimi, M., Depicker, A., and Hilson, P. (2007). Recombinational cloning with plant gateway vectors. Plant physiology *145*, 1144-1154.
Lucas, M., Godin, C., Jay-Allemand, C., and Laplaze, L. (2008). Auxin fluxes in the root apex co-regulate gravitropism and lateral root initiation. Journal of experimental botany *59*, 55-66.
Malamy, J.E., and Benfey, P.N. (1997). Organization and cell differentiation in lateral roots of Arabidopsis thaliana. Development *124*, 33-44.

Moreno-Risueno, M.A., Van Norman, J.M., Moreno, A., Zhang, J., Ahnert, S.E., and Benfey, P.N. (2010). Oscillating gene expression determines competence for periodic Arabidopsis root branching. Science *329*, 1306-1311.
Rouse, D., Mackay, P., Stirnberg, P., Estelle, M., and Leyser, O. (1998). Changes in auxin response from mutations in an AUX/IAA gene. Science *279*, 1371-1373.
Strader, L.C., Wheeler, D.L., Christensen, S.E., Berens, J.C., Cohen, J.D., Rampey, R.A., and Bartel, B. (2011). Multiple facets of Arabidopsis seedling development require indole-3-butyric acid-derived auxin. The Plant cell *23*, 984-999.
Svistoonoff, S., Creff, A., Reymond, M., Sigoillot-Claude, C., Ricaud, L., Blanchet, A., Nussaume, L., and Desnos, T. (2007). Root tip contact with low-phosphate media reprograms plant root architecture. Nature genetics *39*, 792-796.
Swarup, R., Kargul, J., Marchant, A., Zadik, D., Rahman, A., Mills, R., Yemm, A., May, S., Williams, L., Millner, P., *et al.* (2004). Structure-function analysis of the presumptive Arabidopsis auxin permease AUX1. The Plant cell *16*, 3069-3083.
Swarup, R., Kramer, E.M., Perry, P., Knox, K., Leyser, H.M., Haseloff, J., Beemster, G.T., Bhalerao, R., and Bennett, M.J. (2005). Root gravitropism requires lateral root cap and epidermal cells for transport and response to a mobile auxin signal. Nature cell biology *7*, 1057-1065.
Van Norman, J.M., Xuan, W., Beeckman, T., and Benfey, P.N. (2013). To branch or not to branch: the role of pre-patterning in lateral root formation. Development *140*, 4301-4310.
Vanneste, S., De Rybel, B., Beemster, G.T., Ljung, K., De Smet, I., Van Isterdael, G., Naudts, M., Iida, R., Gruissem, W., Tasaka, M., *et al.* (2005). Cell cycle progression in the pericycle is not sufficient for SOLITARY ROOT/IAA14-mediated lateral root initiation in Arabidopsis thaliana. The Plant cell *17*, 3035-3050.
Weijers, D., Van Hamburg, J.P., Van Rijn, E., Hooykaas, P.J., and Offringa, R. (2003). Diphtheria toxin-mediated cell ablation reveals interregional communication during Arabidopsis seed development. Plant physiology *133*, 1882-1892.
Willemsen, V., Bauch, M., Bennett, T., Campilho, A., Wolkenfelt, H., Xu, J., Haseloff, J., and Scheres, B. (2008). The NAC domain transcription factors FEZ and SOMBRERO control the orientation of cell division plane in Arabidopsis root stem cells. Developmental cell *15*, 913-922.

GRASSES

Boundless grasses over the plain,
Come and go with every season;
No prairie fire can destroy the grass,
It shoots up again with the spring breeze blows;
Sweet they press on the old high-road,
And reach the crumbling city-gate;
Oh, Prince of friends, you are gone again...
I hear them sighing after you.

Bai Juyi (A poet from Tang Dynasty)

Chapter 4

A novel small molecule reveals the role of auxin receptor TIR1 on root branching

A novel small molecule reveals the role of auxin receptor TIR1 on root branching

Wei Xuan[1,2], Dominique Audenaert[1,2#], Bert De Rybel[1,2¥], Paul Overvoorde[3], Stefan Kepinski[4], Mark Estelle[5] and Tom Beeckman[1,2*]

Affiliations:

[1]Department of Plant Systems Biology, VIB, Ghent, Belgium.

[2]Department of Plant Biotechnology and Bioinformatics, Ghent University, Gent, Belgium.

[3]Department of Biology, Macalester College, St. Paul, Minnesota, USA.

[4]Centre for Plant Sciences, University of Leeds, Leeds, UK.

[5]Department of Biology, Indiana University, Bloomington, Indiana 47405, USA

[#]Present address: Compound Screening Facility, VIB, Ghent University, Gent, Belgium

[¥]Present address: Laboratory of Biochemistry, Wageningen University, Dreijenlaan 3, 6703HA Wageningen, The Netherlands.

[†] Correspondence to: tobee@psb.vib-ugent.be

Abstract

Auxin has been demonstrated to control root branching in plants. In the plant model *Arabidopsis thaliana*, the auxin signal is mediated by the auxin receptor transport inhibitor response 1 (TIR1). However, the regulation of root branching by TIR1 remains elusive. Here, we identified a novel small molecule, tirlin, TIR1-dependent lateral root inducer, as a chemical tool to unravel the molecular mechanism of Tir1 on lateral root development. We found that tirlin strongly induces lateral root formation without moderating auxin perception by TIR1. Genetic evidence shows that tirlin might act downstream of TIR1 and ARF7-ARF19 to regulate lateral root formation. By screening a fast-neutron mutagenesis population, we identified LBD proteins as potential targets of tirlin. Our work suggests that LBD proteins may act as the core downstream components of TIR1-dependent signaling on the regulation of lateral root formation.

Introduction

The complexity and architecture of the plant root system is mainly controlled by root branching. It plays a crucial role in the adaptation of the plant to environment stimuli. In the plant model *Arabidopsis thaliana*, the process of root branching is under the temporal control of oscillating gene expression in the oscillation zone (OZ) close to the root tip, which has been designated as the root clock (Moreno-Risueno et al., 2010; Van Norman et al., 2013). This periodic gene oscillation in the OZ leads to the spatial formation of prebranch sites, patches of cells in the OZ that subsequently will develop as lateral root (LR) primordia.

Auxin has been demonstrated as a key regulator of repeatable organogenesis in *Arabidopsis*. The expression of the transcriptional auxin response reporter DR5 was found to oscillate in OZ and forms static expression pattern in the prebranch sites, which implies a role for auxin on regulating the rook clock. Recently, a root cap-specific auxin source driven by indole-3-butyric acid (IBA) and TIR1/AFB-dependent auxin signaling were also demonstrated to moderate the strength of the DR5 oscillation, and thus regulate prebrach sites formation (Xuan et al., chapter 2). In *Arabidopsis*, auxin signaling is perceived by the TIR1/AFB family of F-box proteins acting in concert with the Aux/IAA transcriptional repressors (Dharmasiri et al., 2005; Gray et al., 2001). Gain-of-function mutations in AUX/IAA proteins, including IAA28, SLR/IAA14, CRANE/IAA18 and SHY2/IAA3, decrease the number of LRs, indicating that AUX/IAA-dependent auxin signaling is necessary for LR formation (De Rybel et al., 2010; Rogg et al., 2001; Uehara et al., 2008; Vanneste et al., 2005; Vermeer et al., 2014).

However, several lines of evidence suggest that different combination of TIR1/AFB auxin receptors and AUX/IAA proteins displayed a wide range of auxin binding affinities, and as much contributes to the complexity of auxin responses and diverse root phenotypes (Calderon Villalobos et al., 2012; Parry et al., 2009). In addition, the exact role of each auxin receptor type and their downstream signaling components during the process of LR development remains unclear. By using a chemical genetic approach we established previously, we identified several small molecules, as non-auxin-like lateral root inducers in *Arabidopsis* (De Rybel et al., 2012).

One small molecule, which we named tirlin for TIR1-dependent lateral root inducer, enhanced LR development in a TIR1-mediated fashion. In this way, tirlin could act as a unique chemical tool for understanding the signaling pathways involved in TIR1-mediated lateral root formation, and also to get insight into the redundant and non-redundant functions of different auxin receptors.

Results

Identification and characterization of non-auxin like lateral root inducers

To identify new synthetic molecules that stimulate the process of lateral root development, we screened a diverse 10,000-compound library for activators of expression of CYCB1;1, a cell cycle gene that marks cellular divisions (Supplementary Fig. 1). In xylem pole pericycle cells, the induction of *CYCB1;1* promoter expression coincides with cell division of pericycle cells and thus reports the formation of new lateral root primordia (Himanen et al., 2002; Himanen et al., 2004; Vanneste et al., 2005). To report cell division in pericycle cells, we used transgenic seedlings containing a construct comprising the CYCB1;1 promoter fused to β-glucuronidase (GUS) (pCYCB1;1::GUS) in a high-throughput adaptation of a previously described 'lateral root inducible system' (Himanen et al., 2004). Eighty-eight molecules were identified to induce expression of *pCYCB1;1::GUS* in the xylem pole pericycle cells after 24 h (Fig. 1a), suggesting they were potent activators of the early stages of lateral root development. To avoid the selection of auxin-like compounds that would also affect other auxin-related processes, we excluded all molecules with a chemical structure similar to that of known auxins, such as IAA, NAA, 2,4-D or sirtinol, and retained nine hit molecules for further analysis (Fig. 1a and Supplementary Fig. 1; De Rybel et al., 2012). Phenotypic characterization shows that these hit compounds increased lateral root densities in a dose-dependent manner compared to the mock-treated control seedlings (Fig. 1b). Two of these molecules, A11 and A12, which we named naxillin for non-auxin-like lateral root inducer, shared a core structure and act on IBA-to-IAA conversion pathway (De Rybel et al., 2012). Another molecule, A14, displayed the strongest induction on lateral root formation without inducing a transcriptional auxin response in the basal meristem compared to NAA (Fig. 1b and Supplementary Fig. 1). In addition, similar to naxillin, A14 had less effect on primary root elongation and shoot development compared to the synthetic auxin NAA (Fig. 1c). In A14-treated Col-0 seedlings, we also observed lateral roots that were formed adjacent to one another or that fused at the base, indicating that lateral inhibition of organ formation is interrupted by A14 (Fig. 1e). Structure-activity analysis showed that removal of any substructure of this molecule led to the loss of A14 function on lateral root induction. Taken together, these data suggested that A14 and NAA might activate different modes of action to regulate lateral root formation.

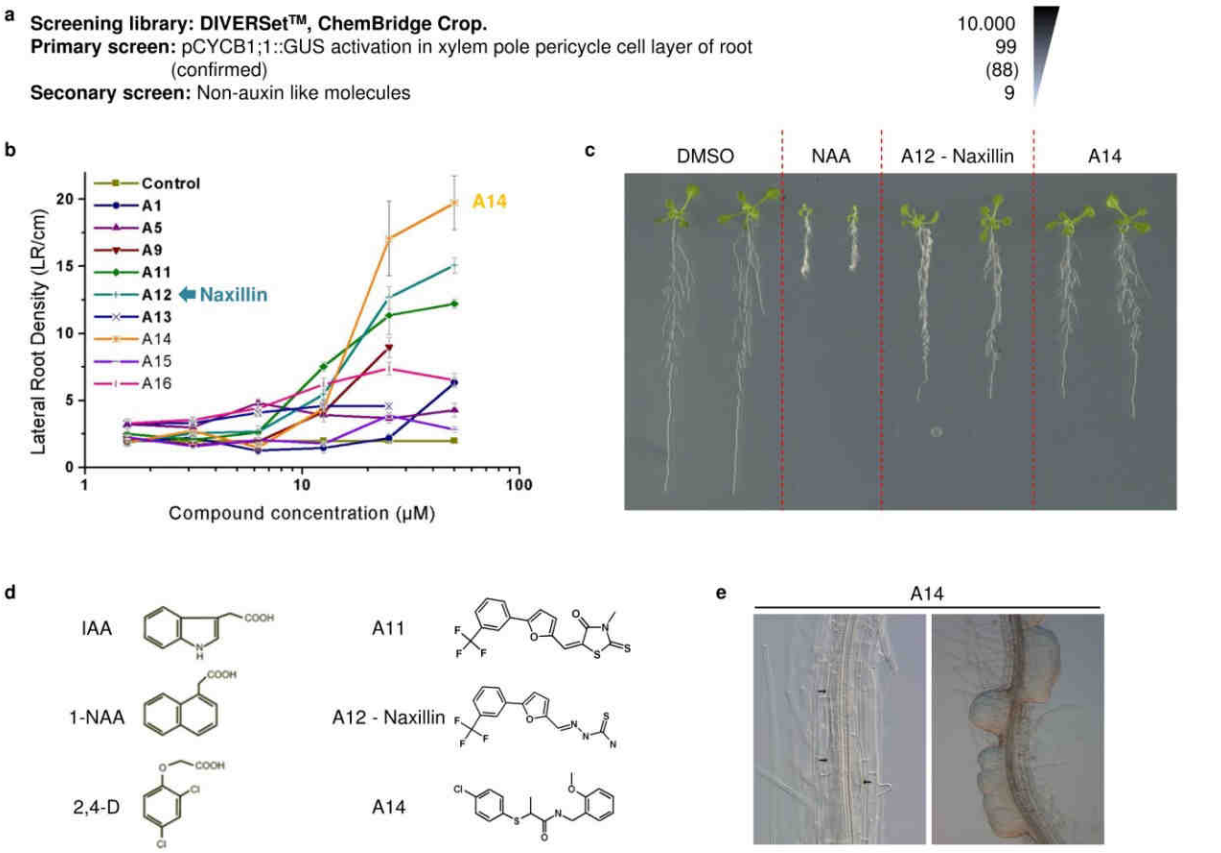

Figure 1. Identification of non-auxin like lateral root inducers. (a) Overview of the procedure to screen for activators of lateral root development with the *pCYCB1;1::GUS* marker (also see **Supplemental Figure 1**). (b) Dose-response analysis of lateral root (LR) density of seedlings grown on control medium until 3 d after germination and transferred to medium supplemented with the indicated hit molecule at the indicated concentration for five additional days. (c) Phenotype of plants grown on control medium for 3 d and then transferred to mock medium (DMSO) or medium supplemented with 10 µM NAA, 10 µM A12-naxillin, or 10 µM A14 for five additional days. (d) Chemical structure of auxin analogues, A11, naxillin and A14. (e) Lateral root primordia phenotype of three-day-old Col-0 seedling under A14 treatment for five additional days. (Updated from De Rybel et al., 2012)

A14 induces auxin response in the transition zone

It has been suggested that the auxin response in the OZ oscillates periodically and leads to the formation of prebranch sites, which is regulated by the amplitude of auxin response in the OZ (De Rybel et al., 2012; Xuan et al., chapter 2). To assess the effect of A14 on auxin response in the OZ, a transgenic line expressing DII-VENUS, an Aux/IAA-based auxin signaling sensor (Brunoud et al., 2012), was treated with A14. Interestingly, similar to NAA, A14 treatment induced a transient degradation of DII-VENUS in the OZ after 2 hours treatment (Fig. 2a). However, the reduction of DII expression level by A14 treatment was less pronounced compared to the global reduction of DII by NAA treatment, indicating that A14 affects auxin signaling in a more subtle way.

In *Arabidopsis*, auxin signaling is monitored by the binding of auxin and its main receptors TIR1/AFBs, which trigger the degradation of AUX/IAA proteins to activate downstream transcription. We further performed pull-down assays to determine whether A14 induces DII-VENUS degradation by affecting the binding of TIR1 to AUX/IAA proteins. Unlike NAA, A14 did not affect the interaction between TIR1-myc and AUX/IAA proteins in the presence or absence of NAA application, which is similar to the behavior of naxillin (Fig. 2b). This suggests that A14 does not act as a typical auxin.

The establishment of local auxin maxima in lateral root primordia is an important determinative factor in the development of lateral roots. In *Arabidopsis*, these auxin maxima are established by the constitutive cycling of the PIN-FORMED (PIN) family of auxin efflux carriers between the plasma membrane and endosomes (Benkova et al., 2003; De Smet et al., 2007; Kitakura et al., 2011). Therefore, we further tested the possibility of A14 on PIN endocytosis. As shown in Fig 3c, BFA treatment inhibits PINs trafficking from endosomes to the plasma membrane and causes the accumulation of PIN1/PIN2 in endosomes, which could be reversed by the application of NAA. By contrast, A14 treatments could not suppress the BFA-induced PIN accumulations, further demonstrating that A14 and NAA have different modes of action.

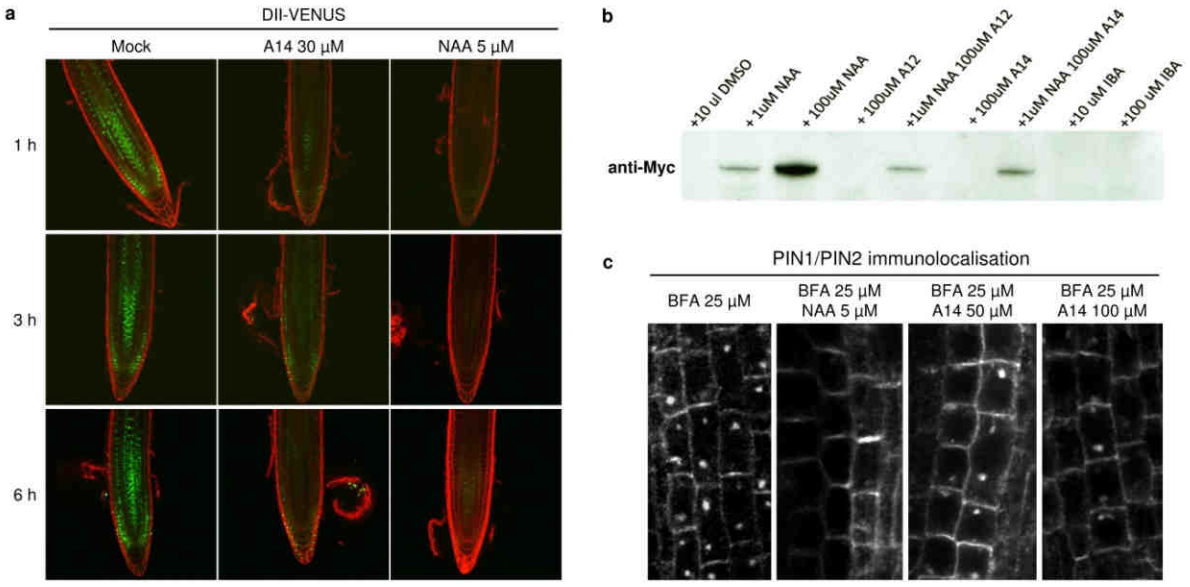

Figure 2. A14 does not interfere with TIR1-AUX/IAA interaction. (a) Time-course analysis of DII-VENUS expression on Col-0 seedlings germinated for five days and transfferd to mock medium (DMSO) or medium supplemented with indicated compounds for 1, 3 and 6 hours. Seedling harvested at indicated time points were used for confocal imaging. (b) The effect of different compounds on the binding assay of TIR1 and AUX/IAA proteins. c-myc-tagged TIR1 was pulled-down using biotinylated Aux/IAA domain II peptides in the presence of 1 µM NAA, 10 µM IBA, 100 µM A12, 100 µM A14, or the combination of different compounds as indicated, and compared to DMSO treatment. Each lane is from identical aliquots of the same batch of TIR1-myc extract and the Aux/IAA peptide is pipetted in and then captured on beads. (c) PIN1/PIN2 immunolocalization in wild-type seedlings treated with BFA alone, or BFA together with NAA or A14 at indicated concentrations for 90 min. (Updated from De Rybel et al., 2012)

A14 function requires the auxin receptor TIR1

To identify the signaling pathways that are essential for A14 activity on lateral root formation, we analyzed the effect of A14 on various mutants from different signaling pathways, which have been demonstrated to be involved in lateral root formation. First, the IBA-to-IAA conversion triple loss-of-function mutant *ibr1ibr3ibr10* maintained sensitivity to A14 treatment (Supplemental Fig. 1) (De Rybel et al., 2012). Meanwhile, A14 could also induce lateral root formation in *smb-3*, *brn1brn2* and *arf7* (Supplemental Fig. 1), mutants that were shown to control the periodicity of lateral root production (Moreno-Risueno et al., 2010). Furthermore, the *acr4* mutation, which interferes with the asymmetric cell division during lateral root initiation (De Smet et al., 2008), also did not suppress the effect of A14 induction on lateral root formation (Supplemental Fig. 1). However, A14 failed to induced lateral root formation in the *arf7 arf19* double loss-of-function mutant (Supplemental Fig. 1), suggesting that A14's function is dependent on the ARF7-ARF19 pathway.

To assess whether A14 affects the early events of auxin signaling, we first determine the effect of A14 on the tir1-1, auxin receptor TIR1mutant (Dharmasiri et al., 2005). Interestingly, the A14-response on lateral root formation and primary root elongation was suppressed in the *tir1*mutant background (Fig. 3a and b). To further test the effect of A14 effect on other auxin receptors, we also analyzed the lateral root phenotype of *afb1*, *afb2* and *afb3* auxin receptor mutants under A14 treatment. Unlike *tir1*, *afb* mutants still show sensitivity to A14, whereas the combination of *tir1* and *afb* mutants were resistant to A14 treatment (Fig. 3a and b). These data suggests A14 might specifically act through a TIR1-dependent signaling pathway. Therefore we named A14 tirlin for "TIR1-dependent lateral root inducer".

At the transcript level, analysis of the auxin response showed that A14-induced DR5:GUS expression level in the OZ and pericycle cells was also reduced in the *tir1* mutant background, further confirming tirlin-induced auxin response during early lateral root development was dependent on TIR1-mediated signaling.

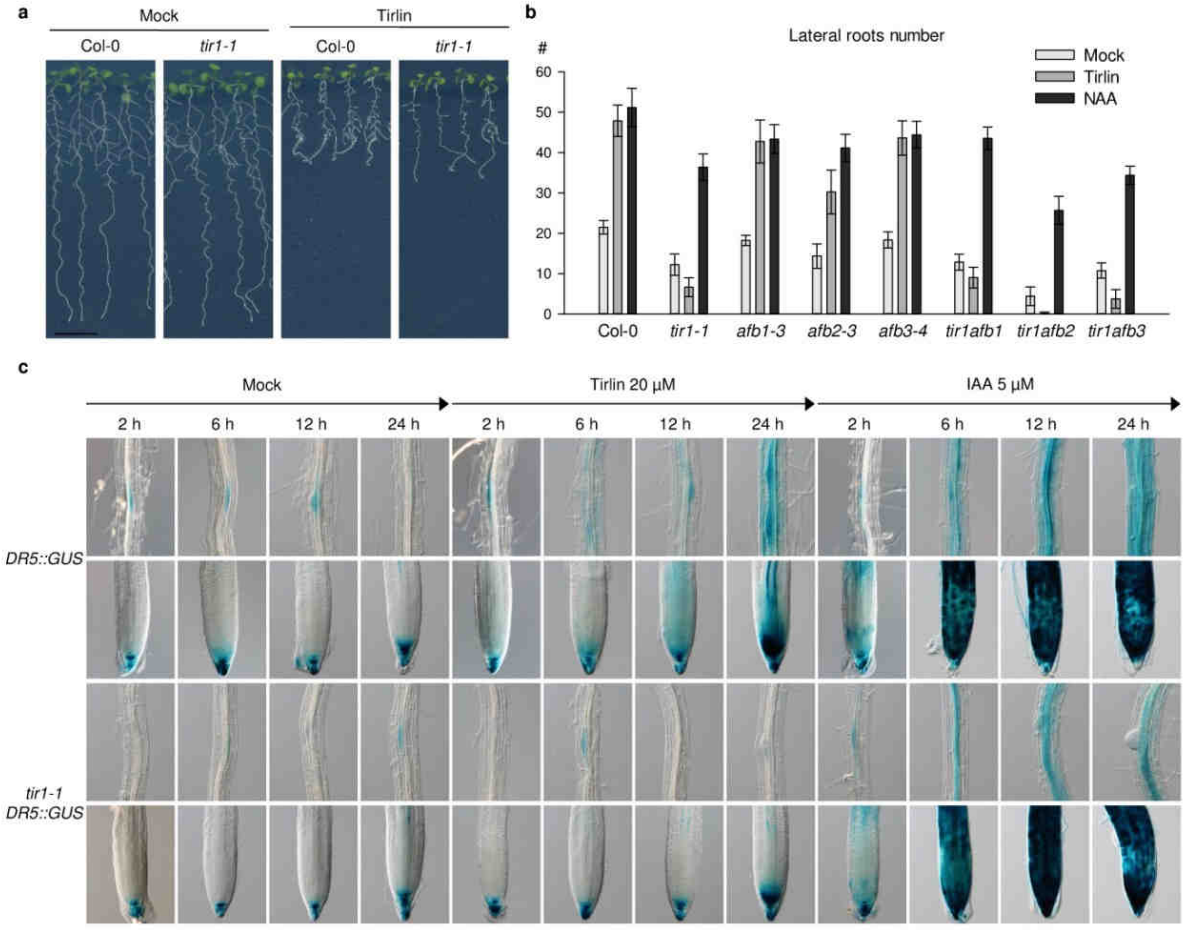

Figure 3. A14 function on lateral root events requires TIR1. (a) Phenotype of Col-0 and *tir1-1* seedlings grown on control medium for 3 d and then transferred to mock medium (DMSO) or medium supplemented with 20 µM A14 for five additional days. (b) Quantification of lateral root number of indicated transgenic seedlings grown on control medium until 3d after germination and transferred to medium supplemented with the indicated hit molecule at the indicated concentration for five additional days. (c) Time-course analysis of DR5::GUS expression on Col-0 and *tir1-1* seedling grown on control medium for 3d and then transferred to mock medium (DMSO) or medium supplemented with indicated compounds for five additional days. Seedling harvested from indicated time points were used for staining to analyze the β-glucuronidase activity.

Identification of potential A14 targets in *Arabidopsis*

Interestingly, the *tir1* mutant also display ~ 50% reduction on lateral root number compared to WT (Fig. 3b), implying an important role of TIR1 on the LR development. To explore the potential targets of tirlin and TIR1-dependent downstream signaling components, we performed a suppressor screen in *Arabidopsis* to identify mutants that were resistant or hyper-sensitive to tirlin-dependent induction of lateral root formation. For this purpose, a fast-neutron mutagenized Col-0 population was screened upon tirlin treatment and the *31-2R, 23-5R, 17-5R,* and *61-108R* mutants were identified as tirlin-resistant mutants, whereas the *9-15S* mutant was selected as a tirlin-hypersensitive mutant (Fig. 4a and b). Among the resistant mutant alleles, the *31-2R* allele showed complete resistance to tirlin-induced lateral root formation and primary root elongation (Fig. 4a and b). Subsequent positional cloning identified a deletion on chromosome 2 close to two genetic markers T20P8 and T16B24 (Fig. 4c). Interestingly, several *LATERAL ORGAN BOUNDARIES DOMAIN/ASYMMETRIC LEAVES2-LIKE* (*LBD*/*ASL*) genes, which encode proteins containing the LOB (for lateral organ boundaries) domain, were found to be located in this region (Fig. 4d) (Matsumura et al., 2009). Among them, LBD16 and LBD18 have been shown to regulate lateral root formation in *Arabidopsis* (Goh et al., 2012). *lbd16* and *lbd18* loss-of-function mutants were less sensitive to tirlin-induced lateral root formation compared to WT, however, an slightly increased lateral root number could still be detected in tirlin-treated *lbd16* and *lbd18* single mutants when compared to Mock-treated seedlings (Fig. 4e). By contrast, *lbd33, lbd16lbd33, lbd16lbd18lbd33* mutants completely inhibited the tirlin response (Fig. 4d and e).Meanwhile, we noticed that LBD33 gene is not located in the predicted deletion region, indicating tirlin might acts on other LBD proteins to regulate LR formation. In addition, lateral root phenotype in *lbd16lbd18lbd33* triple mutant is similar to it in *tir1afb2* mutant, indicating a possible link between TIR1 and LBD proteins. Therefore, we propose that tirlin might be dependent on LBD proteins downstream of TIR1 to regulate lateral root formation.

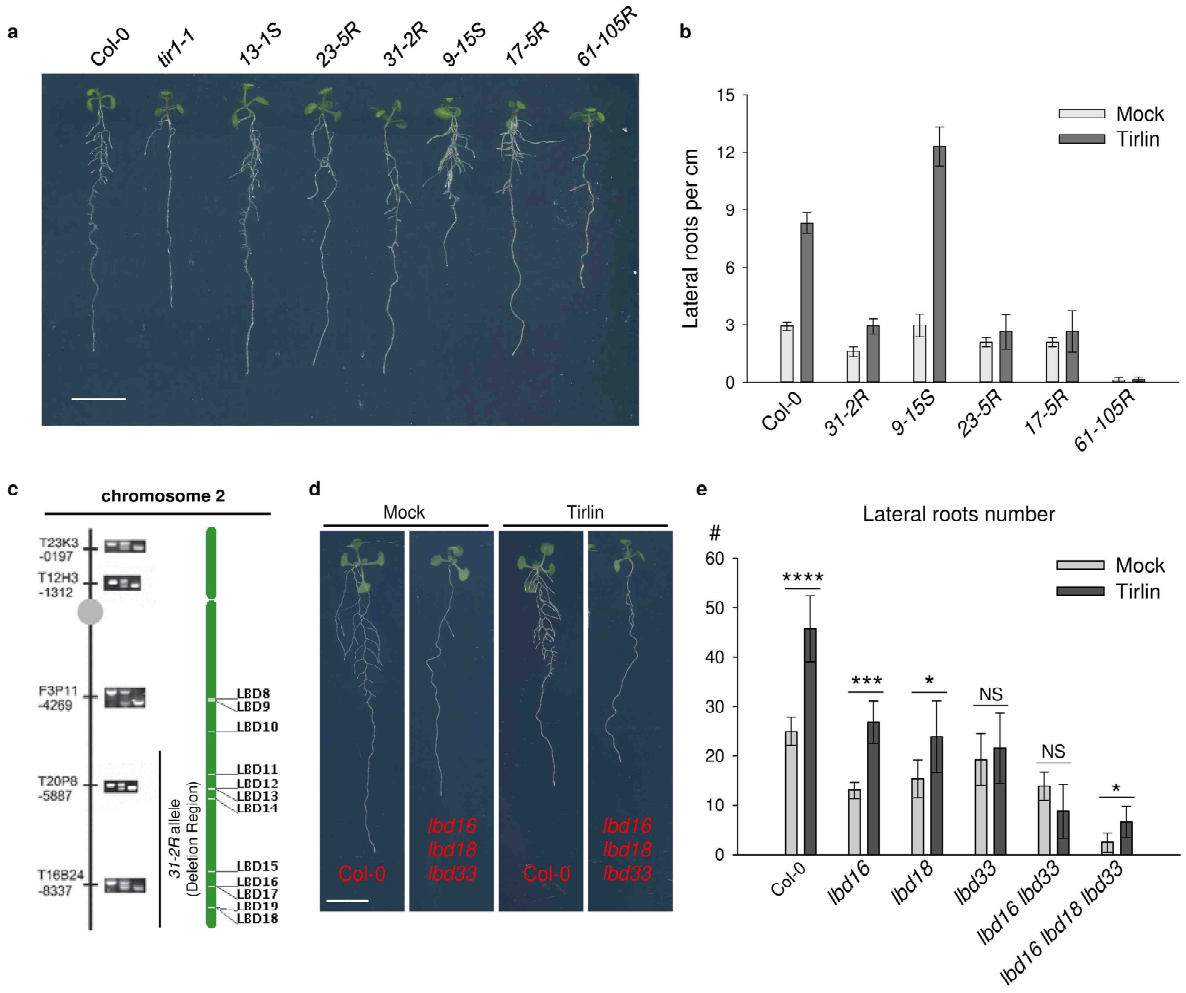

Figure 4. Identification of LBD proteins as the potential targets of Tirlin. (a) Root phenotype of 3-d-old seedlings from different mutant alleles transferred to medium containing 10 µM Tirlin for five more days. (b) Quantification of lateral root phenotype of indicated mutant alleles grown on control medium until 3 d after germination and transferred to medium supplemented with or without 10 µM Tirlin for five additional days. (c) Localization of the potential deletion region and LBD genes in chromosome 2 in Arbidopsis genome. (d) Root phenotype of 3-d-old Col-0 and *lbd16lbd18lbd33* mutant seedlings transferred to medium containing 10 µM Tirlin for five more days. (e) Quantification of lateral root phenotype of seedlings from indicated mutants grown on control medium until 3 d after germination and transferred to medium supplemented with or without 10 µM Tirlin for five additional days ($n > 12$, $*P < 0.01$, $***P < 10^{-4}$, and $**** P < 10^{-5}$ by two-sided Student's *t* test indicated statistically significant differences).

Discussion

For decades, auxin has been demonstrated to control new organ formation in plants, especially in the case of lateral and adventitious root formation. In plant model *Arabidopsis*, auxin perception is mediated by the F-Box proteins TIR1/AFBs (Dharmasiri et al., 2005; Gray et al., 2001). A mutation the main auxin receptor TIR1 results in a reduced number of lateral roots, implying an important role of TIR1 in lateral root formation (Fig. 3). However, the molecular mechanism and signaling components downstream of the auxin receptors for lateral root formation are not yet identified. The observation that auxins such as NAA can still increase LRs in *tir1* or *tir1afb2afb3* triple mutants also indicates functional redundancy of the different auxin receptors for the process of lateral root formation (Fig. 3). In our study, we identified a novel small molecule, tirlin, a strong lateral root inducing molecule that acts in a TIR1-dependent manner and similar to the artificial auxin analogue NAA. However, the effect of tirlin on lateral root formation is not based on alteration in auxin transport but is exclusively dependent on the auxin receptor TIR1, and not on other auxin receptors, indicating the distinguished roles of auxin receptors in different plant developmental processes. The identification of a strong lateral root inducing molecule specifically acting through TIR1therefore underlines the importance of this receptor for lateral root formation as compared to the other auxin receptors. This is coinciding with our previous findings in which we demonstrated that the TIR1-AFB2 pathway controlled the periodic prebranch sites formation by regulating the DR5 oscillation strength in OZ.

Biochemistry data showed that tirlin did not affect the binding affinities of TIR1 and AUX/IAA proteins nor PIN-mediated endocytosis (Fig. 2). These data indicate that tirlin does not directly bind the TIR1 protein; instead, it might target the signaling components downstream of TIR1. By a forward genetic approach, LBD proteins were suggested as potential targets of Tirlin. It has been demonstrated that the expression level of LBD proteins, i.e. LBD16 and LBD18, is regulated by auxin, and they were shown to act downstream of the auxin response factors ARF7- and ARF19-dependent auxin signaling pathway in *Arabidopsis* roots (Okushima et al., 2007). Meanwhile, tirlin function on lateral root development is also dependent on ARF7-ARF19 pathway (Supplemental Fig. 1). In addition, *lbd* triple mutants phenotypically mimic the *tir1afb2* mutants at the level of lateral root formation. Our data therefore suggest the involvement of LBDs in TIR1-dependent signaling pathway for lateral root formation. However, we cannot exclude the possibilities that tirlin might also acts on unknown signaling pathways that are downstream of TIR1, which will be further addressed.

Altogether, identification of tirlin by using a chemical genetics approach, led to the clarification of the role of the auxin receptor TIR1 on lateral root developmental process, and provides candidate genes potentially involved in the TIR1-downstream signaling cascades.

Acknowledgements

We thank Malcolm Bennett (University of Nottingham, UK), Mark Estelle (University of California, San Diego, CA, USA), Hidehiro Fukaki (Kobe University, Kobe, Japan) for sharing seed lines.

Materials and Methods

Compound screening and growth conditions

A commercial 10,000 compound library (DIVERSet™, ChemBridge Corporation) was screened for induction of *pCYCB1;1::GUS* expression in xylem pole pericycle cells. About three seeds of this marker line in *Arabidopsis thaliana*. Col-0 background were sown in 96-well filter plates (Multiscreen HTS MSBVS1210; Millipore) in liquid medium derived from standard Murashige and Skoog (MS) medium, supplemented with 10 µM of the auxin transport inhibitor naphtylphtalamic acid (NPA), resulting in a primary root devoid of lateral roots and allowing synchronization of lateral root development. Subsequently, seeds were incubated in a growth chamber under continuous light (110 $\mu E.m^{-2}.s^{-1}$ photosynthetically active radiation) at 21°C. Three days after germination, the liquid NPA medium was removed and replaced with fresh liquid medium. Compounds were added to the 96-well plates to a final concentration of 50 µM for 24 hours. Plants incubated in 2% DMSO or 10 µM NAA were used as negative and positive control, respectively. Next, all plants were incubated in GUS buffer as described (Vanneste et al., 2005) and analysed for GUS staining in xylem pole pericycle cells. Only compounds that showed similar staining profiles in all seedlings were considered. For all subsequent phenotypic analyses, plants were grown on square plates (Greiner Labortechnik) with solid medium derived from standard MS medium under the same conditions supplemented with compounds dissolved in DMSO when indicated as described previously (De Rybel et al., 2009).

Plant lines used

The *Arabidopsis* accessions Columbia (Col-0) were used for this study. *lbd* mutant lines were kind gifts from Hidehiro Fukaki (Kobe University, Kobe, Japan); the auxin receptor

mutants were kindly supplied by Mark Estelle (University of California, San Diego, CA, USA); DII-VENUS transgenic line was a gift from Malcolm Bennett (University of Nottingham, UK) Double and higher-order mutants harboring various marker lines were generated by crossing. F3 homozygous seedlings were analyzed in all experiments.

Root phenotype analyses

To quantify the lateral root phenotype in wild-type plants and mutants, emerged lateral roots of the whole seedlings were counted under a dissecting microscope 8 days after germination. Subsequently, whole seedlings were scanned for further analysis of the primary root length. For compound treatments, three-day-old seedlings from the indicated lines were transferred to ½ MS medium containing compounds at the indicated concentrations for extra five days. Subsequently, the emerged lateral roots and primary root length were quantified.

Pull-down experiments

Pull-down experiments were done as described previously (Kepinski and Leyser, 2005).

A fast neutron mutagenesis screening and positional cloning

About 50,000 seedlings from 100 fast neutron-mutagenised pools (kindly supplied by Malcolm Bennett lab in University of Nottingham, UK) were germinated on standard MS medium. To exclude effects on germination, these plants were subsequently transferred to 10 µM tirlin three days after germination. Plants resistant to the lateral root inducing effect of tirlin were selected after five more days. Before positional cloning, mutants were back-crossed to Col-0 and selected again for the resistant phenotype. For PCR-based positional cloning using SSLP markers, the mutant was crossed with *Ler* and subsequently selfed. 40 resistant F2 seedlings were used to map the mutation to chromosome 3 between T20P8 (11.6 Mb) and T16B24 (16.4 Mb).

Histochemical and histological analysis and microscopy

The GUS assays were performed as described previously (Vanneste et al., 2005). For microscopic analysis, samples were cleared by mounting in 90% lactic acid (Acros Organics) or by clearing as described previously (Malamy and Benfey, 1997). All samples were analyzed by differential interference contrast microscopy (Olympus BX51). For anatomical sections, GUS-stained samples were fixed overnight and embedded as described previously (De Smet et al., 2004). Fluorescence imaging of roots was performed with an Olympus FV10-ASW or Zeiss 710 confocal laser scanning microscope. For the propidium iodide (PI)-treated

root images, seedlings were stained with 2 µg/mL PI for 3 minutes, washed with water, and used for confocal imaging.

Reference

Benkova, E., Michniewicz, M., Sauer, M., Teichmann, T., Seifertova, D., Jurgens, G., and Friml, J. (2003). Local, efflux-dependent auxin gradients as a common module for plant organ formation. Cell *115*, 591-602.
Brunoud, G., Wells, D.M., Oliva, M., Larrieu, A., Mirabet, V., Burrow, A.H., Beeckman, T., Kepinski, S., Traas, J., Bennett, M.J., *et al.* (2012). A novel sensor to map auxin response and distribution at high spatio-temporal resolution. Nature *482*, 103-106.
Calderon Villalobos, L.I., Lee, S., De Oliveira, C., Ivetac, A., Brandt, W., Armitage, L., Sheard, L.B., Tan, X., Parry, G., Mao, H., *et al.* (2012). A combinatorial TIR1/AFB-Aux/IAA co-receptor system for differential sensing of auxin. Nature chemical biology *8*, 477-485.
De Rybel, B., Audenaert, D., Vert, G., Rozhon, W., Mayerhofer, J., Peelman, F., Coutuer, S., Denayer, T., Jansen, L., Nguyen, L., *et al.* (2009). Chemical inhibition of a subset of Arabidopsis thaliana GSK3-like kinases activates brassinosteroid signaling. Chemistry & Biology *16*, 594-604.
De Rybel, B., Audenaert, D., Xuan, W., Overvoorde, P., Strader, L.C., Kepinski, S., Hoye, R., Brisbois, R., Parizot, B., Vanneste, S., *et al.* (2012). A role for the root cap in root branching revealed by the non-auxin probe naxillin. Nat Chem Biol *8*, 798-805.
De Rybel, B., Vassileva, V., Parizot, B., Demeulenaere, M., Grunewald, W., Audenaert, D., Van Campenhout, J., Overvoorde, P., Jansen, L., Vanneste, S., *et al.* (2010). A novel aux/IAA28 signaling cascade activates GATA23-dependent specification of lateral root founder cell identity. Current biology : CB *20*, 1697-1706.
De Smet, I., Chaerle, P., Vanneste, S., De Rycke, R., Inze, D., and Beeckman, T. (2004). An easy and versatile embedding method for transverse sections. J Microsc *213*, 76-80.
De Smet, I., Tetsumura, T., De Rybel, B., Frei dit Frey, N., Laplaze, L., Casimiro, I., Swarup, R., Naudts, M., Vanneste, S., Audenaert, D., *et al.* (2007). Auxin-dependent regulation of lateral root positioning in the basal meristem of Arabidopsis. Development *134*, 681-690.
De Smet, I., Vassileva, V., De Rybel, B., Levesque, M.P., Grunewald, W., Van Damme, D., Van Noorden, G., Naudts, M., Van Isterdael, G., De Clercq, R., *et al.* (2008). Receptor-like kinase ACR4 restricts formative cell divisions in the Arabidopsis root. Science *322*, 594-597.
Dharmasiri, N., Dharmasiri, S., and Estelle, M. (2005). The F-box protein TIR1 is an auxin receptor. Nature *435*, 441-445.
Goh, T., Joi, S., Mimura, T., and Fukaki, H. (2012). The establishment of asymmetry in Arabidopsis lateral root founder cells is regulated by LBD16/ASL18 and related LBD/ASL proteins. Development *139*, 883-893.
Gray, W.M., Kepinski, S., Rouse, D., Leyser, O., and Estelle, M. (2001). Auxin regulates SCF(TIR1)-dependent degradation of AUX/IAA proteins. Nature *414*, 271-276.
Hilson, P., Allemeersch, J., Altmann, T., Aubourg, S., Avon, A., Beynon, J., Bhalerao, R.P., Bitton, F., Caboche, M., Cannoot, B., *et al.* (2004). Versatile gene-specific sequence tags for Arabidopsis functional genomics: transcript profiling and reverse genetics applications. Genome Res *14*, 2176-2189.

Himanen, K., Boucheron, E., Vanneste, S., de Almeida Engler, J., Inze, D., and Beeckman, T. (2002). Auxin-mediated cell cycle activation during early lateral root initiation. The Plant cell *14*, 2339-2351.
Himanen, K., Vuylsteke, M., Vanneste, S., Vercruysse, S., Boucheron, E., Alard, P., Chriqui, D., Van Montagu, M., Inze, D., and Beeckman, T. (2004). Transcript profiling of early lateral root initiation. Proceedings of the National Academy of Sciences of the United States of America *101*, 5146-5151.
Karimi, M., Depicker, A., and Hilson, P. (2007). Recombinational cloning with plant gateway vectors. Plant Physiol *145*, 1144-1154.
Kepinski, S., and Leyser, O. (2005). The Arabidopsis F-box protein TIR1 is an auxin receptor. Nature *435*, 446-451.
Kitakura, S., Vanneste, S., Robert, S., Lofke, C., Teichmann, T., Tanaka, H., and Friml, J. (2011). Clathrin mediates endocytosis and polar distribution of PIN auxin transporters in Arabidopsis. The Plant cell *23*, 1920-1931.
Liu, X., Cohen, J.D., and Gardner, G. (2011). Low-fluence red light increases the transport and biosynthesis of auxin. Plant Physiology *157*, 891-904.
Malamy, J.E., and Benfey, P.N. (1997). Organization and cell differentiation in lateral roots of Arabidopsis thaliana. Development *124*, 33-44.
Matsumura, Y., Iwakawa, H., Machida, Y., and Machida, C. (2009). Characterization of genes in the ASYMMETRIC LEAVES2/LATERAL ORGAN BOUNDARIES (AS2/LOB) family in Arabidopsis thaliana, and functional and molecular comparisons between AS2 and other family members. The Plant journal : for cell and molecular biology *58*, 525-537.
Moreno-Risueno, M.A., Van Norman, J.M., Moreno, A., Zhang, J., Ahnert, S.E., and Benfey, P.N. (2010). Oscillating gene expression determines competence for periodic Arabidopsis root branching. Science *329*, 1306-1311.
Okushima, Y., Fukaki, H., Onoda, M., Theologis, A., and Tasaka, M. (2007). ARF7 and ARF19 regulate lateral root formation via direct activation of LBD/ASL genes in Arabidopsis. The Plant cell *19*, 118-130.
Parry, G., Calderon-Villalobos, L.I., Prigge, M., Peret, B., Dharmasiri, S., Itoh, H., Lechner, E., Gray, W.M., Bennett, M., and Estelle, M. (2009). Complex regulation of the TIR1/AFB family of auxin receptors. Proceedings of the National Academy of Sciences of the United States of America *106*, 22540-22545.
Rogg, L.E., Lasswell, J., and Bartel, B. (2001). A gain-of-function mutation in IAA28 suppresses lateral root development. The Plant cell *13*, 465-480.
Uehara, T., Okushima, Y., Mimura, T., Tasaka, M., and Fukaki, H. (2008). Domain II mutations in CRANE/IAA18 suppress lateral root formation and affect shoot development in Arabidopsis thaliana. Plant & cell physiology *49*, 1025-1038.
Van Norman, J.M., Xuan, W., Beeckman, T., and Benfey, P.N. (2013). To branch or not to branch: the role of pre-patterning in lateral root formation. Development *140*, 4301-4310.
Vanneste, S., De Rybel, B., Beemster, G.T., Ljung, K., De Smet, I., Van Isterdael, G., Naudts, M., Iida, R., Gruissem, W., Tasaka, M., *et al.* (2005). Cell cycle progression in the pericycle is not sufficient for SOLITARY ROOT/IAA14-mediated lateral root initiation in Arabidopsis thaliana. The Plant cell *17*, 3035-3050.
Vermeer, J.E., von Wangenheim, D., Barberon, M., Lee, Y., Stelzer, E.H., Maizel, A., and Geldner, N. (2014). A spatial accommodation by neighboring cells is required for organ initiation in Arabidopsis. Science *343*, 178-183.

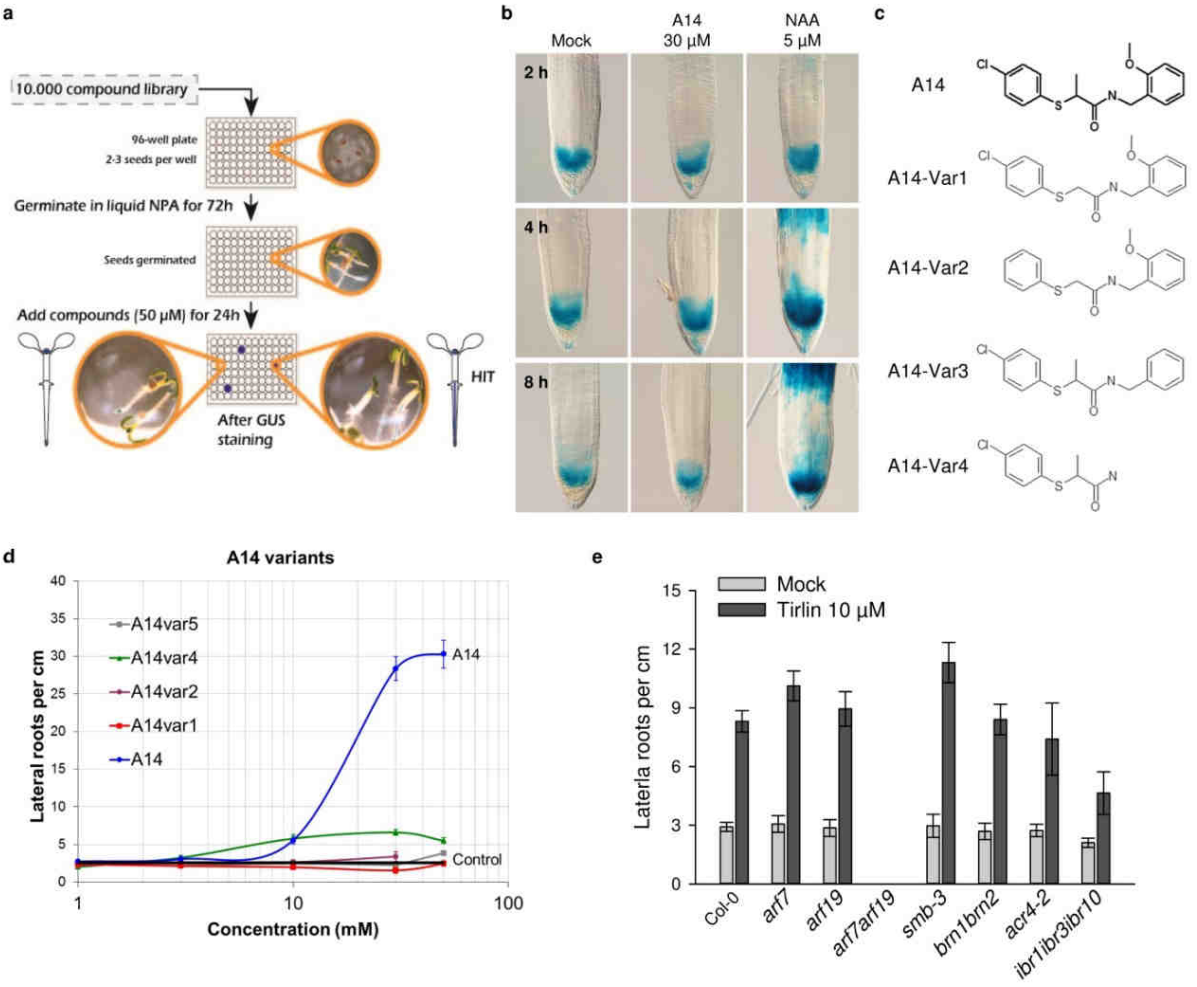

Supplemental Figure 1. Identification and characterization of A14-tirlin. (a) Overview of the procedure to screen for activators of lateral root development with the pCYCB1;1::GUS marker. (b) Time-course experiment on three-day-old pDR5::GUS seedlings germinated on 10 µM NPA and subsequently treated with or without 30 µM A14 or 5 µM NAA for indicated hours, followed by staining for β-glucuronidase activity to assess the rate of lateral root development. (c) The chemical structures of A14 variants. (d) Analysis of lateral root density of seedlings grown on control medium until 3 d after germination and transferred to medium supplemented with the various A14 variants at the indicated concentration for five additional days. (e) Lateral root phenotype of three-day-old seedlings from indicated mutants were further treated with or without 10 µM tirlin for five days. (Updated from De Rybel et al., 2012)

Knowledge is a matter of science, and no dishonesty or conceit whatsoever is permissible.

Mao Tse-tung

Chapter 5

Concluding remarks

Concluding remarks

Root cap contributes to the root patterning

Plant roots grow in the soil in order to support plant growth by absorbing water and nutrients. Root growth rate is controlled by cell elongation in the elongation zone and cell divisions in the apical meristem, the latter being covered by the root cap. As helmets are required for protecting peoples head during hazardous activities, root cap cells serve a similar purpose in plants. Besides protecting the root apical meristem, the root cap further contributes in the perception of environmental signals, in mediating interactions between the soil and the plant and in controlling the direction of root growth (Filleur et al., 2005). More recently, the root cap was found to release a broad variety of chemical compounds into the soil to mediate rhizospheric interactions both at the plant–microbiome levels (Driouich et al., 2013; Turner et al., 2013b).

Our studies revealed a novel role of the root cap in patterning of root branching in *Arabidopsis*. First, local auxin biosynthesis in the root cap controls the prebranch site formation by regulating the oscillation amplitude in the OZ (Chapter 2). Secondly, auxin transport through the lateral root cap and epidermis is involved in the transduction of the root cap signal to the prebranch site and finally the earlier described periodic root cap cell death is correlated with and seems to be crucial for the oscillatory nature of the process (Chapter 3). Moreover, the NAC domain transcriptional factors SMB and FEZ, known to regulate root cap formation, are also required for setting the root clock (Moreno-Risueno et al., 2010).

Based on our findings it is tempting to speculate that the root cap might act as a transmission medium linking the environmental stimuli with root pre-patterning. When the root cap perceives external signals, it might moderate its growth dynamics by altering the cell division rate and by delaying or accelerating its programmed cell death. Through the mechanism that we have proposed in this thesis, such an alteration in the growth dynamics of the root cap might affect the patterning of lateral organs in the primary root. In other words, the growth dynamics in the root cap might help the plant to produce more or less lateral roots along the primary root axis dependent on the environmental conditions. Interestingly, *Low Phosphate Root1* (*LPR1*) and *Nitrate Transporter* (*NRT1*) genes are expressed in the root cap cells (Krouk et al., 2010; Svistoonoff et al., 2007), indicating the altered primary root and lateral root phenotype under varying nutrient conditions might be also determined by the signal perception and transduction in the root cap. Therefore, further research is required to

focus on the mechanism by which the root cap is capable in sensing the environment signal, and to determine whether this signal could be converted into the positional information for root patterning.

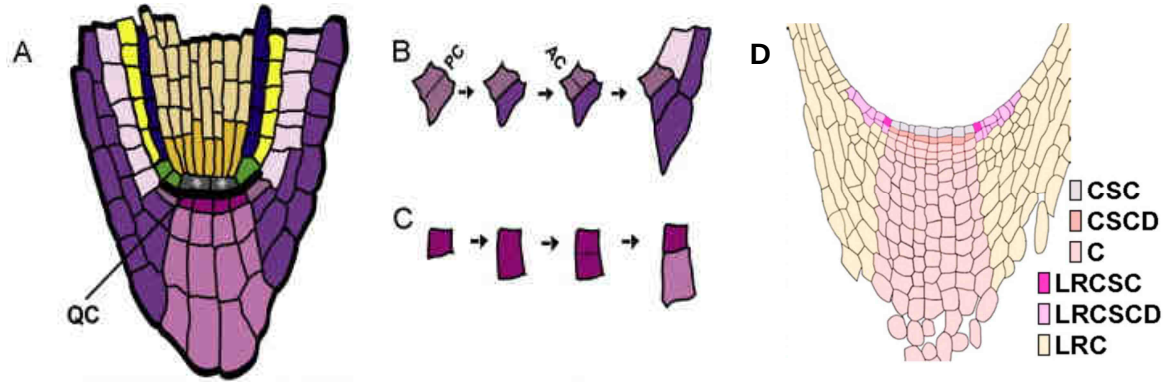

Figure 1. The root cap models in plants. (A) Schematic of the *Arabidopsis* root cap.(B) Schematic showing PC division in the Epi/LRC stem cell (dark pink) division that generates the LRC (purple) and anticlinal cell division that generates the epidermis (light pink).(C) Schematic of anticlinal COL stem cell division, with the stem cell in red and the differentiated COL cell in pink. (D) Schematic drawing of the root cap in rice. CSC: columella stem cell. CSCD: columella stem cell daughter. C: columella. LRCSC: lateral root cap stem cell. LRCSCD: lateral root cap stem cell daughter. LRC: lateral root cap.

Furthermore, in chapter 3, we also show that the formation and programmed cell death of root cap cells is crucial for the root clock. In *Arabidopsis*, the root cap develops from two sets of meristematic cells, a central group of initials that gives rise to the columella and a surrounding ring of cells that gives rise to both the lateral root cap and the epidermis through periclinal cell divisions of common stem cells (Fig.1) (Dolan et al., 1993; Scheres et al., 2002). At the distal end of the lateral root cap, cells are released from the root triggered by programmed cell death (Fendrych et al., 2014). This process is restricted by SMB and FEZ, the NAC domain transcriptional factors in *Arabidopsis* (Bennett et al., 2010; Willemsen et al., 2008). Meanwhile, the mutants of *QUASIMODO 1* (*QUA1*) and *QUASIMODO 2* (*QUA2*) genes, which encode putative glycosyltransferases in *Arabidopsis*, have root cap cells that separate from each other when they are released (Durand et al., 2009). Normally, the wild type Arabidopsis root tip does not produce isolated border cells per se, but it does produce and release cells that remain attached to each other, forming a block of several cell layers called border-like cells (Vicre et al., 2005). Interestingly, the *quasimodo* mutants display an altered lateral root phenotype compared to WT, suggesting that a formative build-up of root cap

tissue is required for root prepatterning in *Arabidopsis*. More recently, signaling components were identified to be involved in the root cap formation. The QC-expressed transcription factor WUSCHEL-RELATED HOMEOBOX5 (WOX5) was found to negatively regulate the SMB activity during columella development. Besides WOX5, RETINOBLASTOMA-RELATED protein, and the ARF10- and ARF16-mediated auxin response factors also play a role in the determination of columella stem cells activity, which further affects the root cap formation (Bennett et al., 2014). However, up to present, it is not clear if all these factors also regulate the root cap cell death and root prepatterning.

In order to identify more and specific signaling pathways that might have a function in root cap differentiation, secretory activity and PCD, a comprehensive transcriptomic fate map of the LRC would be preferable. Actually, the exciting transcriptomic data sets of the *Arabidopsis* root generated by the Benfey's lab (Brady et al., 2007) do not allow to distillate transcriptional data on the separated root cap cell types, such as columella, LRC initials, differentiating cells, differentiated cells, and cells undergoing PCD). To excess the different developmental stages of the root cap, we are recently involved in a project that will make use of cell-type and developmental specific reporter lines, such as J3411(Lateral root cap), J0951 (out layer of LRC), PET111 (Columella), J1092 (LRC initials), pPASPA1:GFP, and SMB:GFP to perform cell sorting and further RNA sequencing. This novel dataset might enhance our insight in the various functions of the root cap including its role in root prepatterning.

Unlike *Arabidopsis*, in the monocot plant *Oryza sativa*, columella and lateral root cap arise from a set of root cap stem cells that do not contribute to the generation of the epidermis (Fig.2) (Wang et al., 2014). In rice, the root cap stem cells are located below the cap junction, a distinct cell layer composed with approximately 13 cells. The central root cap stem cells divide anticlinally to develop a columella, whereas the outer stem cells form the lateral root cap by several rounds of periclinal and anticlinal cell divisions. This process is regulated by OsIAA23-mediated auxin signaling and the glutamate receptor-like gene, *GLR3;1* (Jun et al., 2011; Li et al., 2006; Ni et al., 2014). However, the role of these genes on root prepatterning in is not characterized yet.

Taken together, despite the dissimilar pattern of root cap formation in *Arabidopsis* and *Oryza sativa*, it is still unclear whether the control on the pattern of root branching occurs in a similar way in these two different species. Moreover, it is not clear yet whether the root cap is

also controlling root branching in other species. As mentioned higher, the lateral root phenotype of the *quasimodo* mutants indicate that there might be a correlation with the presence of border-like cells and normal lateral root patterning. Furthermore, the occurrence of border-like cells seems to be specific for the Brassicaceae family as it also occurs in rapeseed (*Brassica napus*), mustard (*Brassica juncea*), and Brussels sprout (*Brassica oleracea gemmifera*) (Driouich et al., 2007) and is absent in many other plant species analyzed so far. It is therefore still possible that root prepatterning occurs differently in other plant species.

Root pre-patterning in plants

In *Arabidopsis*, root prepatterning has been described as a biological clock process that translates a temporal signal into spatial information for lateral organ formation along the primary root axis. A large scale of experiments has been applied to study the molecular mechanism of this process in *Arabidopsis*, and several signaling components have been discovered to control this process. However, it is not certain whether the occurrence of a root clock is a shared mechanism for root branching in other plant species. In addition, the existence and the function of the identified signaling pathways for root branching still need to be investigated in in other species and is mainly hampered by the lack of suitable research tools such as in vivo markers to monitor auxin reponses.

In *Zea mays* and *Oryza sativa*, two important commercial crop plants, several lines of research have been performed to reveal the pattern of lateral root primordium development. In contrast to *Arabidopsis*, in which lateral roots are specifically initiated and developed from a patch of protoxylem pole pericycle cells (De Smet et al., 2008; Malamy and Benfey, 1997), LR development in *Zea mays* and *Oryza sativa* is more painful to analyze because monocot roots are composed of several cortex layers and a varying number of cells per layer. In *Zea mays*, LR initiation occurs in the pericycle cells opposite the phloem poles, and xylem pole pericycle cells are not competent for LRI (Jansen et al., 2012). In *Oryza sativa*, the LR primordium is initiated from pericycle cells at the phloem pole and endodermis (Kawata and Shibayama, 1965). Similar to *Arabidopsis*, DR5 was also detected to be expressed in the meristem in *Zea mays* and *Oryza sativa*. Longitudinal sections of the *Zea mays* root tip showed the expression of DR5:RFP mainly in the QC, root cap, epidermis, and vascular tissue, whereas transversal sections reveals that the DR5 signal starts in the meta-xylem precursor cells and the proto-xylem poles close to the root tip, and subsequently also appears in the phloem pole. In the upper root, the DR5 signal only remains in the phloem poles, which might

be linked to the activation of phloem pole pericycle cells for lateral root initiation (Jansen et al., 2012). While in the *Oryza sativa* root tip, DR5:GUS expression was observed specifically in the root cap, quiescent center, xylem cells in the root apical meristem and lateral roots (Zhou et al., 2014), which resembles the expression pattern of DR5 obtained in *Arabidopsis*. Moreover, similar expression patterns of DR5 were also found in *Medicago truncatula*, soybean and tomato during the lateral root developmental process (Dubrovsky et al., 2008; Herrbach et al., 2014; Turner et al., 2013a). Thus, to reveal the root prepatterning or lateral root initiation events in other species, auxin responsive elements base marker lines such as DR5 could serve as a general and useful maker for the further research.

Spatial control of the root clock by auxin

In *Arabidopsis*, local auxin sources have been found to play a central role in the regulation of organ formation. In chapter 2, we have identified that a root-cap specific auxin source, derived from IBA, could moderate the amplitude of DR5 oscillation, and thus presumably the auxin response levels, in the OZ to regulate the prebanch sites formation. In addition, we also found that the DR5 signal intensity and the amplitude of the oscillations were reduced in the auxin receptor mutant *tir1afb2* (Chapter 2). Interestingly, the periodicity of DR5 expression oscillating in OZ is not disturbed in auxin biosynthesis or signaling mutants, indicating that oscillations of the root clock could occur even in the absence of local auxin signaling. It also shows that auxin is required to maintain clock oscillations and suggests that the arrest of transition from oscillations to prebranch sites is linked to the level of auxin and its signaling in the OZ. Thus, we propose a two-tier mechanism for the root clock; while oscillating genes might regulate the temporal signals, auxin may act as a local gradient facilitating the spatial formation of prebranch sites in OZ.

IBA was reported to supply 30% of total auxin biosynthesis in *Arabidopsis*, and in our study, we found that IBA-to-IAA conversion contributed to 50% of total lateral root production. This indicates that other auxin sources might also be involved in root prepatterning. It has been reported that overexpressing TAA1 and YUC genes significantly promotes lateral root formation in *Arabidopsis* (Mashiguchi et al., 2011), indicating a possible role for the tryptophan (Trp)-dependent auxin biosynthesis pathway on root patterning, however, the mechanism and the contribution of this auxin biosynthesis for root branching is not fully characterized yet.

Beside the local auxin biosynthesis, several lines of evidence showed that auxin signaling is also important for lateral root development. Gain-of-function mutants of AUX/IAA genes, such as *IAA28*, *SLR/IAA14*, *CRANE/IAA18* and *SHY2/IAA3*, severely reduce the lateral root formation. Moreover, tissue-specific auxin signaling also affects lateral root development at different developmental stages. For instance, endodermis auxin signaling is required for the swelling of the LRFC and the execution of the asymmetric cell division of pericycle cells (Vermeer et al., 2014), and auxin signaling in xylem pole pericycle is essential for lateral root initiation (De Smet et al., 2007). Cortex auxin signaling is also found to be involved in lateral root emergence and lateral root primordium shape (Lucas et al., 2013). Interestingly, IAA2 and IAA14 are found to be expressed in the lateral root cap cells (Swarup et al., 2005; Vanneste et al., 2005), indicating a possible role of auxin signaling in the root cap. However, our data argue for a scenario in which local auxin signaling is not required for this process; instead, auxin transport might mediate auxin movement from the root cap into the OZ (Chapter 3). In addition, although AUX/IAA genes were expressed in the endodermis and pericycle cells, there is no clear evidence of the existence of a local auxin source in these tissues, whereas several auxin flux carriers were found to be localized in the cell layers surrounding LRP. The auxin signaling in these tissues might therefore be activated by auxin transported from other tissues. It has been demonstrated that in *Arabidopsis*, the root tip has a high activity on auxin biosynthesis (Petersson et al., 2009), and this auxin is further taken by auxin transport to generate an auxin maximum in other tissues through “auxin reflux loop” model (Grieneisen et al., 2007; Laskowski et al., 2008). So it will be also interesting to investigate whether root cap-derived auxin source could also contribute to the LR initiation and LRP development. Moreover, we cannot exclude the possibility that the auxin signaling in these tissues might be activated by other signaling components rather than auxin itself, which also has to be further determined.

Other hormones or signaling molecules, such as cytokinins and carotenoids, are known to display negative effects on root patterning and a change on DR5 activity in their pathway mutants or under exogenous compound treatment have been observed (Bielach et al., 2012; Van Norman et al., 2014), suggesting a link between these hormones and auxin on regulating root patterning. Interestingly, recent studies also show that cytokinin could act through auxin efflux to regulate the auxin response in the root meristem and lateral root development (Bishopp et al., 2011; Marhavy et al., 2014). Because our results suggested that an auxin flux, mediated by auxin transport carriers AUX1 and PINS, is essential to establish the DR5

oscillations in the OZ, it will be interesting to evaluate whether cytokinins act on this early step of lateral root formation through the interference with PIN function (Chapter 3). The impact of cytokinin on auxin transport could thus represent a potential role of cytokinin on root prepatterning. According to the opposite function on root branching by IBA and cytokinin, the cross-talk between IBA and cytokinin would be an interesting topic for further research. Additionally, the function of other hormones on root patterning could also be mediated by auxin-independent signaling pathways and still have to be analyzed.

Gene oscillation in the root cells: a mystery unraveled

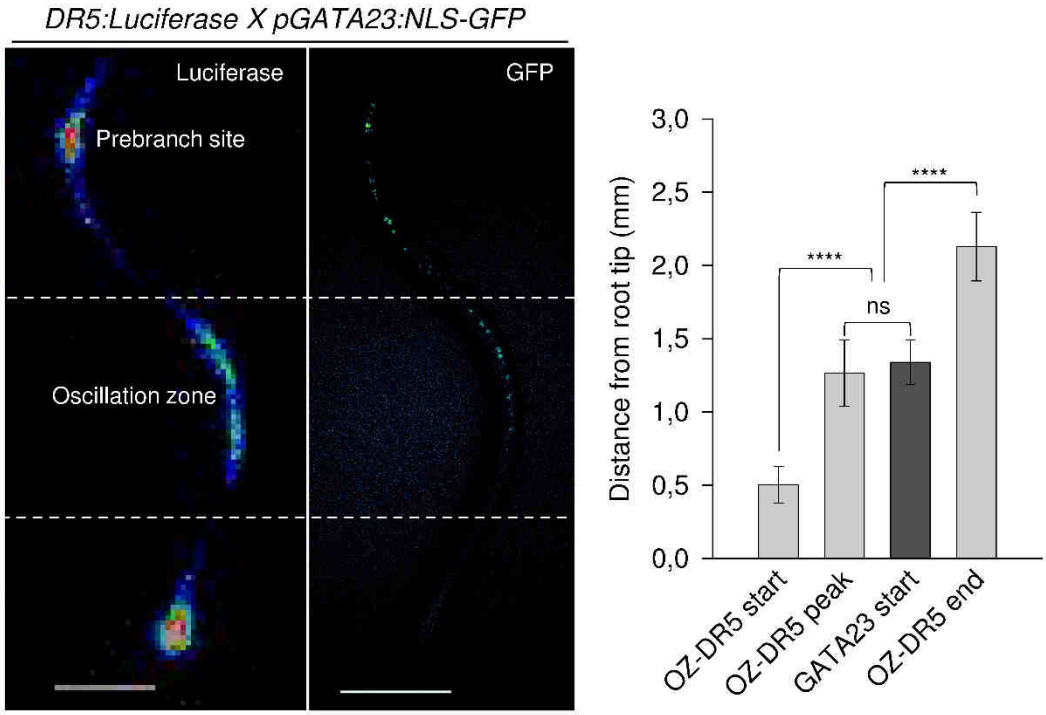

Figure 2. Spatial distribution of DR5 oscillation signal and GATA23 signal in OZ and the prebranch sites. *pGATA23:NLS-GFP* reporter and *DR5:luciferase* reporter were used to quantifying DR5 signal and GATA23signal in OZ and the prebranch sites respectively ($n > 40$). Scale bar = 0.5 mm.

In *Arabidopsis*, gene oscillatory patterns of expression were detected by capturing the bioluminescence signal from firefly luciferase driven by the promoters of oscillating genes. Because of the low resolution images captured by CCD cameras compared to laser scanning confocal microscopes, the oscillating model could only be observed at the organ level. By contrast, in animals, gene oscillation could be detected at the cell level by visualizing signal

from fluorescence proteins (i.e. YFP and GFP) during somitogenesis. In this respect, it will be crucial for future research in plants to reveal expression patterns of oscillating genes in the OZ at the cellular level.

To this end, we developed an experimental set-up using a macro-view microscope that enables us to detect fluorescence signals with higher resolution, thus serving as a powerful technique to access the gene oscillating pattern at the tissue level. Expression pattern of DR5:Luciferase throughout the root was observed to be synchronized with the dynamic of oscillating genes, thus we performed live imaging on auxin response reporter line carrying a DR5-promoter-driven nuclear yellow fluorescent proteins over a longer period. The DR5 signal appeared to be homogenously expressed in two strains of protoxylem at the start of the OZ and appears in xylem pole pericycle cells later on. When the root cells enter the different zone, the DR5 signal disappears from the xylem pole cells and becomes specifically expressed in lateral root primordia. Under our experimental set-up, we could not detect the changes of DR5 expression level at the cellular level inside the OZ, so it remains unclear which cells are targeted during the oscillation.

Interestingly, by using another maker line, namely pGATA23:NLS-GFP, which marks the founder cell specification and lateral root initiation, we found that the expression of GATA23 already started in the OZ, at the position where the DR5 signal reached the peak value in the OZ (Fig.2). Therefore, we hypothesize that in the OZ the auxin response maximum shifts from protoxylem pole cells to the xylem pole pericycle cells thereby triggering the lateral root initiation events. In this respect a new “DR5” marker (unpublished data, personal communication, Bert De Rybel, University of Wageningen, The Netherlands) was recently generated that shows expression both in protoxylem cells as well as in protoxylem pole pericycle cells. These data strongly indicate that the DR5 oscillation in the OZ is dependent on the signal transition from xylem pole to xylem pole pericycle cells when the root tip receive the development signal, such as root bending, programmed cell death, cell elongation and differentiation.

Although the root clock in plants might be comparable to the segmentation clock in animals to a certain level, our observations argue for a novel oscillating model in plants which requires signal transduction between neighboring cells or tissues, rather than a cell-autonomous mode of action. However, we cannot exclude the possibility that gene oscillating occurs cell autonomously because oscillation might be hard to be traced due to the rapid

process and minute change of expression levels which requires more sensitive fluorescence proteins and more advanced imaging techniques.

Reference

Bennett, T., van den Toorn, A., Sanchez-Perez, G.F., Campilho, A., Willemsen, V., Snel, B., and Scheres, B. (2010). SOMBRERO, BEARSKIN1, and BEARSKIN2 regulate root cap maturation in Arabidopsis. The Plant cell *22*, 640-654.

Bennett, T., van den Toorn, A., Willemsen, V., and Scheres, B. (2014). Precise control of plant stem cell activity through parallel regulatory inputs. Development *141*, 4055-4064.

Bielach, A., Podlesakova, K., Marhavy, P., Duclercq, J., Cuesta, C., Muller, B., Grunewald, W., Tarkowski, P., and Benkova, E. (2012). Spatiotemporal regulation of lateral root organogenesis in Arabidopsis by cytokinin. The Plant cell *24*, 3967-3981.

Bishopp, A., Help, H., El-Showk, S., Weijers, D., Scheres, B., Friml, J., Benkova, E., Mahonen, A.P., and Helariutta, Y. (2011). A mutually inhibitory interaction between auxin and cytokinin specifies vascular pattern in roots. Current biology : CB *21*, 917-926.

Brady, S.M., Orlando, D.A., Lee, J.Y., Wang, J.Y., Koch, J., Dinneny, J.R., Mace, D., Ohler, U., and Benfey, P.N. (2007). A high-resolution root spatiotemporal map reveals dominant expression patterns. Science *318*, 801-806.

De Smet, I., Tetsumura, T., De Rybel, B., Frei dit Frey, N., Laplaze, L., Casimiro, I., Swarup, R., Naudts, M., Vanneste, S., Audenaert, D., *et al.* (2007). Auxin-dependent regulation of lateral root positioning in the basal meristem of Arabidopsis. Development *134*, 681-690.

De Smet, I., Vassileva, V., De Rybel, B., Levesque, M.P., Grunewald, W., Van Damme, D., Van Noorden, G., Naudts, M., Van Isterdael, G., De Clercq, R., *et al.* (2008). Receptor-like kinase ACR4 restricts formative cell divisions in the Arabidopsis root. Science *322*, 594-597.

Dolan, L., Janmaat, K., Willemsen, V., Linstead, P., Poethig, S., Roberts, K., and Scheres, B. (1993). Cellular organisation of the Arabidopsis thaliana root. Development *119*, 71-84.

Driouich, A., Follet-Gueye, M.L., Vicre-Gibouin, M., and Hawes, M. (2013). Root border cells and secretions as critical elements in plant host defense. Current opinion in plant biology *16*, 489-495.

Dubrovsky, J.G., Sauer, M., Napsucialy-Mendivil, S., Ivanchenko, M.G., Friml, J., Shishkova, S., Celenza, J., and Benkova, E. (2008). Auxin acts as a local morphogenetic trigger to specify

lateral root founder cells. Proceedings of the National Academy of Sciences of the United States of America *105*, 8790-8794.

Fendrych, M., Van Hautegem, T., Van Durme, M., Olvera-Carrillo, Y., Huysmans, M., Karimi, M., Lippens, S., Guerin, C.J., Krebs, M., Schumacher, K., *et al.* (2014). Programmed Cell Death Controlled by ANAC033/SOMBRERO Determines Root Cap Organ Size in Arabidopsis. Current biology : CB.

Filleur, S., Walch-Liu, P., Gan, Y., and Forde, B.G. (2005). Nitrate and glutamate sensing by plant roots. Biochemical Society transactions *33*, 283-286.

Grieneisen, V.A., Xu, J., Maree, A.F., Hogeweg, P., and Scheres, B. (2007). Auxin transport is sufficient to generate a maximum and gradient guiding root growth. Nature *449*, 1008-1013.

Herrbach, V., Rembliere, C., Gough, C., and Bensmihen, S. (2014). Lateral root formation and patterning in Medicago truncatula. Journal of plant physiology *171*, 301-310.

Jansen, L., Roberts, I., De Rycke, R., and Beeckman, T. (2012). Phloem-associated auxin response maxima determine radial positioning of lateral roots in maize. Philosophical transactions of the Royal Society of London Series B, Biological sciences *367*, 1525-1533.

Jun, N., Gaohang, W., Zhenxing, Z., Huanhuan, Z., Yunrong, W., and Ping, W. (2011). OsIAA23-mediated auxin signaling defines postembryonic maintenance of QC in rice. The Plant journal : for cell and molecular biology *68*, 433-442.

Kawata, S., Shibayama, H. (1965) On the lateral root primordia formation in the crown roots of rice plants. Proc Crop Sci Soc Jpn *33*, 423-431

Krouk, G., Lacombe, B., Bielach, A., Perrine-Walker, F., Malinska, K., Mounier, E., Hoyerova, K., Tillard, P., Leon, S., Ljung, K., *et al.* (2010). Nitrate-regulated auxin transport by NRT1.1 defines a mechanism for nutrient sensing in plants. Developmental cell *18*, 927-937.

Laskowski, M., Grieneisen, V.A., Hofhuis, H., Hove, C.A., Hogeweg, P., Maree, A.F., and Scheres, B. (2008). Root system architecture from coupling cell shape to auxin transport. PLoS biology *6*, e307.

Li, J., Zhu, S., Song, X., Shen, Y., Chen, H., Yu, J., Yi, K., Liu, Y., Karplus, V.J., Wu, P., *et al.* (2006). A rice glutamate receptor-like gene is critical for the division and survival of individual cells in the root apical meristem. The Plant cell *18*, 340-349.

Lucas, M., Kenobi, K., von Wangenheim, D., Vobeta, U., Swarup, K., De Smet, I., Van Damme, D., Lawrence, T., Peret, B., Moscardi, E., *et al.* (2013). Lateral root morphogenesis is dependent on the mechanical properties of the overlaying tissues. Proceedings of the National Academy of Sciences of the United States of America *110*, 5229-5234.

Malamy, J.E., and Benfey, P.N. (1997). Organization and cell differentiation in lateral roots of Arabidopsis thaliana. Development *124*, 33-44.

Marhavy, P., Duclercq, J., Weller, B., Feraru, E., Bielach, A., Offringa, R., Friml, J., Schwechheimer, C., Murphy, A., and Benkova, E. (2014). Cytokinin controls polarity of PIN1-dependent auxin transport during lateral root organogenesis. Current biology : CB *24*, 1031-1037.

Mashiguchi, K., Tanaka, K., Sakai, T., Sugawara, S., Kawaide, H., Natsume, M., Hanada, A., Yaeno, T., Shirasu, K., Yao, H., *et al.* (2011). The main auxin biosynthesis pathway in Arabidopsis. Proceedings of the National Academy of Sciences of the United States of America *108*, 18512-18517.

Moreno-Risueno, M.A., Van Norman, J.M., Moreno, A., Zhang, J., Ahnert, S.E., and Benfey, P.N. (2010). Oscillating gene expression determines competence for periodic Arabidopsis root branching. Science *329*, 1306-1311.

Ni, J., Zhu, Z., Wang, G., Shen, Y., Zhang, Y., and Wu, P. (2014). Intragenic suppressor of Osiaa23 revealed a conserved tryptophan residue crucial for protein-protein interactions. PloS one *9*, e85358.

Petersson, S.V., Johansson, A.I., Kowalczyk, M., Makoveychuk, A., Wang, J.Y., Moritz, T., Grebe, M., Benfey, P.N., Sandberg, G., and Ljung, K. (2009). An auxin gradient and maximum in the Arabidopsis root apex shown by high-resolution cell-specific analysis of IAA distribution and synthesis. The Plant cell *21*, 1659-1668.

Scheres, B., Benfey, P., and Dolan, L. (2002). Root development. The Arabidopsis book / American Society of Plant Biologists *1*, e0101.

Svistoonoff, S., Creff, A., Reymond, M., Sigoillot-Claude, C., Ricaud, L., Blanchet, A., Nussaume, L., and Desnos, T. (2007). Root tip contact with low-phosphate media reprograms plant root architecture. Nature genetics *39*, 792-796.

Swarup, R., Kramer, E.M., Perry, P., Knox, K., Leyser, H.M., Haseloff, J., Beemster, G.T., Bhalerao, R., and Bennett, M.J. (2005). Root gravitropism requires lateral root cap and epidermal cells for transport and response to a mobile auxin signal. Nature cell biology *7*, 1057-1065.

Turner, M., Nizampatnam, N.R., Baron, M., Coppin, S., Damodaran, S., Adhikari, S., Arunachalam, S.P., Yu, O., and Subramanian, S. (2013a). Ectopic expression of miR160 results in auxin hypersensitivity, cytokinin hyposensitivity, and inhibition of symbiotic nodule development in soybean. Plant physiology *162*, 2042-2055.

Turner, T.R., James, E.K., and Poole, P.S. (2013b). The plant microbiome. Genome biology *14*, 209.

Van Norman, J.M., Zhang, J., Cazzonelli, C.I., Pogson, B.J., Harrison, P.J., Bugg, T.D., Chan, K.X., Thompson, A.J., and Benfey, P.N. (2014). Periodic root branching in Arabidopsis requires synthesis of an uncharacterized carotenoid derivative. Proceedings of the National Academy of Sciences of the United States of America *111*, E1300-1309.

Vanneste, S., De Rybel, B., Beemster, G.T., Ljung, K., De Smet, I., Van Isterdael, G., Naudts, M., Iida, R., Gruissem, W., Tasaka, M., *et al.* (2005). Cell cycle progression in the pericycle is not sufficient for SOLITARY ROOT/IAA14-mediated lateral root initiation in Arabidopsis thaliana. The Plant cell *17*, 3035-3050.

Vermeer, J.E., von Wangenheim, D., Barberon, M., Lee, Y., Stelzer, E.H., Maizel, A., and Geldner, N. (2014). A spatial accommodation by neighboring cells is required for organ initiation in Arabidopsis. Science *343*, 178-183.

Vicre, M., Santaella, C., Blanchet, S., Gateau, A., and Driouich, A. (2005). Root border-like cells of Arabidopsis. Microscopical characterization and role in the interaction with rhizobacteria. Plant physiology *138*, 998-1008.

Wang, L., Chu, H., Li, Z., Wang, J., Li, J., Qiao, Y., Fu, Y., Mou, T., Chen, C., and Xu, J. (2014). Origin and development of the root cap in rice. Plant physiology.

Willemsen, V., Bauch, M., Bennett, T., Campilho, A., Wolkenfelt, H., Xu, J., Haseloff, J., and Scheres, B. (2008). The NAC domain transcription factors FEZ and SOMBRERO control the orientation of cell division plane in Arabidopsis root stem cells. Developmental cell *15*, 913-922.

Zhou, J., Yu, F., Wang, X., Yang, Y., Yu, C., Liu, H., Cheng, Y., Yan, C., and Chen, J. (2014). Specific expression of DR5 promoter in rice roots using a tCUP derived promoter-reporter system. PloS one *9*, e87008.

Summary

Summary

Summary

The root system is essential for plants to uptake water and nutrients from the soil and to adapt the growth pattern in response to changing environment conditions. The root cap is located in the distal end of the root and covers the meristem reaching the transition zone. It acts as principal sensor mediating the interactions between plant roots and the soil, thus representing an interface capable in transmitting external signals to the root thereby determining the growth pattern of the root systems.

The root system is composed of a primary root and lateral roots sequentially forming along the primary root. In plant model *Arabidopsis thaliana,* lateral root formation is linked to a root clock that reflects a temporal oscillating pattern of gene expression in the oscillation zone in the root tip. This recurrent gene expression pattern is translated into a repetitive spatial pattern of prebranch sites, which eventually can further develop as lateral roots (Van Norman et al., 2013). Thus, the spatiotemporal pattern of lateral root formation during primary root growth becomes a curial topic in the present root development research. However, the molecular components that regulate the oscillations remain unknown. In addition, auxin has been demonstrated to control most aspects of lateral rooting events; however, the potential role of auxin in controlling the root clock has not yet been determined.

In this Ph.D thesis, we attempt to address this question. First of all, by using a chemical genetic approach, we identified that IBA-to-IAA conversion contributes to root branching. Following the real-time analysis of *DR5:Lucifease* expression in IBA-to-IAA conversion mutants, we revealed that the IBA-derived auxin in the root cap could moderate the strength of the oscillation, and thus regulate prebranch sites formation. Meanwhile, we showed that the amplitude of oscillation signal is dependent on TIR1/AFB-mediated auxin signaling in OZ. These data led to the understanding of the role of auxin in the root clock. More specifically we showed that auxin might act as a local gradient in OZ to regulate the oscillation strength which in turn determines the establishment of prebranch sites. Our results suggest that the root clock is controlled by a combination of temporal signals (oscillating of gene expression) on the oscillation periodicity and by a spatial signal of TIR1/AFB-dependent auxin signaling that is required for the amplitude in the oscillation.

To explore the downstream signaling components of IBA-derived auxin, we performed an IBA transcriptome analysis and identified novel and IBA-regulated components of root patterning, such as the *MEMBRANE-ASSOCIATED KINASE REGULATOR4* (*MAKR4*). Transcriptional analysis revealed that *MAKR4* expression specifically locates in primordia and moves towards the consecutive prebranch sites. Its plasma membrane localization strongly suggested cell-to-cell communication might be required during the prebanch sites establishment. Moreover, genetic evidence showed that the *makr4* mutant and amiRNA lines have a decreased number of lateral roots and lateral root primordia without affecting the prebranch site formation. Taken together, our data indicated that MAKR4 perceives the oscillation signal and translates it to the prebranch sites resulting into a regular spacing of lateral organs.

Based on these results, we set up a new imaging system using a vertical oriented macroview stereo microscope. It enables us to trace fluorescence signal movement through the root in the normal experimental condition during a long period. By using this novel imaging system, we observed that a periodic degradation of DR5 signal in the root cap triggers the local formation of a lateral root primordium. This process is triggered by periodic programmed cell death of root cap cells. We also found that auxin signaling in root cap is not required for maintaining the root clock behavior. Instead, it requires the coordination of local auxin biosynthesis and auxin transport in the root cap. Our findings demonstrated that the auxin in the root cap is as a crucial for regulating root patterning in Arabidopsis.

In addition, we have shown that TIR1-dependent auxin perception is required for maintaining DR5 oscillation level in OZ, indicating a central role of auxin on root prepatterning. In chapter 4, we further explore the specific signaling pathway downstream TIR1 for lateral root development. We identified a novel small molecule tirlin as a TIR1-dependent lateral root inducer representing a chemical tool to access it. Genetic evidences show that tirlin might act downstream of TIR1 and ARF7-ARF19 pathway to regulate lateral root formation. By screening a fast-neutron mutagenesis population, we propose LBD proteins as the potential target of tirlin. Our work further suggests that LBD proteins may act as downstream components of TIR1-dependent signaling on regulating lateral root formation.

Bidding deputy magistrate Du farewell

《送杜少府之任蜀州》

The capital and palace are guarded by the land of three Qin kingdoms,

In the distance the five ferries are screened by wind and mist.

城阙辅三秦，风烟望五津。

Now comes the time for us to bid farewell to each other,

And we still be officials away from home on duty.

与君离别意，同是宦游人。

As long as we remain bosom friends in our heart of hearts,

We'll still feel like neighbours despite the distance apart.

海内存知己，天涯若比邻。

So don't let us shed tears like youngsters,

At that last moment when we both wave goodbye.

无为在歧路，儿女共沾巾！

Wang Bo 王勃

Acknowledgements

In China, we often use “Fate (缘分)” to define friendship. People always say that the fate brings people together no matter how far apart they may be, otherwise they can't know each other even face to face.

In this respect, before I finished the writing of my Ph.D thesis, I would like to thank all the people who have ever helped me not only during my Ph.D study, but also in my life in the past five years, which is really a fantastic experience for me. I am very pleased with my research here in the past years, and I always feel free and never had the feeling of stress. I also like the academic atmosphere in PSB, people here are motivated and prefer to share the experience, which enable me to learn as much as possible.

First of all, I would like to thank all the root members, especially Tom, who gave me the opportunity to study at PSB, *an international institute with excellent researches*, in Gent, *a city with so many friendly Flemish people*, in Belgium, *a country with the best BEER and CHOCOLATE*! Actually, when there is a shortage of Orval in the market, I always got the feeling of victory because I could drink Orval weekly. Ha~Ha~

As my promoter, Tom spent a lot time on my project, a lot discussions and sending emails all over world to get the materials to keep my research in the highway. I really appreciate these and I sincerely believe Tom is an excellent promoter and a gentleman. I hope Tom could find Orval in the shop again after my leaving….

Next to Tom, I would like to thank my supervisor, Dominique, for guiding me a lot on designing the experiments properly and analyzing the data. Most of my research is performed on Arabidopsis thaliana, a tiny and uneatable plant, which is complete new for me at the beginning of my Ph.D study. With the help from Dominique and Bert, I became familiar with doing experiments *Arabidopsis thaliana*. And also thanks for including me in the chemical genetic projects, from which I could work out the title for my Ph.D thesis.

I will also remember Maria for help me making sections of roots – really very hard but crucial work, and also the delicious Asian&Belgium food. Food….sometimes can be very special, for instant, chick eggs from Gieljon; if the size of eggs in supermarket is scaled as lateral root primordium, Gieljon’s chick is producing founder cells. But many thanks to Xiyangyang for these eggs, several times help on repairing my bike, and also a lot fun during the work.

Lorena, Leen, Giel and Gert, although you have left the lab, I still appreciate the help from you for guiding me basic techniques at the beginning of my Ph.D with great patience. Lorena,

I believe you can become a good teacher; Gert, I still remember the word from you: “Be nice to the people!”

Davy and Hanne (哈娜), thanks a lot for help me with cloning and imagings; I wish you be in love forever and have happiness every moment.

Barbara, thanks for helping me with writing; Boris, thanks for the help on IBA microarray analysis; Marlies, Ianto and Ana, thanks for sharing experience on counting lateral root primordia; Long, Andry (Monkey King) and Hans, I really enjoyed the time sitting in the corner with you, always fun and innovations there.

Kun, Qian and Tao, I wish you success in your research and find a good job in the future.=

In the department, I want to thank Steffen for many useful advices and ideas on my research, especially on auxin transport; although every time I know I will get difficult questions from you and more work to do, but I still like to discuss with you. I also appreciate the help from Daniel for setting up the Olympus imaging systems; it is really fantastic and powerful machine for root development research.

Moreover, I want to thank all the jury members in the committee of my Ph.D defense,

dr. Wout Boerjan (chair), dr. Laurent Laplaze, dr. Lieven De Veylder, dr. Ive de Smet, and dr. Danny Geelen for the critical comments and very kind advices on my future research.

all the PIs in the department:

dr. Dirk Inzé, dr. Moritz Nowack, dr. Geert De Jaeger, dr. Sofie Goormachtig, dr. Ann Depicker, and dr. Jiri Friml for nice discussions on my projects and kindly sharing the materials.

I am also very appreciated all the support from people all over the world:

dr. Philip N. Benfey (Duke University, USA), dr. Malcolm Bennett (University of Nottingham, UK), dr. Bonnie Bartel (Rice University, USA), dr. Mark Estelle (University of California, USA), dr. Leah Band (University of Nottingham, UK), dr. Lucia C. Strader (Washington University, USA), dr. Catherine Bellini (Umeå University, Umeå, Sweden) for the kind gifts of lines and constructs.

For my dear Chinese friends, I really miss the time with you guys in Belgium, and am grateful for all your great help and encouragement.

First of all, I want to thank Dalong, my comrade, who had this adventure together with me, and we helped each other for our Ph.D study. I also want to thank Hanyi, and Weicong, who introduce PSB to me with a lot nice words, which help me make the decision to go here. My wife and I also enjoyed the trip we made together in France very much.

I could not forget the help from Zhang Jing, Zhaojun and He Ying on my research and take care of me at the early period of my study and living in Belgium.

Li Zhen and Deng Lei, I think I will miss the taste of home-made and Belgium-style hafing dish very much after I return, thanks a lot for sharing nice food with me and many nice discussions.

Zhubing and Chunmei, thanks for feeding me with delicious cookies every time when I was hungry. It's really special way for supporting my work.

I am also deeply indebted to all the other Chinese: Huang Jingjing, Chen Jian, Yao Yao, Du yulong, Xiao Xiaojian, Wang Feng, Chen Xu, Zhu Qiang, Gao Zhen, Luo Yu, Zhang Zaichao, Sun Xiaohuan, Han Chao, and Jiang Lingxiang, for your direct and indirect help to me and my work!

In the end, I also want to thank the China scholarship council (CSC), Ghent University, and VIB, who support my Ph.D study for the past five years.

Finally, I am indebted to my families for their continuous support and

To everybody: I hope all of you have enjoyed reading this. Without all your help, I could not finish my Ph.D. Thanks for all the great moments during these last five years. I wish our friendship remain and never can end.

Now it is time for the new adventure…; the future is warm yellow!

All the best,

Wei Xuan (宣伟), on the behavior of my family

Curriculum Vitae

Wei Xuan

Personal details

Birth date:	23/03/1984, Male
Birth place:	Xinghua city, Jiangsu Provence, P.R.China
Nationality:	Chinese
Residence address (Belgium):	Ijzerlaan 7, Gent, B-9000
Contact email:	xuanweichina@gmail.com

Education

2002.9-2006.6 Bachelor of Science, major in Biological Science, College of Life Sciences, Nanjing Agricultural University

2006.9-2009.6 Master of Science, major in Biochemistry & Molecular Biology, College of Life Sciences, Nanjing Agricultural University

2009.11- Present Predoctoral follow, VIB, Department of Plant Systems Biology, Ghent University, Technologiepark 927, 9052 Gent

PERFORMANCE AWARDS

2006 Nanjing Agricultural University scientific competition in Challenge Cup Awards

2008 China Youth Science and Technology Innovation Awards

2009 Jiangsu Province "triple-A" outstanding student

2009 China Scholarship Council (CSC) scholarship

2010 Special Research Fund - Cofunding for Chinese Ph.D students

Selected Publications (SCI/EI)

1. Van Norman, J.M., Xuan, W., Beeckman, T., and Benfey, P.N. (2013). To branch or not to branch: the role of pre-patterning in lateral root formation. Development *140*, 4301-4310.
2. Xuan, W., Murphy, E., Beeckman, T., Audenaert, D., and De Smet, I. (2013). Synthetic molecules: helping to unravel plant signal transduction. Journal of chemical biology *6*, 43-50.
3. De Rybel, B., Audenaert, D., Xuan, W., Overvoorde, P., Strader, L.C., Kepinski, S., Hoye, R., Brisbois, R., Parizot, B., Vanneste, S., *et al.* (2012). A role for the root cap in root branching revealed by the non-auxin probe naxillin. Nature chemical biology *8*, 798-805.
4. Xuan, W., Xu, S., Li, M., Han, B., Zhang, B., Zhang, J., Lin, Y., Huang, J., Shen, W., and Cui, J. (2012). Nitric oxide is involved in hemin-induced cucumber adventitious rooting process. Journal of plant physiology *169*, 1032-1039.
5. Cao, Z., Geng, B., Xu, S., Xuan, W., Nie, L., Shen, W., Liang, Y., and Guan, R. (2011). BnHO1, a haem oxygenase-1 gene from Brassica napus, is required for salinity and osmotic stress-induced lateral root formation. Journal of experimental botany *62*, 4675-4689.
6. Han, Y., Zhang, J., Chen, X., Gao, Z., Xuan, W., Xu, S., Ding, X., and Shen, W. (2008). Carbon monoxide alleviates cadmium-induced oxidative damage by modulating glutathione metabolism in the roots of Medicago sativa. The New phytologist *177*, 155-166.
7. Xuan, W., Xu, S., Yuan, X., and Shen, W. (2008a). Carbon monoxide: A novel and pivotal signal molecule in plants? Plant signaling & behavior *3*, 381-382.
8. Xuan, W., Zhu, F.Y., Xu, S., Huang, B.K., Ling, T.F., Qi, J.Y., Ye, M.B., and Shen, W.B. (2008b). The heme oxygenase/carbon monoxide system is involved in the auxin-induced cucumber adventitious rooting process. Plant physiology *148*, 881-893.
9. Xuan W, Huang LQ, Li M, Huang BK, Xu S, Liu H, Gao Y, Shen WB (2007) Induction of growth elongation in wheat root segments by heme molecules: a regulatory role of carbon monoxide in plants? Plant Growth Regulation 52: 41–51